

การสังเคราะห์และการตรวจสอบสมบัติของสารประกอบใหม่ที่มีออกซาโซล



นางสาวรพรรณ สิวลีพันธ์

วิทยานิพนธ์นี้เป็นส่วนหนึ่งของการศึกษาตามหลักสูตรปริญญาวิทยาศาสตรมหาบัณฑิต

สาขาวิชาปิโตรเคมีและวิทยาศาสตร์พอลิเมอร์


คณะวิทยาศาสตร์ จุฬาลงกรณ์มหาวิทยาลัย

ปีการศึกษา 2546

ISBN 974-17-4217-7

ลิขสิทธิ์ของจุฬาลงกรณ์มหาวิทยาลัย

SYNTHESIS AND CHARACTERIZATION OF NEW OXAZOLE CONTAINING  
COMPOUNDS



Miss Vorapun Sivaleepunth

สถาบันวิทยบริการ  
จุฬาลงกรณ์มหาวิทยาลัย

A Thesis Submitted in Partial Fulfillment of the Requirements  
for the Degree of Master of Science in Petrochemistry and Polymer Science

Faculty of Science  
Chulalongkorn University  
Academic Year 2003  
ISBN 974-17-4217-7

Thesis Title                   SYNTHESIS AND CHARACTERIZATION OF NEW OXAZOLE  
CONTAINING COMPOUNDS  
By                               Miss Vorapun Sivaleepunth  
Field of Study               Petrochemistry and Polymer Science  
Thesis Advisor               Associate Professor Supawan Tantayanon, Ph.D.

---

Accepted by the Faculty of Science, Chulalongkorn University in Partial Fulfillment of  
the Requirements for the Master's Degree

.....Dean of Faculty of Science  
(Professor Piamsak Menasveta, Ph.D.)

THESIS COMMITTEE

.....Chairman  
(Professor Pattarapan Prasassarakich, Ph.D.)

.....Thesis Advisor  
(Associate Professor Supawan Tantayanon, Ph.D.)

.....Member  
(Associate Professor Nuanphun Chantarasiri, Ph.D.)

.....Member  
(Assistant Professor Warinthorn Chavasiri, Ph.D.)

.....Member  
(Wanlapa Aeungmaitrepirom, Ph.D.)

วรพรรณ สีวลีพันธ์: การสังเคราะห์และการตรวจสอบสมบัติของสารประกอบใหม่ที่มี  
ออกซาโซล (SYNTHESIS AND CHARACTERIZATION OF NEW OXAZOLE  
CONTAINING COMPOUNDS) อ.ที่ปรึกษา : รศ.ดร.ศุภวรรณ ตันตยานนท์; 160 หน้า.  
ISBN974-17-4217-7.

4-คลอโร-2,5-ไดเฟนิลออกซาโซล สังเคราะห์ได้จากปฏิกิริยาระหว่างเบนโซอิล ไฮยาไนด์ และ  
เบนซาลดีไฮด์ ให้ผลผลิต 67% ได้เสนอกลไกการเกิดปฏิกิริยาของ 4-คลอโร ออกซาโซล  
ผ่านอินเทอร์มีเดียตเฮกซิลอิมมิโดอิลคลอไรด์ ปฏิกิริยานี้ถูกนำมาใช้สำหรับสังเคราะห์ 1,4-บิส(4-  
คลอโร-5-เฟนิลออกซาโซล-2-อิล)เบนซีน และ 1,4-บิส(4-คลอโร-2-เฟนิลออกซาโซล-5-อิล)เบนซีน  
โดยผ่านปฏิกิริยาระหว่างเบนโซอิลไฮยาไนด์ กับ เทเรพทาไดคาร์บอกซาลดีไฮด์ และ เทเรพทาโลอิล  
ไฮยาไนด์ กับ เบนซาลดีไฮด์ ตามลำดับ สามารถเตรียมได้ร้อยละ 59 และ 52 ตามลำดับ การรีดักชัน  
ของ 1,4-บิส(4-คลอโร-5-เฟนิลออกซาโซล-2-อิล)เบนซีน เป็น 1,4-บิส(5-เฟนิลออกซาโซล-2-อิล)  
เบนซีน หรือ พีไอพีไอพี เกิดขึ้นผ่านไฮโดรจีเนชัน โดยใช้ 10% แพลลาเดียมบนคาร์บอนเป็น  
ตัวเร่งปฏิกิริยา ผลผลิตทั้งหมดถูกตรวจสอบโดยเทคนิคทางสเปกโทรสโกปี และในการศึกษานี้ได้มี  
การสังเคราะห์โพลิโอมเมอร์ที่มีออกซาโซล และยังศึกษาสมบัติทางด้านแสงของสารประกอบใน  
สารละลายต่างๆ พบว่า 1,4-บิส(4-คลอโร-5-เฟนิลออกซาโซล-2-อิล)เบนซีน และ 1,4-บิส(4-คลอโร-2-  
เฟนิลออกซาโซล-5-อิล)เบนซีน ให้ค่าฟลูออเรสเซนซ์ควอนตัมยี่ลด์ของสารสูงกว่า 4-คลอโร-2,5-ได  
เฟนิลออกซาโซล

หลักสูตร.....ลายมือชื่อนิสิต.....  
สาขาวิชา...ปิโตรเคมีและวิทยาศาสตร์พอลิเมอร์...ลายมือชื่ออาจารย์ที่ปรึกษา.....  
ปีการศึกษา...2546...

# # 4572469123 : MAJOR PETROCHEMISTRY AND POLYMER SCIENCE

KEY WORD : 2,5-DIPHENYLOXAZOLE/ SCINTILLATOR/ POPOP/ HETEROCYCLIC/  
FLUORESCENCE

VORAPUN SIVALEEPUNTH : SYNTHESIS AND CHARACTERIZATION OF NEW  
OXAZOLE CONTAINING COMPOUNDS. THESIS ADVISOR : ASSOC. PROF.  
SUPAWAN TANTAYANON, Ph.D., 160 pp. ISBN 974-17-4217-7.

4-Chloro-2,5-diphenyloxazole was synthesized from the reaction of benzoyl cyanide with benzaldehyde and gave the yield 67%. The mechanism of 4-chloro-oxazole formation was proposed to occur *via* acylimidoyl chloride intermediate. Similarly, reaction was used for the synthesis of 1,4-bis(4-chloro-5-phenyloxazol-2-yl)benzene and 1,4-bis(4-chloro-2-phenyloxazol-5-yl)benzene. These compounds have been synthesized by reacting between benzoyl cyanide and terephthalaldehyde, and terephthaloyl cyanide and benzaldehyde, respectively in dried diethyl ether and saturated with hydrogen chloride gas that gave the yield 59% and 52%, respectively. The reduction of 1,4-bis(5-phenyloxazol-2-yl)benzene or POPOP can occur *via* catalytic hydrogenation employing 10% Pd/C as catalyst. All these products were identified by the spectroscopic techniques. The synthesis of oligomer containing oxazole moiety in the backbone was also attempted. The optical property of these compounds in various solvents had been investigated. It was found that 1,4-bis(4-chloro-5-phenyloxazol-2-yl)benzene and 1,4-bis(4-chloro-2-phenyloxazol-5-yl)benzene gave higher fluorescence quantum yields than 4-chloro-2,5-diphenyloxazole.

Program.....Student's signature.....

Field of study...Petrochemistry and Polymer Science...Advisor's signature.....

Academic year....2003....

## ACKNOWLEDGEMENTS

The author wishes to express sincere thanks and grateful appreciation to Associate Professor Dr. Supawan Tantayanon, her advisor who has been giving all her support and guidance throughout the research work. Although this thesis had obstacles, finally it could be completed by her advice. The author feels great gratitude to her teacher. In addition, her appreciation also extends to all committee members for their comments regarding this thesis.

Moreover, the author would like to thank Supramolecular Chemistry Research Unit (SCRU), the Chemistry Department, Chulalongkorn University for allowing her to use Fluorometer for this research and the author would like to thank Assist. Prof. Dr. Nongnuj Muangsin (Chulalongkorn University) and Assist. Prof. Dr. Chavang Pakavatchai (Prince Songkla University) for X-ray diffraction data collections. In addition, the author also would like to acknowledge Dr. Ichiro Imae, JAIST, Japan who tried the measurement of 500 MHz<sup>1</sup>H and 125 MHz<sup>13</sup>C NMRs, COSY, HMQC, and HMBC to confirm the characterization of these samples.

Furthermore, the author also greatest thanks Department of Chemistry for the equipment and facilities throughout the course of her thesis. The Graduate School, Chulalongkorn University and the Ministry of University Affairs are gratefully acknowledged for providing partial financial support for this research.

Special thanks are expanded to Mr. Theppawut Israsena Na Ayudhya and Mr. Wongwit Wongwitwichote for their cheerful and energetic willingness to do her a huge favor. Additionally, the author is grateful to anyone else whose names are not mentioned here, who helped and encouraged her over the years of this study.

Finally, the author wishes to express to her gratitude to her family for their encouragement and strong moral support. Many thanks to her friends and colleagues who contributed suggestions and support during the course of her research.

## CONTENTS

	PAGE
ABSTRACT (INTHAI).....	iv
ABSTRACT (IN ENGLISH).....	v
ACKNOWLEDGMENTS.....	vi
CONTENTS.....	vii
LIST OF TABLES.....	xi
LIST OF FIGURES.....	xii
LIST OF SCHEMES.....	xiii
LIST OF ABBREVIATIONS.....	xiv
CHAPTER I: INTRODUCTION	
1.1 Introduction.....	1
1.2 Objectives.....	2
1.3 Scope of the Research.....	2
CHAPTER II: THEORY AND LITERATURE REVIEW	
2.1 Oxazole.....	4
2.2 Luminescence Process.....	4
2.3 Effect of Transition Type on Luminescence.....	8
2.4 Photoluminescence and the structure of Organic Molecules.....	9
2.5 Fluorescence Quenching and Energy Transfer in Organic Compounds.....	14
2.6 Single crystal X-ray diffraction.....	17
2.7 Literature Reviews.....	18
CHAPTER III: EXPERIMENTAL	
3.1 Apparatus.....	22
3.2 Synthesis of starting materials and products for studying on the optical property.....	23
3.2.1 Preparation of benzoyl cyanide.....	23
3.2.2 Preparation of terephthaloyl cyanide.....	24



## CONTENTS (continued)

	PAGE
3.2.3 Synthesis of 4-chloro-2,5-diphenyloxazole.....	25
3.2.4 Synthesis of 1,4-bis(4-chloro-5-phenyloxazol-2-yl)benzene.....	26
3.2.5 Synthesis of 1,4-bis(4-chloro-2-phenyloxazol-5-yl)benzene.....	27
3.2.6 Reduction of 1,4-bis(5-phenyloxazol-2-yl)benzene.....	28
3.2.7 The larger molecules of the oxazole containing compound synthesis.....	29
3.3 Optical property.....	30
3.3.1 UV-Absorption analysis.....	30
3.3.1.1 UV-Absorption analysis of 4-chloro-2,5-diphenyloxazole.....	30
3.3.1.2 UV-Absorption analysis of 1,4-bis(4-chloro-5-phenyloxazol-2-yl)benzene...30	
3.3.1.3 UV-Absorption analysis of 1,4-bis(4-chloro-2-phenyloxazol-5-yl)benzene...31	
3.3.1.4 UV-Absorption analysis of 2,5-diphenyloxazole.....	31
3.3.1.5 UV-Absorption analysis of 1,4-bis(5-phenyloxazol-2-yl)benzene.....	32
3.3.2 Fluorescence analysis.....	33
-General Experimental Considerations.....	33
-Procedure.....	33
-Calculation of Fluorescence Quantum Yields from Acquired Data.....	34
3.3.2.1 Fluorescence analysis of anthracene.....	34
3.3.2.2 Fluorescence analysis of 4-chloro-2,5-diphenyloxazole.....	34
3.3.2.3 Fluorescence analysis of 1,4-bis(4-chloro-5-phenyloxazol-2-yl)benzene.....	35
3.3.2.4 Fluorescence analysis of 1,4-bis(4-chloro-2-phenyloxazol-5-yl)benzene.....	35
3.3.2.5 Fluorescence analysis of 2,5-diphenyloxazole.....	35
3.3.2.6 Fluorescence analysis of 1,4-bis(5-phenyloxazol-2-yl)benzene.....	36

## CHAPTER IV: RESULTS AND DISCUSSION

4.1 Preparation of Starting materials.....	37
4.1.1 Preparation of benzoyl cyanide.....	37
4.1.2 Preparation of terephthaloyl cyanide.....	38
4.2 Synthesis of 4-chloro-2,5-diphenyloxazole.....	39
4.3 Synthesis of 1,4-bis(4-chloro-5-phenyloxazol-2-yl)benzene.....	44



## CONTENTS (continued)

	PAGE
4.4 Synthesis of 1,4-bis(4-chloro-2-phenyloxazol-5-yl)benzene.....	54
4.5 Reduction of 1,4-bis(5-phenyloxazol-2-yl)benzene.....	62
4.6 The larger molecules of the oxazole containing compound.....	65
4.7 The results of UV-Absorption analysis.....	67
4.8 The results of Fluorescence analysis.....	69
4.8.1 Fluorescence analysis of 4-chloro-2,5-diphenyloxazole.....	69
4.8.2 Fluorescence analysis of 2,5-diphenyloxazole.....	70
4.8.3 Fluorescence analysis of 1,4-bis(4-chloro-5-phenyloxazol-2-yl)benzene.....	71
4.8.4 Fluorescence analysis of 1,4-bis(4-chloro-2-phenyloxazol-5-yl)benzene.....	72
4.8.5 Fluorescence analysis of 1,4-bis(5-phenyloxazol-2-yl)benzene.....	73
4.8.6 Comparison the fluorescence emission spectra.....	74
 CHAPTER V: CONCLUSION	
5.1 Conclusion.....	78
5.2 Proposal for future work.....	79
 REFERENCES.....	 80
 APPENDICES	
APPENDIX A .....	83
APPENDIX B .....	101
APPENDIX C .....	115
APPENDIX D .....	144
 VITA.....	 160

## LIST OF TABLES

TABLES	PAGE
2-1. Comparison of $n, \pi^*$ and $\pi, \pi^*$ Singlet States.....	8
2-2. Effects of Substituents upon the Fluorescence of Aromatics.....	12
4-1 Interpretation of IR spectra of benzoyl chloride, benzoyl cyanide.....	38
4-2 Interpretation of IR spectra of terephthaloyl chloride, terephthaloyl cyanide.....	39
4-3 $^{13}\text{C}$ NMR chemical shifts (ppm) of 4-chloro-2,5-diphenyloxazole.....	41
4-4 Mass spectroscopic data of 4-chloro-2,5-diphenyloxazole.....	42
4-5 NMR chemical shifts (ppm) of compound A.....	46
4-6 Mass spectroscopic data of 4-(4-chloro-5-phenyloxazol-2-yl)-benzaldehyde.....	47
4-7 NMR chemical shifts (ppm) of 1,4-bis(4-chloro-5-phenyloxazol-2-yl)benzene.....	51
4-8 Mass spectroscopic data of 1,4-bis(4-chloro-5-phenyloxazol-2-yl)benzene.....	52
4-9 NMR chemical shifts (ppm) of 1,4-bis(4-chloro-2-phenyloxazol-5-yl)benzene.....	56
4-10 Mass spectroscopic data of 1,4-bis(4-chloro-2-phenyloxazol-5-yl)benzene.....	57
4-11 Crystal and experimental data of 1,4-bis(4-chloro-2-phenyloxazol-5-yl)benzene ....	59
4-12 Bond lengths (Å) and angles of 1,4-bis(4-chloro-2-phenyloxazol-5-yl)benzene.....	60
4-13 NMR chemical shifts (ppm) of 1,4-bis(5-phenyloxazol-2-yl)benzene.....	64
4-14 UV absorption spectral data of the compounds.....	67
4-15 The results of UV-Absorption analysis.....	76
4-16 The results of Fluorescence analysis.....	77

## LIST OF FIGURES

FIGURES	PAGE
1.1 The photomultiplier/scintillation counter system.....	1
2.1 Structure of oxazole molecule.....	4
2.2 State diagram depicting the unimolecular processes .....	5
2.3 Comparison of electronic processes for molecules having lowest $n, \pi^*$ and $\pi, \pi^*$ states.....	9
2.4 Room-temperature fluorescence spectra of three aromatic hydrocarbons in methanol.....	10
2.5 Dapoxyl sulfonic acid.....	20
4.1 Chemical structure of 4-chloro-2,5-diphenyloxazole with atomic numbering.....	40
4.2 The structure of 4-(4-chloro-5-phenyloxazol-2-yl)-benzaldehyde.....	47
4.3 Chemical structure of 1,4-bis(4-chloro-5-phenyloxazol-2-yl)benzene with atomic numbering.....	49
4.4 Chemical structure of 1,4-bis(4-chloro-2-phenyloxazol-5-yl)benzene with atomic numbering.....	54
4.5 An ORTEP drawing of 1,4-bis(4-chloro-2-phenyloxazol-5-yl)benzene.....	62
4.6 Chemical structure of 1,4-bis(5-phenyloxazol-2-yl)benzene with atomic numbering.....	63
4.7 The UV-absorption spectra of the oxazole containing compounds.....	68
4.8 The emission spectra of 4-chloro-2,5-diphenyloxazole.....	70
4.9 The emission spectra of 2,5-diphenyloxazole.....	71
4.10 The emission spectra of 1,4-bis(4-chloro-5-phenyloxazol-2-yl)benzene.....	72
4.11 The emission spectra of 1,4-bis(4-chloro-2-phenyloxazol-5-yl)benzene.....	73
4.12 The emission spectra of 1,4-bis(5-phenyloxazol-2-yl)benzene.....	74
4.13 The fluorescence emission spectra of the compounds.....	75

## LIST OF SCHEMES

SCHEMES	PAGE
2.1 Synthesis of 2,5-diphenyloxazole by Fischer synthesis.....	18
2.2 Synthesis of 2,5-diphenyloxazole by Robinson-Gabriel synthesis .....	19
2.3 Synthesis of 4-chloro-2,5-diphenyloxazole by modified Fischer synthesis .....	19
3.1 Preparation of benzoyl cyanide.....	23
3.2 Preparation of terephthaloyl cyanide.....	24
3.3 Synthesis of 4-chloro-2,5-diphenyloxazole .....	25
3.4 Synthesis of 1,4-bis(4-chloro-5-phenyloxazol-2-yl)benzene.....	26
3.5 Synthesis of 1,4-bis(4-chloro-2-phenyloxazol-5-yl)benzene.....	27
3.6 Reduction of 1,4-bis(5-phenyloxazol-2-yl)benzene.....	28
3.7 The larger molecules of the oxazole containing compound synthesis.....	29
4.1 The fragmentation pathways of 4-chloro-2,5-diphenyloxazole.....	42
4.2 Proposed mechanism of 4-chloro-oxazole formation.....	43
4.3 The fragmentation pathways of 4-(4-chloro-5-phenyloxazol-2-yl)-benzaldehyde.....	48
4.4 The fragmentation pathways of 1,4-bis(4-chloro-5-phenyloxazol-2-yl)benzene.....	53
4.5 The fragmentation pathways of 1,4-bis(4-chloro-2-phenyloxazol-5-yl)benzene.....	58

สถาบันวิทยบริการ  
จุฬาลงกรณ์มหาวิทยาลัย

## LIST OF ABBREVIATIONS

cm <sup>-1</sup>	Unit of wavenumber
m.p.	Melting Point
°C	Degree ceisius
(Å)	Angstrom
MS	Mass Spectrometry
m/z	Mass per charge
NMR	Nuclear Magnetic Resonance
J	Coupling constant
Hz	Hertz
ppm	Parts Per Million
δ	Chemical shift
s	Singlet (NMR)
d	Doublet (NMR)
dd	Doublet of doublet (NMR)
t	Triplet (NMR)
m	Multiplet (NMR)
ε	Extinction coefficient
M	Molar
mmol	Millimol
ml	Milliter
THF	tetrahydrofuran
PPO	2,5-diphenyloxazole
POPOP	1,4-bis(5-phenyloxazol-2-yl)benzene
HMQC	Heteronuclear Multiple Quantum Coherence
HMBC	Heteronuclear Multiple Bond Coherence
UV	Ultraviolet
atm	atomosphere

# CHAPTER I

## INTRODUCTION

### 1.1 Introduction

Oxazole containing compounds are generally used for luminescence because the properties of oxazole have high fluorescence quantum yields, fast emission decay, low photochemical fatigue and structure tenability. Therefore, oxazole has several applications such as pharmaceuticals, fluorescent whitening agents, photography and scintillator.

Scintillator is employed in scintillation counters to detect various types of radiation. Scintillation counting is a method of counting flashes of light emitted by fluorescent molecules when impacted by ionizing radiation, in order to establish the presence or amount of radioactivity. The scintillator is defined as a flash emitter of light, which is a consequence of receiving excitation energy from the radiation source. The energy absorbed by the scintillator is converted into fluorescence emission of photons. The emitted photons are not usually counted directly. To increase the sensitivity and accuracy of measurement photomultipliers are commonly used.

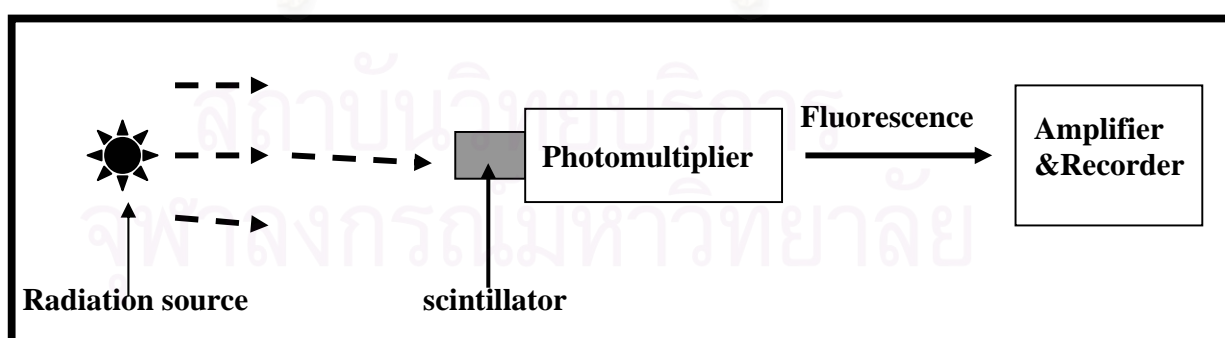


**Figure 1.1** The photomultiplier/scintillation counter system

Figure 1.1 shows the principle of a photomultiplier/scintillation counter system. Characteristics to be considered in the selection of the scintillator are internal absorption of fluorescence, scintillation decay time, fluorescence quantum yield, and pulse height, which is influenced by the sensitivity of the photomultiplier at the wavelengths of fluorescence emission of the particular scintillator.<sup>1</sup> For instance, 2,5-diphenyloxazole, PPO and 1,4-bis(5-phenyloxazol-2-yl)benzene, POPOP are the most efficient fluorescent compounds which can be used as scintillators.

In this research, the synthesis of new oxazole compounds was achieved *via* modified Fischer Synthesis. It involves only one step and the products could be separated and purified easily. In addition, the optical properties of products are investigated. They give higher efficiency in the utilization than 2,5-diphenyloxazole.

## 1.2 Objectives

The aim of this research is to synthesize new oxazole containing compounds *via* modified Fischer Synthesis for studying the optical property.

## 1.3 Scope of the Research

1. To synthesize new oxazole containing compounds.

1.1 Synthesis of 4-chloro-2,5-diphenyloxazole.

The reaction shows in the following steps:

1.1.1 Cyclization reaction of 4-chloro-2,5-diphenyloxazole  
between benzoyl cyanide and benzaldehyde

1.1.2 Characterization of 4-chloro-2,5-diphenyloxazole.



## 1.2 Synthesis of 1,4-bis(4-chloro-5-phenyloxazol-2-yl)benzene.

The reaction shows in the following steps:

- 1.2.1 Preparation of benzoyl cyanide
- 1.2.2 Cyclization reaction of 1,4-bis(4-chloro-5-phenyloxazol-2-yl)benzene between benzoyl cyanide and terephthalaldehyde
- 1.2.3 Characterization of 1,4-bis(4-chloro-5-phenyloxazol-2-yl)benzene.

## 1.3 Synthesis of 1,4-bis(4-chloro-2-phenyloxazol-5-yl)benzene.

The reaction shows in the following steps:

- 1.3.1 Preparation of terephthaloyl cyanide
- 1.3.2 Cyclization reaction of 1,4-bis(4-chloro-2-phenyloxazol-5-yl)benzene between terephthaloyl cyanide and benzaldehyde
- 1.3.3 Characterization of 1,4-bis(4-chloro-2-phenyloxazol-5-yl)benzene.

## 1.4 Synthesis of 1,4-bis(5-phenyloxazol-2-yl)benzene.

The reaction shows in the following steps:

- 1.4.1 Synthesis of 1,4-bis(4-chloro-5-phenyloxazol-2-yl)benzene.
- 1.4.2 Reduction of 1,4-bis(4-chloro-5-phenyloxazol-2-yl)benzene by Catalytic Hydrogenation employing 10% Pd/C as catalyst.
- 1.4.3 Characterization of 1,4-bis(5-phenyloxazol-2-yl)benzene.

## 1.5 The larger molecules of the oxazole containing compound synthesis.

2. To investigate the optical property of synthesized new oxazole containing compounds.

## CHAPTER II

### THEORY AND LITERATURE REVIEW

#### 2.1 Oxazole

**Oxazole** is a class of five-membered ring, heteroaromatic compound and derived from this species by replacing two of the carbons with a nitrogen atom and another heteroatom. Oxazole has an oxygen atom and a pyridine-type nitrogen atom at the 1 and 3 positions of the ring, and, like pyridines, oxazole is weakly basic substances.<sup>2</sup>

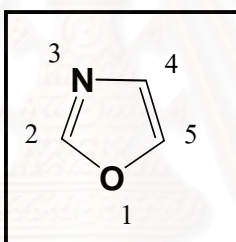


**Figure 2.1** Structure of oxazole molecule

#### 2.2 Luminescence Process

Luminescence processes can be interpreted only in terms of the excited state from which luminescence emission occurs and its relationship to the ground state of the molecule. Although the simple picture of photon to give luminescence seems to be quite straightforward, there are nonradiative processes that precede and compete with photon emission. Therefore, it is important to consider all processes, which occur after photon absorption by a molecule and their relationship to luminescence.

The term “luminescence” refers to the emission of radiation from an excited state and covers two phenomena; fluorescence and phosphorescence. The unimolecular processes

leading to these radiative deactivation steps are conveniently introduced by reference to a “Jablonski Diagram” of the type shown Figure 2.2. The lowest energy state of the vast majority of organic molecules is a singlet state. This state is depicted as  $S_0$  in Figure 2.2. *Absorption*, occurring with retention of spin, promotes an electron from the highest occupied molecular orbital into one of higher energy, creating a molecule in a higher excited state  $S_n$ .<sup>3</sup>

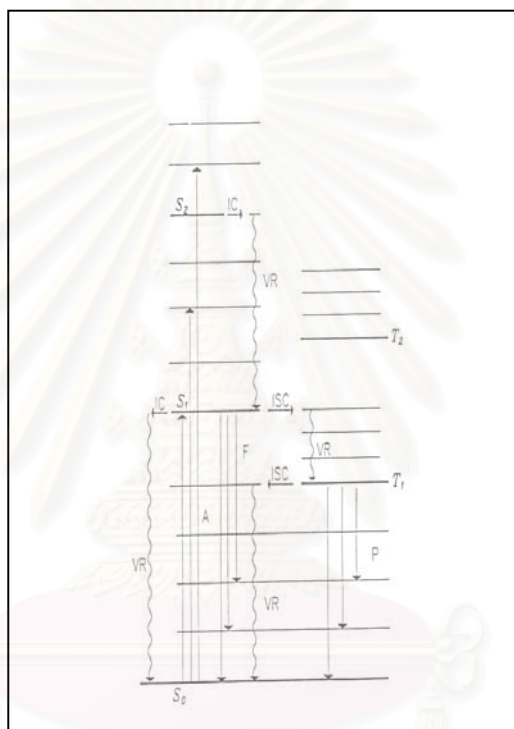


**Figure 2.2** State diagram depicting the unimolecular processes of A-absorption; F-fluorescence; IC-internal conversion; ISC-intersystem crossing; P-phosphorescence and VR-vibrational relaxation.<sup>3</sup>

*Vibrational levels* of the excited state are also populated and a range of wavelengths is absorbed in the excitation process as revealed in the absorption spectrum. The processes of internal conversion and vibrational relaxation (the intermolecular exchange of energy whereby a vibrationally “hot” species achieves thermal equilibrium with its surroundings) rapidly

render the molecule in the lowest vibrational level of the  $S_1$  state. Consequently, the proportion of the energy initially absorbed which can be accessed by the spectroscopist, as luminescence, is determined by the relative efficiencies of the process which serve to deactivate  $S_1$ . Once a molecule arrives at the lowest vibrational level of an excited singlet state, it can do a number of things, one of which is to return to the ground state by photon emission. This process is called *fluorescence* (the radiative deactivation of  $S_1$ ). Fluorescence ( $S_1 \rightarrow S_0$  radiative transitions occur to the various vibrational levels of  $S_1$ : in condensed media, fluorescence results in the appearance of a broad “band” spectrum at energies lower than that of the absorption band).

The quantum efficiency of fluorescence is defined as the fraction of excited molecules that will fluoresce. For highly fluorescent molecules the quantum efficiency of fluorescence approaches unity, while for other molecules fluorescence is so weak that one is unable to observe it and the quantum efficiency of fluorescence approaches zero. It should be noted that even though a quantum of radiation is emitted in fluorescence, this quantum would be of lower energy on the average than the quantum absorbed by the molecule, due to vibrational relaxation. The change in photon energy causes a shift of the fluorescence spectrum to longer wavelengths, relative to the absorption spectrum, and is referred to as a Stokes Shift. Then, the process of fluorescence consists of photon absorption by a molecule to go to an excited singlet state, photon emission to a vibrationally excited level of the ground state, and again relaxation of the molecule to the lowest vibrational level of the ground state. In addition to fluorescence, one also encounters radiationless processes whereby molecules in an excited singlet state may return to the ground state without the emission of a photon, converting all of the excitation energy into heat. The process, called *internal conversion*, is not well understood and its efficiency is very difficult to measure, followed by vibrational cascade is one means whereby  $S_1$  is radiationlessly converted into  $S_0$ . Generally, internal conversion between an excited singlet state and the ground state should be an inefficient process and it probably accounts for only a small fraction of the total excitation energy in most molecules.

This is particularly true in aromatic hydrocarbons, where it is thought that internal conversion between the lowest excited singlet state and the ground state is nonexistent. On the other hand, the energy separation between the ground state and the first excited singlet state is small, and therefore an efficient internal conversion process removes the excitation energy from the first excited singlet state. Another non-radiative route is that of intersystem crossing. Intersystem crossing is an isoenergetic transition, involving spin inversion, leading to population of an upper vibrational level of a triplet state. In condensed media, excess energy is rapidly lost and subsequent deactivation occurs from the lowest vibrational level of the lowest triplet state,  $T_1$ . Return to the ground state from  $T_1$  may be effected by two unimolecular processes. Non-radiative deactivation is accomplished via intersystem crossing to an upper vibrational level of  $S_0$ , followed by vibrational relaxation. The radiative process of phosphorescence, populating the various vibrational levels of the ground state produces a band spectrum, in condensed media, which is disposed at lower energies than that of fluorescence. The various modes of deactivation of  $S_1$  or  $T_1$  combine to determine the lifetime of the excited state. For example, under the influence of the unimolecular processes of fluorescence (F), internal conversion (IC) and intersystem crossing (ISC), a “steady-state” population of  $S_1$  excited states, following instantaneous cessation of excitation. In condensed media, excited singlet states are generally characterized by lifetimes, which lie in the nanosecond to microsecond range. Phosphorescent states on the other hand are longer lived (conversion to the ground state being spin “forbidden”) and, dependent upon chromophore, environment, etc., exist upon timescales which might range from the microsecond domain to tens of seconds. As a consequence, by choosing appropriate combinations of fluorescent and phosphorescent sensors, the polymer chemist can access an extremely broad range of “test frequencies”.

### 2.3 Effect of Transition Type on Luminescence

Internal conversion to the lowest excited singlet state of a molecule prior to emission of a photon is very important in determining the luminescence characteristics of a molecule. This means that the behavior of a molecule after excitation will not depend upon the state to which it was excited initially, but rather on the nature of the lowest excited singlet state. If the lowest excited singlet state is a  $\pi, \pi^*$  state, the molecule will show behavior characteristic of a  $\pi, \pi^*$  state, whereas if the lowest excited singlet state is an  $n, \pi^*$  state, it will show characteristics of an  $n, \pi^*$  state. Because  $\pi, \pi^*$  and  $n, \pi^*$  states represent the two major types of excited states found in organic molecules, it is important to compare those characteristics which affect their luminescence.

Table 2-1 compares approximate values for maximum extinction coefficient, lifetime of the state, singlet-triplet split, and relative rate of intersystem crossing for  $n, \pi^*$  and  $\pi, \pi^*$  states. Because  $n \rightarrow \pi^*$  transitions generally are less intense than  $\pi \rightarrow \pi^*$  transitions,  $n, \pi^*$  excited states have longer lifetimes, a factor which tends to enhance intersystem crossing from  $n, \pi^*$  states. The smaller singlet-triplet split for  $n, \pi^*$  states also tends to enhance intersystem crossing. These two factors account for the fact that intersystem crossing occurs with a much greater probability from an  $n, \pi^*$  excited state than from a  $\pi, \pi^*$  state.

**Table 2-1.** Comparison of  $n, \pi^*$  and  $\pi, \pi^*$  Singlet States

	$n, \pi^*$ states	$\pi, \pi^*$ states
$\epsilon_{\max}$ ( $\text{cm}^{-1}\text{M}^{-1}$ )	$10^3$ - $10^5$	$10^3$ - $10^5$
Lifetime ( $\text{s}^{-1}$ )	$10^{-7}$ to $10^{-5}$	$10^{-9}$ to $10^{-7}$
Singlet-triplet split	Small	Generally large
Rate of intersystem Crossing	Greater than for fluorescence	the same order as fluorescence



This situation is illustrated in Figure 2.3. Absorption of a photon to produce an excited singlet state is indicated by A, with internal conversion to the lowest excited singlet state by IC. For molecule “a”, where the lowest excited singlet state is  $\pi,\pi^*$ , competition between the usual processes for the loss of excitation energy occurs. This means that the molecule may fluoresce or may undergo intersystem crossing to the triplet state and then return to the ground state by phosphorescence. If the lowest excited singlet state is  $n,\pi^*$  as in the case of molecule “b”, intersystem crossing is enhanced at the expense of fluorescence, removing fluorescence as a major pathway for the loss of excitation energy, but retaining all other processes.<sup>4</sup>

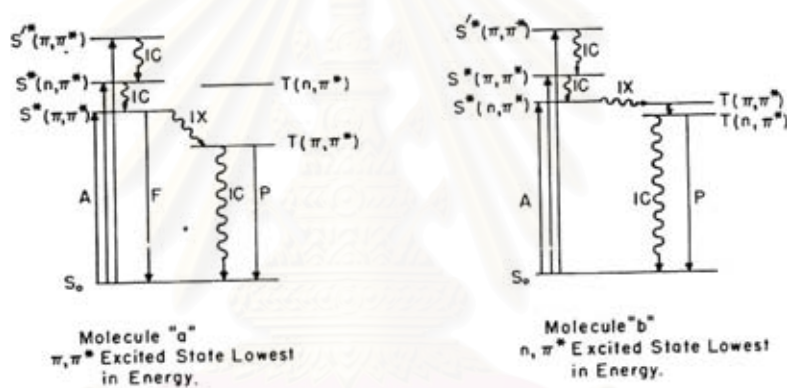


**Figure 2.3** Comparison of electronic processes for molecules having lowest  $n,\pi^*$  and  $\pi,\pi^*$  states : A, absorption; IC, internal conversion; IX, intersystem crossing; P, phosphorescence; F, fluorescence;  $S^*$ , excited singlet state; T, triplet state;  $S_0$ , ground state.<sup>4</sup>

## 2.4 Photoluminescence and the Structure of Organic Molecules

Fluorescence and phosphorescence spectroscopy are not broadly useful methods for determining molecular structure in the same way that, for example, infrared or microwave



spectroscopy is. Nonetheless, significant qualitative information concerning molecular structure can be obtained from fluorescence studies.<sup>5</sup>

A great majority of the organic compounds which exhibit intense analytically useful fluorescence possess cyclic, conjugated structures. However, the fact that a molecule possesses these structural characteristics does not guarantee that the species will fluoresce. This section discusses the fluorescence characteristics of the different classes of aromatic and heterocyclic compounds, and some of the effects of molecular structure upon the luminescence of such compounds.

### 1. Aromatic Hydrocarbons

In liquid solution, most unsubstituted aromatic hydrocarbons exhibit fluorescence, either in the visible or ultraviolet. In general, the greater the number of condensed rings in an aromatic hydrocarbon, the lower will be the energy of emission. Thus, benzene and naphthalene fluoresce in the ultraviolet, anthracene exhibits blue fluorescence, naphthalene fluoresces green, and pentacene exhibits a red emission. Various aromatic hydrocarbons may fluoresce at widely differing frequencies, a fact which is of considerable analytical importance. Solutions of the aromatic hydrocarbons anthracene, phenanthrene, and fluorene fluoresce as shown in Figure 2.4.

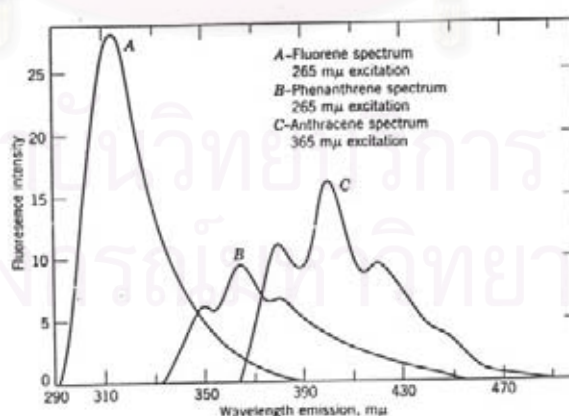


**Figure 2.4** Room-temperature fluorescence spectra of three aromatic hydrocarbons in methanol. From Thommes and Leininger<sup>6</sup>

Note that the three spectra do not overlap completely; it is therefore possible, by careful choice of exciting and emitting wavelengths, to determine each hydrocarbon quantitatively in the presence of the other two. One can often analyze mixtures of two or three aromatic hydrocarbons, without prior separation, by selective choice of excitation and emission wavelengths. Of course, such a procedure will fail if the fluorescence spectra of the various components of the mixture coincide or if certain types of energy transfer occur.

Two major difficulties are encountered in the measurement of the room-temperature fluorescence of aromatic hydrocarbons. First, the fluorescence of many polynuclear aromatic hydrocarbons is extremely sensitive to oxygen quenching; thus, solutions of aromatic hydrocarbons should be carefully purged of oxygen before fluorescence intensities are measured. Second, the fluorescence of solutions of condensed ring aromatic hydrocarbons is often extraordinarily sensitive to the presence of small concentrations of impurities. Therefore, it is necessary to use carefully purified solutes and solvents when investigating the fluorescence properties of aromatic hydrocarbons.

## 2. *Substituted Aromatic Hydrocarbons*

Certain functional groups on an aromatic ring exert definite, predictable influences upon both the energy and intensity of emission. These substituent effects are listed in Table 2-2, and a few of them are discussed briefly below.

สถาบันวิทยบริการ  
จุฬาลงกรณ์มหาวิทยาลัย

**Table 2-2.** Effects of Substituents upon the Fluorescence of Aromatics

Substituent	Effect on frequency	
	of emission	Effect on intensity
Alkyl	None	Very slight increase or decrease
OH, OCH <sub>3</sub> , OC <sub>2</sub> H <sub>5</sub>	Decrease	Increase
CO <sub>2</sub> H	Decrease	Large decrease
NH <sub>2</sub> , NHR, NR <sub>2</sub>	Decrease	Increase
NO <sub>2</sub> , NO	-	Total quenching
CN	None	Increase
SH	Decrease	Decrease
F	Decrease	Decrease
Cl		
Br		
I		
SO <sub>3</sub> H	None	None

a. **Alkyl Groups.** In general, addition of alkyl groups of an aromatic nucleus has little influence upon the energy or intensity of emission, unless steric factors are involved. In a number of aromatic compounds, substitution of methyl or ethyl groups causes substantial increases in the phosphorescence-to-fluorescence intensity ratio.

b. **Halogens.** McClure<sup>7</sup> noted, for halogen-substituted naphthalenes, that as the series F, Cl, Br, I was traversed, the fluorescence diminished in intensity while the phosphorescence efficiency increased. It is generally termed the “intramolecular heavy-atom effect”. Thus, bromo- or iodo-substituted aromatics exhibit intense phosphorescence, but only very weak fluorescence. Furthermore, many iodo-substituted aromatic compounds are subject to

predissociation or photodissociation in liquid solution, rendering the observation of any fluorescence even less probable.

In a study of the mechanism of the heavy-atom effect, it has been indicated that the halogen substituent enhances the spin-orbit coupling mechanism of the aromatic hydrocarbon and, in addition, introduces a new spin-orbit coupling process of its own. The heavy atom need not be a constituent of the emitting molecule in order to manifest this perturbation; a heavy-atom-containing *solvent* will also quench the fluorescence of the solute.

c. **Nitro Groups.** As a general rule, nitro-substituted aromatics may exhibit phosphorescence, but do not fluoresce. It appears that heavy-atom effects and predissociation are both involved in the quenching of fluorescence by nitro groups. Some dyes containing nitro groups, which absorb at very long wavelengths, do emit fluorescence.

d. **Hydroxyl and Amino Groups.** These groups are mainly of interest due to the unusual acid-base dissociation properties of excited organic compounds.

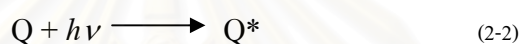
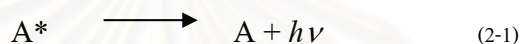
### 3. *Other Heterocyclic Compounds*

Fluorescence and phosphorescence of oxygen, sulfur, and silicon heterocycles is just beginning to be investigated systematically. A number of phenyl-substituted oxazoles have been used in liquid scintillation counting; for example, 2,5-diphenyloxazole is the well-known scintillator, "PPO". Oxygen heterocycles generally do not appear to fluoresce unless the oxygen-containing ring is fused to at least one aromatic ring. The same can be said for sulfur heterocycles. Thiophene does not appear to fluoresce or phosphoresce, but dibenzothiophene and other condensed sulfur heterocycles are known to phosphoresce.<sup>8</sup>

## 2.5. Fluorescence Quenching and Energy Transfer in Organic Compounds

### A. Transfer of Singlet and Triplet Excitation Energy

The transfer of singlet excitation energy from one organic molecule to another is a subject of intense research activity at the present time. The most obvious mechanism by which an excited organic molecule,  $A^*$ , can transfer energy to a ground-state molecule of another species,  $Q$ , is by fluorescence of  $A^*$  followed by absorption of the emitted quantum by  $Q$ :

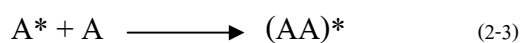


Since this process involves emission and re-absorption of radiant energy, it is commonly called “radiative energy transfer”.

### B. Quenching of Fluorescence in Liquid Solution

Having presented the fundamental aspects of electronic energy transfer in a qualitative fashion. The influence of energy transfer processes upon various subjects of analytical interest. One phenomenon of which the analytical chemist cannot remain unaware is fluorescence quenching. *Quenching* of fluorescence is defined as any process that results in a decrease in the *true* fluorescence efficiency of a molecule; quenching processes divert the absorbed energy into channels other than fluorescence.

Although it is recognized that extraneous organic solutes can quench fluorescence of a given organic compound by means of intermolecular energy transfer, the fact that fluorescence of an organic molecule can also be quenched by other molecules of the same species is less widely appreciated. Particularly if a solute is present in high concentration, an excited organic molecule can form a transient dimer with a ground state molecule of the same species:



The dimeric species  $(AA)^*$  is called an “excimer”. Excimers are capable of characteristic emission; the formation of an excimer which emits and then decomposes after emission, to yield two ground state A molecules, clearly tends to quench the fluorescence of  $A^*$ .

### C. Energy Transfer in Organic Liquid Scintillators

Energy transfer phenomena are of great importance in the action of organic scintillators for the detection of high energy radiation.

In liquid organic scintillators, a solution is prepared which usually contains a single fluorescent solute. The incident energy produces ionization and electronic excitation of solvent molecules. The solvent ions thus produced may decompose, transfer their charge to another solvent molecule, or may be neutralized to yield highly excited singlet or triplet states which then internally convert to lower singlet states. These excited solvent molecules may transfer electronic energy to solute molecules, which then fluoresce. Although the preponderance of excitation processes affect the *solvent*, emission of the *solute* is observed. Clearly, then, high energy transfer efficiencies are necessary for useful scintillation properties.

Energy transfer from solvent to solute should be rapid, efficient, and irreversible. The first important consideration in this regard is the nature of the solvent. For high scintillation efficiency, the solvent must have a large excitation coefficient and must transfer a large fraction of its excitation energy irreversibly to the fluorescent solute. Furst and Kallmann<sup>9</sup> reported that, when the fluorescence of a given solute was tested in different solvents, nearly equal intensities were found under ultraviolet excitation but large differences were observed under high energy irradiation. A proposed scintillation mixture must therefore be tested under high energy irradiation in order to effectively gauge its scintillation efficiency. Most of the “good” scintillation solvents are unsaturated; examples are benzene, toluene, and the xylenes. Dioxane, although saturated, is an effective scintillation solvent. Solvents with “poor” scintillation properties include acetone, chloroform, ethanol, hexane, and diethyl ether.



Unfortunately, many of the “good” scintillation solvents do not dissolve a wide range of materials. If solubility poses a problem, it is often possible to dissolve the solute in a “poor” solvent and then add as much “good” solvent as possible.

The nature of the solute is also important. According to Heller<sup>10</sup>, the most effective scintillation solutes are molecules which do not possess highly rigid structures (for example, terphenyl and diphenyloxazole).

The prospective scintillation solute must exhibit intense fluorescence in a region of the spectrum convenient to measure, such as the visible or near ultraviolet. Of the possible substituents, CH<sub>3</sub>, OCH<sub>3</sub>, F, and Cl do not adversely affect scintillator efficacy, but as expected, NO<sub>2</sub>, Br, and I should be avoided.

#### D. Energy Transfer in Organic Plastic Scintillators

Plastics containing dissolved scintillating chemicals have been used for detection of high energy radiation. While the mode of action of scintillator plastics is not completely understood, it appears that the fluorescence process is initiated principally by excitation of the polymer molecules, which then transfer energy to the fluorescent solute. Since plastics are heterogeneous mixtures of long-chain molecules, it is possible that intramolecular energy transfer can occur along the polymer chain. If the solute molecules can attach themselves in some manner to the polymer chain, the energy may be transferred to the solute, the fluorescence of which will then be observed. In some plastics, the scintillation efficiency depends upon the molecular weight of the polymer; the efficiency increases sharply with molecular weight up to a certain value and then levels off.

#### E. Energy Transfer in Organic Crystal Scintillators

Very pure organic crystals can also be used as scintillators. In general, energy-transfer from the host material to another molecular species present in the crystal is not desirable, and



purity of the crystalline materials thus becomes a crucial factor, due to the very high efficiency of energy transfer in the organic solid state. The most effective scintillating crystals are characterized by large  $\pi$ - electron systems, high molecular symmetry, and the absence of appreciable steric hindrance. Crystalline aromatic hydrocarbons are widely used. The choice of suitable compounds to serve as crystal scintillators is much more limited than for plastic or liquid scintillators.

## 2.6 Single crystal X-ray diffraction

X-ray diffraction from crystalline solids occurs as a result of the interaction of X-rays with the electron charge distribution in the crystal lattice.<sup>11</sup> The pattern of scattered X-rays can be directly recorded, either on photographic film or on a variety of other X-rays sensitive detectors, then the recombination which is impossible physically can be performed mathematically, with the aid of computers. The components of the material which interact with the incident X-rays and scatter them. These are the electrons in the atoms. Concentrations of electron density in the image correspond to atoms, somewhat spread out by time averaged vibration, and the results are usually interpreted and presented as atomic positions. The process of crystal structure determination is simple. Measurement of the diffraction pattern geometry and symmetry tells us the unit cell geometry and gives some information about the symmetry of arrangement of the molecules in the unit cell. Then from the individual intensities of the diffraction pattern, the process of working out the atoms in the unit cell, adding together the individual waves with their correct relative amplitudes and phases. The phase problem was seen because the measured diffraction pattern provides directly only the amplitudes and not the required phases.<sup>12,13</sup>

The diffraction maxima are sometimes individually considered to be the result of diffraction of the incident X-rays beam of wavelength from crystal lattice planes, having

Miller indices  $hkl$  and spacing  $d_{hkl}$ . Diffraction occurs at an angle of incidence equal to the Bragg angle  $\theta_B$ , i.e. Bragg's law is obeyed:

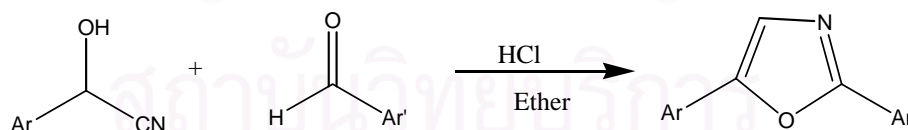
$$\lambda = 2 d_{hkl} \sin \theta_B$$

The intensities of diffraction pattern and the arrangement of atoms in the unit cell of the crystal structure are related to each other by Fourier transformation: the diffraction pattern is the Fourier transform of the electron density, and the electron density is itself the Fourier transform of the diffraction pattern.

## 2.7 Literature Reviews

In general 2,5-diaryloxazoles, such as 2,5-diphenyloxazole, PPO and 1,4-bis(5-phenyloxazol-2-yl)benzene, POPOP, are the most efficient fluorescent compounds which can be used as scintillators.

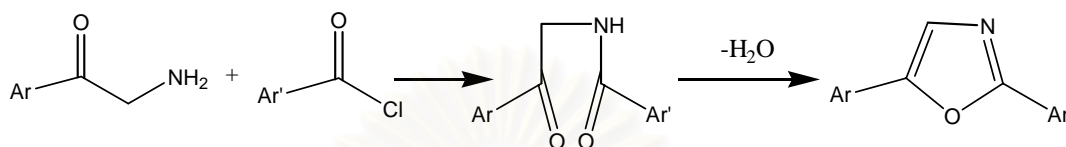
Fischer<sup>14</sup> [1896] studied to synthesize of 2,5-diphenyloxazole that has been prepared using the Fischer synthesis from the one step reaction between aryl cyanohydrin and an aryl aldehyde in ether at 0°C with dried hydrogen chloride.



**Scheme 2.1** Synthesis of 2,5-diphenyloxazole by Fischer synthesis

The reaction always gives the main byproduct as 2,5-diaryl-oxazolid-4-one in high yields. There is also a certain ambiguity in that the starting materials may exchange hydrogen cyanide, thus causing scrambling of the phenyl ring in the product if these bear different substituents. The yield of the oxazole is low.

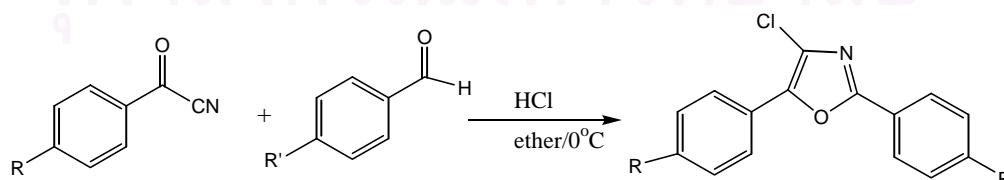
Robinson<sup>15</sup> [1909] studied to synthesize 2,5-diphenyloxazole by using another method, especially POPOP, is condensation of an  $\alpha$ -aminomethyl-arylketone followed by cyclodehydration of the resulting  $\alpha$ -aminomethyl-arylketones. (Robinson-Gabriel synthesis)



**Scheme 2.2** Synthesis of 2,5-diphenyloxazole by Robinson-Gabriel synthesis

Effect the ring closure will use concentrated sulfuric acid or phosphorus pentachloride as dehydrating agent. It was found that the presence of the dehydrating agent leads to the formation of byproducts, which are very difficult to remove. Thus this method is not suitable for the production purity of scintillator grade oxazoles. Another problem with this synthesis is the difficulty of obtaining the starting materials that often require several synthetic steps.

Ternai et al<sup>16</sup> [1977] studied to synthesize 2,5-diaryl-4-chloro(or bromo)oxazoles by modified Fischer synthesis, using an acyl cyanide instead of a cyanohydrin. This method, is known as the Ternai synthesis, used the only one step reaction. It is suitable for the commercial production oxazole based scintillators. Due to the convenience of using stable starting materials, gave the oxazoles in high yields without byproducts and in high purity.



**Scheme 2.3** Synthesis of 4-chloro-2,5-diphenyloxazole by modified Fischer synthesis

Pei et al <sup>17</sup> [1995] reported the synthesis, characterization, and optical properties of three 1,3,4-oxadiazole-containing polymers with different solubility and conjugation length. It was found that 1,3,4-oxadiazole-containing polymer, with an even longer conjugation length, has strong blue fluorescence and can be used this polymer as the electroluminescent layer in LEDs.

Sutherland et al <sup>18</sup> [1997] have synthesized a variety of 4-functionalized-2,5-diphenyloxazoles and evaluated their scintillation efficiencies for use as reporter tags in molecular recognition systems.

Clapham and Sutherland <sup>19</sup> [2000] have developed a series of scintillant containing chemically functionalized polystyrene resin beads for application in combinatorial chemistry.

Diwu et al <sup>20</sup> [2000] investigated the spectral properties and potential biological applications of water-soluble Dapoxyl sulfonic acid (5-(4''-dimethylaminophenyl)-2-(4'-sulfophenyl)oxazole, sodium salt). It can be explored to study a variety of biological events and processes, in addition to its long emission wavelength, large extinction coefficient, high fluorescence quantum yield and large Stokes shift and excellent photostability.

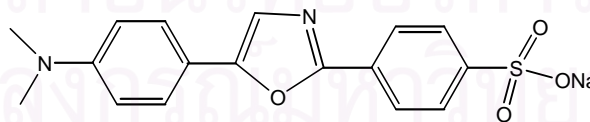


**Figure 2.5** Dapoxyl sulfonic acid (5-(4''-dimethylaminophenyl)-2-(4'-sulfophenyl)oxazole, sodium salt)

Hay et al <sup>21</sup> [2000] studied to synthesis 4-hydroxymethyl-2,5-diphenyloxazole that was reacted with 3-isocyanatopropyltriethoxysilane to form a functionalized silicon alkoxide precursor (3-ICPS-PPO adduct). The sol-gel glasses were found to be highly efficient detectors of  $\beta^-$  radioactivity.

Doroshenko et al <sup>22</sup> [2000] have studied spatially hindered polynuclear aromatic derivatives of oxazole and oxadiazole, namely, *ortho* analogues of POPOP, which is extensively used in liquid and polymeric scintillators.

Megelski et al <sup>23</sup> [2001] have investigated means of fluorescence microscopy, single-crystal imaging, and space filling arguments led to new information about the orientation of dye molecules by observing made on POPOP in the channels of zeolite L crystals.



สถาบันวิทยบริการ  
จุฬาลงกรณ์มหาวิทยาลัย

## CHAPTER III

### EXPERIMENTAL

#### 3.1 Apparatus

NMR spectra were obtained at 200 MHz ( $^1\text{H}$ ) or 50 MHz ( $^{13}\text{C}$ ) on a Bruker AC and Varian Inc., UNITY *INOVA* 500 for 500 MHz ( $^1\text{H}$ ), 125 MHz ( $^{13}\text{C}$ ), COSY, HMQC, and HMBC. Chemical shift ( $\delta$ ) is in ppm using the residual proton or carbon signal in deuterated solvents as internal references and coupling constants ( $J$ ) are in Hz.

Infrared spectra were acquired using a Nicolet Impact 410. Solid samples were prepared by pressing the sample with KBr. Infrared spectra were recorded between  $400\text{ cm}^{-1}$  and  $4000\text{ cm}^{-1}$  in transmittance mode.

Mass spectrometry was determined using FISSONS Instrument Mass spectrometer model Trioto 2000 in EI mode at 70 eV.

Melting points were determined using an Electrothermal 9100 melting point apparatus.

Ultraviolet absorption spectra were run on Cary Eclipse UV-Visible spectrophotometer VARIAN with different concentrations of solutions in 1 cm. path-length quartz cuvettes.

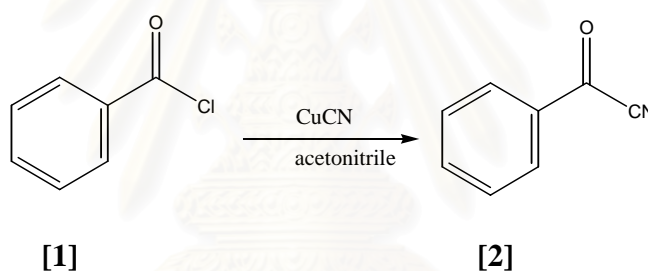
Emission spectra were recorded on Cary Eclipse Fluorescence Spectrophotometer VARIAN with different concentrations of solutions in 1 cm. path-length quartz cuvettes.

Elemental analyses were recorded on CHNS/O Analyzer Perkin Elmer PE2400 Series II).

All reactions were followed by thin layer chromatography (TLC). Tetrahydrofuran and diethyl ether were distilled from Na/benzophenone. Dichloromethane, benzene and acetonitrile were distilled from CaH<sub>2</sub>. Other chemicals were obtained from Aldrich, Fluka or Merck and used as received. Evaporation refers to the rotary evaporation of solvent under aspirator pressure.

### 3.2 Synthesis of starting materials<sup>24,25</sup> and products for studying on the optical property

#### 3.2.1 Preparation of benzoyl cyanide [2]<sup>24</sup>

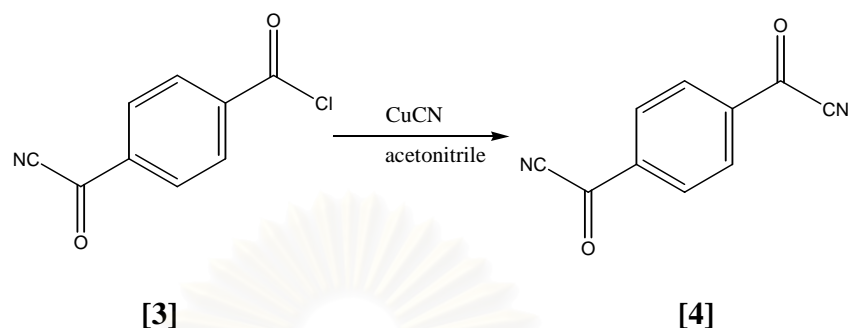


**Scheme 3.1**

The mixture of benzoyl chloride [1] 19 ml (21 g, 150 mmol) and copper cyanide 15.2 g (170 mmol) in dried acetonitrile 150 ml was refluxed for 3 h. The mixture became dark brown. The crude product was evaporated to remove the residue solvent. The solvent free product was dissolved in dried benzene, filtered and evaporated. The yellow brown oil was distilled under reduced pressure to give 16.3 g of [2] as a colorless liquid with 92% yield; IR ( $\nu$ , cm<sup>-1</sup>) 3068 (CH), 2222 (CN), 1685 (C=O); 200 MHz <sup>1</sup>H NMR (CDCl<sub>3</sub>)  $\delta$  7.56 (t, 1H, J = 6 Hz), 7.77 (t, 2H, J = 2 Hz) and 8.10 (d, 2H, J = 2 Hz); 50 MHz <sup>13</sup>C NMR (CDCl<sub>3</sub>)  $\delta$  112.8, 128.5, 129.6, 130.3, 133.3, 136.9 and 167.9.



### 3.2.2 Preparation of terephthaloyl cyanide [4]<sup>25</sup>

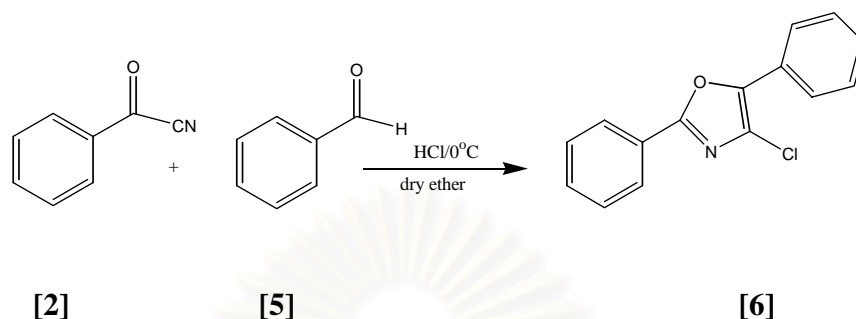


**Scheme 3.2**

In a 500 ml round bottom flask equipped with a reflux condenser and a magnetic stirrer was placed 180 ml of dried acetonitrile and 28.19 g (315 mmol) of copper cyanide. The reaction flask was fitted with drying tube. The suspended mixture was stirred for about 15 min, and then 30.45 g (150 mmol) of terephthaloyl chloride [3] was added slowly to the reaction flask. Gentle reflux overnight, the mixture became dark brown. The crude product was evaporated to remove the residue solvent and was filtered with hot benzene 500 ml. The resulting residue was evaporated and sublimed under reduced pressure to give 10.14 g of [4] as a white crystal with 37% yield, m.p.149.2-149.9 °C (Lit.<sup>25</sup>, 140-143 °C); IR ( $\nu$ ,  $\text{cm}^{-1}$ ) 3092 (CH), 2231 (CN), 1687 (C=O), 1502 and 1411 (C=C); 200 MHz  $^1\text{H}$  NMR (DMSO- $d_6$ )  $\delta$  8.23 (s, 4H, J = 3.5 Hz); 50 MHz  $^{13}\text{C}$  NMR (DMSO- $d_6$ )  $\delta$  113.3, 130.2, 138.1, 166.2 and 188.9.

สถาบันวิทยบริการ  
จุฬาลงกรณ์มหาวิทยาลัย

### 3.2.3 Synthesis of 4-chloro-2,5-diphenyloxazole [6]

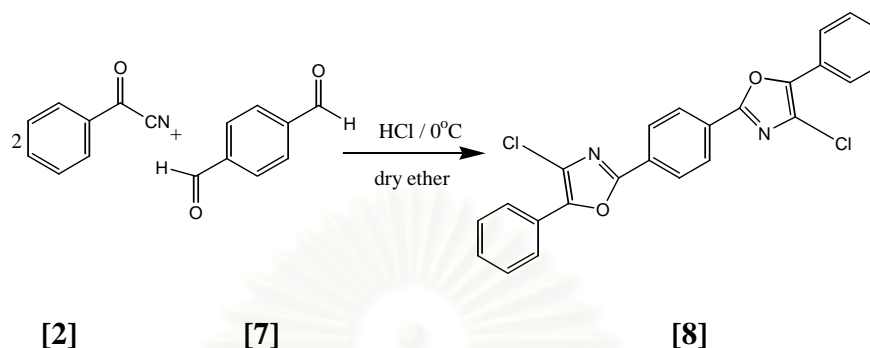


**Scheme 3.3**

Hydrogen chloride was passed into an ice-cooled solution of benzoyl cyanide [2] 1.42 ml (1.57 g, 12 mmol) and benzaldehyde [5] 1 ml (1.06 g, 10 mmol) in 10 ml of dried diethyl ether for 2 h. The reaction mixture was kept at 0°C for 90 h. The mixture was then poured onto crushed ice (300 g) and the precipitate was collected by filtration. Recrystallization from ethanol gave pure white crystal of 4-chloro-2,5-diphenyloxazole [6] 1.70 g with 67% yield, m.p. 70-71°C. The  $R_f$  value was 0.80 when using an aluminum plate as an absorbent and the mixture of 5% ethyl acetate in hexane as the developing solvent. IR ( $\nu$ ,  $\text{cm}^{-1}$ ) 3057 (CH), 1604, 1448 (C=C), 1580 (-NCO), 983 (C-Cl); 500 MHz  $^1\text{H}$  NMR ( $\text{CDCl}_3$ )  $\delta$  8.11-8.08 (m, 2H), 7.95 (d, 2H,  $J = 7$  Hz), 7.51-7.48 (m, 5H) and 7.39 (t, 1H,  $J = 7$  Hz); 125 MHz  $^{13}\text{C}$  NMR ( $\text{CDCl}_3$ )  $\delta$  125.0, 126.4, 126.4, 126.5, 126.9, 128.7, 128.8, 128.9, 130.9, 143.9 and 158.9; MS ( $m/z$ ) 255(100) ( $M^+$ ), 257(34) ( $M+2$ ).

สถาบันวิทยบริการ  
จุฬาลงกรณ์มหาวิทยาลัย

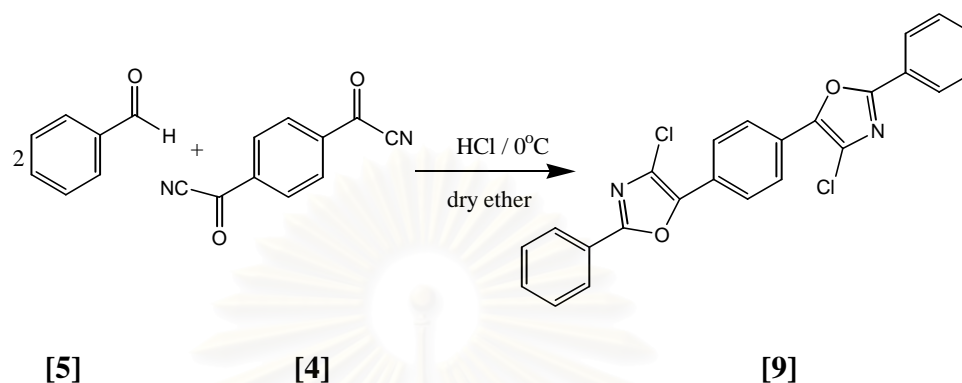
### 3.2.4 Synthesis of 1,4-bis(4-chloro-5-phenyloxazol-2-yl)benzene [8]



**Scheme 3.4**

Terephthalcarboxaldehyde [7] (5.4 g, 40 mmol) was added to a solution of benzoyl cyanide [2] 11.9 ml (13.2 g, 100 mmol) in 100ml of dried diethyl ether. The mixture was cooled to 0°C in an ice-bath for 3 h and saturated with hydrogen chloride. The reaction mixture was kept at 0°C for 7 days and was then poured onto crushed ice (500 g). The yellow solid was recrystallized from ethanol to give [8] 10.2 g with 59% yield, m.p. 249.0-249.4°C. The  $R_f$  value was 0.75 when using an aluminum plate as an absorbent and mixtures of 5% ethyl acetate in hexane as developing solvent. IR ( $\nu$ ,  $\text{cm}^{-1}$ ) 3054 (CH), 1574 (-NCO), 1605, 1445 (C=C) and 985 (C-Cl); 500 MHz  $^1\text{H}$  NMR ( $\text{CDCl}_3$ )  $\delta$  8.19 (s, 4H), 7.96 (d, 4H,  $J = 7$  Hz), 7.50 (t, 4H,  $J = 7$  Hz) and 7.40 (t, 2H,  $J = 7$  Hz); 125 MHz  $^{13}\text{C}$  NMR ( $\text{CDCl}_3$ )  $\delta$  125.2, 126.7, 126.8, 126.8, 128.3, 128.9, 128.9, 144.6 and 158.0; MS ( $m/z$ ) 432 (100) ( $\text{M}^+$ ), 434 (82) ( $\text{M}+2$ ), 436 (10) ( $\text{M}+4$ ); Found C 66.59%, H 3.25%, N 6.49%,  $\text{C}_{24}\text{H}_{14}\text{Cl}_2\text{N}_2\text{O}_2$  requires C 66.53%, H 3.26%, N 6.47%.

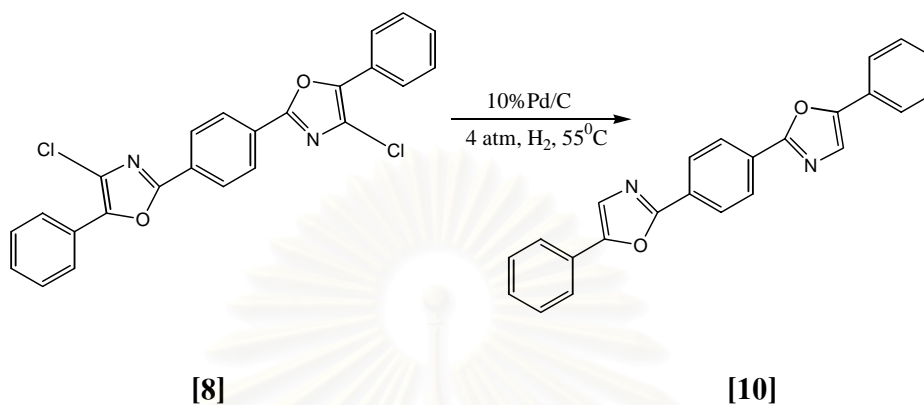
### 3.2.5 Synthesis of 1,4-bis(4-chloro-2-phenyloxazol-5-yl)benzene [9]



**Scheme 3.5**

The mixture of terephthaloyl cyanide [4] (0.92 g, 5 mmol) and benzaldehyde [5] (2.81 ml, 2.65 g, 25 mmol) in 18 ml of dried diethyl ether was saturated with hydrogen chloride and cooled in an ice-bath for 3 h. The reaction mixture was kept at 0°C for 7 days. The yellow mixture was then poured onto crushed ice (300 g) and the precipitate was collected by filtration. Recrystallization from ethanol gave pure yellow compound of 1,4-bis(4-chloro-2-phenyloxazol-5-yl)benzene 0.67 g with 52% yield, m.p. 273.5-275.5°C. The  $R_f$  value was 0.75 when using an aluminum plate as an absorbent and a mixture of 5% ethyl acetate in hexane as developing solvent. IR ( $\nu$ ,  $\text{cm}^{-1}$ ) 3060 (CH), 1587 (-NCO), 1600, 1447 (C=C), 984 (C-Cl); 500 MHz  $^1\text{H}$  NMR ( $\text{CDCl}_3$ )  $\delta$  8.12-8.10 (m, 4H), 8.08 (s, 4H) and 7.53-7.50 (m, 6H); 125 MHz  $^{13}\text{C}$  NMR ( $\text{CDCl}_3$ )  $\delta$  125.2, 126.3, 126.5, 126.8, 127.3, 128.9, 131.2, 143.4 and 159.4; MS ( $m/z$ ) 432 (100) ( $\text{M}^+$ ), 434 (65) ( $\text{M}+2$ ), 436 (10) ( $\text{M}+4$ ); Found C 66.50%, H 3.49%, N 6.39%,  $\text{C}_{24}\text{H}_{14}\text{Cl}_2\text{N}_2\text{O}_2$  requires C 66.53%, H 3.26%, N 6.47%.

### 3.2.6 Reduction<sup>26</sup> of 1,4-bis(5-phenyloxazol-2-yl)benzene [10]

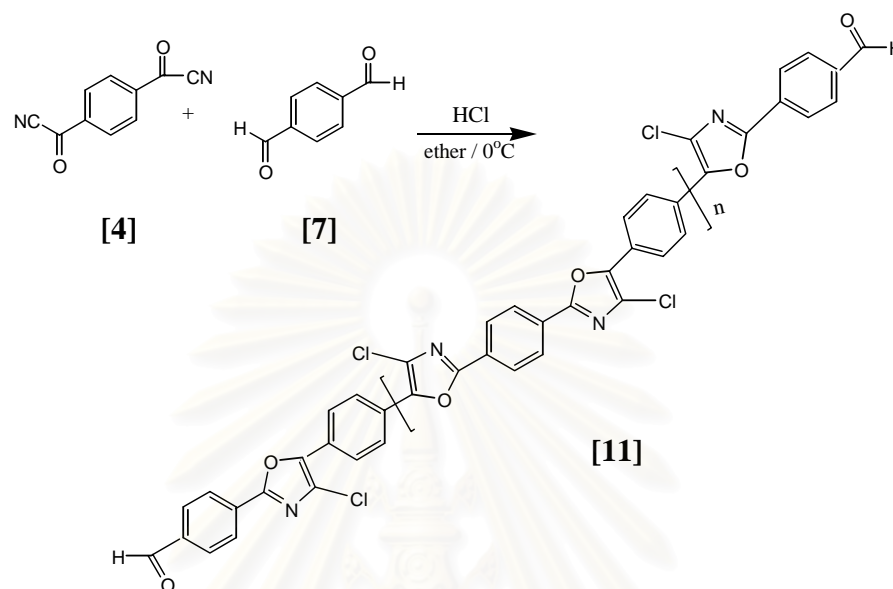


Scheme 3.6

#### 3.2.6.1 The preparation of catalytic Hydrogenation employing 10% Pd/C as catalyst from 1,4-bis(4-chloro-5-phenyloxazol-2-yl)benzene : Isolation of 1,4-bis(5-phenyloxazol-2-yl)benzene

To 1,4-bis(4-chloro-5-phenyloxazol-2-yl)benzene [8] (2.165 g, 5 mmol) dissolved in tetrahydrofuran (80 ml) containing sodium acetate anhydrous (1.1-1.5 equivalents per halogen) (0.6153 g) was added 10% palladium on carbon (10%-equal amount by weight) (0.2165 g). The mixture was shaken in a Parr hydrogenation reactor under 4 atmospheres of hydrogen at 55 °C for 24 h. The catalyst removed by filtration and the tetrahydrofuran was evaporated. The product could be further purified by chromatography on silica gel (25 g) eluting with 5% and 10% ethyl acetate in hexane to give the 10% yield of 1,4-bis(5-phenyloxazol-2-yl)benzene [10], m.p. 242-243°C. IR ( $\nu$ ,  $\text{cm}^{-1}$ ) 3099 (CH), 1486 (C=C), 1584 (-NCO); 200 MHz  $^1\text{H}$  NMR ( $\text{CDCl}_3$ )  $\delta$  8.2 (s, 2H), 7.71 (d, 4H,  $J = 7$  Hz) and 7.51-7.30 (m, 8H); 125 MHz  $^{13}\text{C}$  NMR ( $\text{CDCl}_3$ )  $\delta$  125.0, 123.8, 124.3, 126.6, 127.8, 128.7, 129.0, 151.8 and 160.5.

### 3.2.7 The larger molecules of the oxazole containing compounds [11]



**Scheme 3.7**

Hydrogen chloride was passed into an ice-cooled solution of terephthaloyl cyanide [4] 0.092 g (0.5 mmol) and terephthalaldehyde [7] 0.101 g (0.75 mmol) in 18 ml of dried diethyl ether for 3 h. The reaction mixture was kept at 0°C for 20 days. The mixture was then poured onto crushed ice (200 g) and the precipitate was collected by filtration to give yellow powder 0.0280 g. IR ( $\nu$ ,  $\text{cm}^{-1}$ ) 2857 (ald.), 1720 (C=O ald.), 1610, 1417 (C=C), 1581 (-NCO) and 839 (C-Cl); 200 MHz  $^1\text{H}$  NMR ( $\text{CDCl}_3$ )  $\delta$  10.12 (s, 2H) and 8.28-7.99 (m, 20H).

### 3.3 Optical property

All UV absorption spectra were recorded at wavelengths 250-500 nm at room temperature (25°C) with air-saturated solutions. The fluorescence emission spectra were recorded at wavelengths 300-600 nm at room temperature (25°C) with air-saturated solutions. Plots of all UV absorption and fluorescence emission data are shown in Appendix B and Appendix C.

#### 3.3.1 UV-Absorption analysis

##### 3.3.1.1 UV-Absorption analysis of 4-chloro-2,5-diphenyloxazole.

The UV absorption spectrum of 4-chloro-2,5-diphenyloxazole [6] was recorded in THF solvent at concentrations of  $9.9 \times 10^{-6}$  M,  $10 \times 10^{-6}$  M and  $19.6 \times 10^{-6}$  M. The spectra, as shown in Figure B1, displayed the maximum absorption at 308 nm with an extinction coefficient,  $\epsilon$ , of  $37377 \text{ cm}^{-1}\text{M}^{-1}$  ( $\log \epsilon = 4.57$ ). Based on 4-chloro-2,5-diphenyloxazole was determined in dichloromethane solvent at concentrations of  $9.9 \times 10^{-6}$  M,  $14.8 \times 10^{-6}$  M,  $19.6 \times 10^{-6}$  M,  $24.4 \times 10^{-6}$  M and  $29.1 \times 10^{-6}$  M. The spectra showed the maximum absorption (Figure B2) at 310 nm with an extinction coefficient,  $\epsilon$ , of  $31933 \text{ cm}^{-1}\text{M}^{-1}$  ( $\log \epsilon = 4.50$ ).

##### 3.3.1.2 UV-Absorption analysis of 1,4-bis(4-chloro-5-phenyloxazol-2-yl)benzene.

The UV absorption spectrum of 1,4-bis(4-chloro-5-phenyloxazol-2-yl)benzene [8] was determined in dichloromethane at concentrations of  $3.32 \times 10^{-6}$  M,  $6.62 \times 10^{-6}$  M,  $10 \times 10^{-6}$  M,  $11 \times 10^{-6}$  M and  $13.16 \times 10^{-6}$  M. The spectra showed the maximum absorption (Figure B3) at 369 nm with an extinction coefficient,  $\epsilon$ , of  $60578 \text{ cm}^{-1}\text{M}^{-1}$  ( $\log \epsilon = 4.78$ ), THF solvent at concentrations of



$4.98 \times 10^{-6}$  M,  $7.89 \times 10^{-6}$  M,  $9.09 \times 10^{-6}$  M and  $10.7 \times 10^{-6}$  M. The spectra displayed the maximum absorption (Figure B12) at 368 nm with an extinction coefficient,  $\epsilon$ , of  $74514 \text{ cm}^{-1}\text{M}^{-1}$  ( $\log \epsilon = 4.87$ ), and *n*-butanol at concentrations of  $9.9 \times 10^{-6}$  M,  $10 \times 10^{-6}$  M,  $19.6 \times 10^{-6}$  M and  $24.4 \times 10^{-6}$  M, the spectra showed the maximum absorption (Figure B4) at 368 nm with an extinction coefficient,  $\epsilon$ , of  $38595 \text{ cm}^{-1}\text{M}^{-1}$  ( $\log \epsilon = 4.59$ ).

### 3.3.1.3 UV-Absorption analysis of 1,4-bis(4-chloro-2-phenyloxazol-5-yl)benzene.

The UV absorption spectrum of 1,4-bis(4-chloro-2-phenyloxazol-5-yl)benzene [9] was determined in dichloromethane at concentrations of  $3.3 \times 10^{-6}$  M,  $6.62 \times 10^{-6}$  M,  $10 \times 10^{-6}$  M and  $13.16 \times 10^{-6}$  M. The spectra showed the maximum absorption (Figure B5) at 363 nm with an extinction coefficient,  $\epsilon$ , of  $41852 \text{ cm}^{-1}\text{M}^{-1}$  ( $\log \epsilon = 4.62$ ), THF at concentrations of  $4.98 \times 10^{-6}$  M,  $7.89 \times 10^{-6}$  M,  $9.09 \times 10^{-6}$  M and  $10.7 \times 10^{-6}$  M. The spectra displayed the maximum absorption (Figure B13) at 363 nm with an extinction coefficient,  $\epsilon$ , of  $79082 \text{ cm}^{-1}\text{M}^{-1}$  ( $\log \epsilon = 4.90$ ), and *n*-butanol at concentrations of  $9.9 \times 10^{-6}$  M,  $19.6 \times 10^{-6}$  M,  $24.4 \times 10^{-6}$  M,  $29.1 \times 10^{-6}$  M,  $33.8 \times 10^{-6}$  M and  $38.5 \times 10^{-6}$  M. The spectra showed the maximum absorption (Figure B6) at 362 nm with an extinction coefficient,  $\epsilon$ , of  $22849 \text{ cm}^{-1}\text{M}^{-1}$  ( $\log \epsilon = 4.36$ ).

### 3.3.1.4 UV-Absorption analysis of 2,5-diphenyloxazole.

The UV absorption spectrum of 2,5-diphenyloxazole was recorded in THF solvent at concentrations of  $9.9 \times 10^{-6}$  M,  $14.8 \times 10^{-6}$  M and  $16.6 \times 10^{-6}$  M. The spectra, as shown in Figure B7, displayed the maximum absorption at 305 nm with an extinction coefficient,  $\epsilon$ , of  $49483 \text{ cm}^{-1}\text{M}^{-1}$  ( $\log \epsilon = 4.69$ ). Based on 4-chloro-2,5-diphenyloxazole was determined in dichloromethane at concentrations of  $9.9 \times 10^{-6}$  M,  $14.8 \times 10^{-6}$  M,  $19.6 \times 10^{-6}$  M,  $24.4 \times 10^{-6}$  M, the spectra showed the

maximum absorption (Figure B8) at 306 nm with an extinction coefficient,  $\epsilon$ , of  $41421 \text{ cm}^{-1}\text{M}^{-1}$  ( $\log \epsilon = 4.62$ ).

### 3.3.1.5 UV-Absorption analysis of 1,4-bis(5-phenyloxazol-2-yl)benzene.

The UV absorption spectrum of 1,4-bis(5-phenyloxazol-2-yl)benzene [10] was determined in dichloromethane at concentrations of  $4.98 \times 10^{-6} \text{ M}$ ,  $9.9 \times 10^{-6} \text{ M}$ ,  $10 \times 10^{-6} \text{ M}$ ,  $10.7 \times 10^{-6} \text{ M}$ . The spectra showed the maximum absorption (Figure B9) at 361 nm with an extinction coefficient,  $\epsilon$ , of  $70654 \text{ cm}^{-1}\text{M}^{-1}$  ( $\log \epsilon = 4.85$ ). In THF at concentrations of  $4.98 \times 10^{-6} \text{ M}$ ,  $7.89 \times 10^{-6} \text{ M}$ ,  $9.09 \times 10^{-6} \text{ M}$ ,  $9.9 \times 10^{-6} \text{ M}$  and  $10.7 \times 10^{-6} \text{ M}$ , the spectra displayed the maximum absorption (Figure B11) at 361 nm with an extinction coefficient,  $\epsilon$ , of  $72232 \text{ cm}^{-1}\text{M}^{-1}$  ( $\log \epsilon = 4.86$ ), and in *n*-butanol at concentrations of  $4.98 \times 10^{-6} \text{ M}$ ,  $9.9 \times 10^{-6} \text{ M}$ ,  $14.8 \times 10^{-6} \text{ M}$ ,  $19.6 \times 10^{-6} \text{ M}$  and  $24.4 \times 10^{-6} \text{ M}$ . The spectra showed the maximum absorption (Figure B10) at 361 nm with an extinction coefficient,  $\epsilon$ , of  $32561 \text{ cm}^{-1}\text{M}^{-1}$  ( $\log \epsilon = 4.51$ ).

### 3.3.2 Fluorescence analysis

#### **General Experimental Considerations<sup>27</sup>:**

Standard samples. The standard samples should be chosen to ensure that they absorb at the excitation wavelength of choice for the test sample, and, if possible, emit in a similar region to test sample. The standard sample must be well characterized and suitable for such use.

Cuvettes. Standard 10 mm path length fluorescence cuvettes are sufficient for running the fluorescence measurements. In order to minimize errors in calculating the absorbance of each solution, it is advisable to use absorption cuvettes with extended path lengths.

Sample preparation. It is vital that all glassware be kept scrupulously clean, and solvents must be of spectroscopic grade and checked for background fluorescence.

#### **Procedure:**

1. Record the UV-vis absorption spectrum of the solvent background for the chosen sample. Note down the absorbance at the excitation wavelength to be used.
2. Record the fluorescence spectrum of the same solution in the 10 mm fluorescence cuvette. Calculate and note down the integrated fluorescence intensity from the fully corrected fluorescence spectrum.
3. Repeat steps 1 and 2 for five solutions with increasing concentrations of the chosen sample.
4. Plot a graph of integrated fluorescence intensity *vs* absorbance. The result should be a straight line with gradient  $m$ , and intercept = 0.
5. Repeat steps 1 to 4 for the remaining samples.

### Calculation of Fluorescence Quantum Yields from Acquired Data:

The gradients of the graphs obtained in 4. above are proportional to the quantum yield of the different samples. Absolute values are calculated using the standard samples which have a fixed and known fluorescence quantum yield value, according to the following equation:

$$\phi_x = \phi_{ST} \frac{(Grad_x)(\eta_x^2)}{(Grad_{ST})(\eta_{ST}^2)}$$

Where the subscripts ST and X denote standard and test respectively,  $\phi$  is the fluorescence quantum yield, *Grad* is the gradient from the plot of integrated fluorescence intensity vs absorbance, and  $\eta$  is the refractive index of the solvent.

#### 3.3.2.1 Fluorescence analysis of anthracene. (The reference standard)

The fluorescence quantum yields were determined using anthracene in ethanol as the reference standard. ( $\phi_f=0.27$ )<sup>28</sup>. The fluorescence emission spectra of the reference standard were recorded at excitation wavelength 356 nm. (Figure C1)

#### 3.3.2.2 Fluorescence analysis of 4-chloro-2,5-diphenyloxazole.

The 4-chloro-2,5-diphenyloxazole solutions were prepared by diluting the stock solution. The solutions in dichloromethane solvent and in THF solvent respectively (Figures C2, C3) were analyzed by fluorescence emission spectroscopy at the excitation wavelength of 300 nm using air saturated solutions. Fluorescence spectra of these solutions were recorded at an excitation wavelength of 372 nm and 369 nm respectively using air-saturated solution.

### 3.3.2.3 Fluorescence analysis of 2,5-diphenyloxazole.

The 2,5-diphenyloxazole in dichloromethane solvent and in THF solvent was prepared by diluting the stock solution, which were analyzed by fluorescence emission spectroscopy at the excitation wavelength of 300 nm. Emission spectra of these solutions were recorded at an excitation wavelength of 363 nm and 362 nm respectively (Figures C8, C9).

### 3.3.2.4 Fluorescence analysis of 1,4-bis(4-chloro-5-phenyloxazol-2-yl)benzene.

The 1,4-bis(4-chloro-5-phenyloxazol-2-yl)benzene in dichloromethane solvent, in THF solvent and in *n*-butanol solvent were prepared by diluting the stock solution which were analyzed by fluorescence emission spectroscopy at the excitation wavelength of 300 nm. Emission spectra of these solutions were recorded at an excitation wavelength of 427 nm, 425 nm and 423 nm respectively (Figures C4, C13 and C5).

### 3.3.2.5 Fluorescence analysis of 1,4-bis(4-chloro-2-phenyloxazol-5-yl)benzene.

The 1,4-bis(4-chloro-2-phenyloxazol-5-yl)benzene in dichloromethane solvent in THF solvent and in *n*-butanol solvent was prepared by diluting the stock solution which were analyzed by fluorescence emission spectroscopy at the excitation wavelength of 300 nm. Emission spectra of these solutions were recorded at an excitation wavelength of 416 nm, 417 nm and 415 nm respectively (Figures C6, C14 and C7).

### 3.3.2.6 Fluorescence analysis of 1,4-bis(5-phenyloxazol-2-yl)benzene.

The 1,4-bis(5-phenyloxazol-2-yl)benzene in dichloromethane solvent, in THF solvent and in *n*-butanol solvent were prepared by diluting the stock solution which were analyzed by fluorescence emission spectroscopy at the excitation wavelength of 300 nm. Emission spectra of these solutions were recorded at an excitation wavelength of 418 nm, 417 nm and 418 nm respectively (Figures C10, C12 and C11).



## CHAPTER IV

### RESULTS AND DISCUSSION

#### **Part I : Synthesis**

In this research, the synthesis of new oxazole containing compounds was described using a modified Fischer synthesis. It involved only one step and the products could be separated and easily purified. Although 4-chloro-2,5-diphenyloxazole had been synthesized by the other research groups<sup>16, 18</sup>, not much detail has been reported.

#### **4.1 Preparation of Starting Materials**

As mentioned in chapter 2, the formation of 4-chloro-2,5-diphenyloxazole or 4-chloro-PPO occurred *via* the cyclization of the aromatic aldehyde and benzoyl cyanide.

##### **4.1.1 Preparation of benzoyl cyanide**

The preparation of benzoyl cyanide was synthesized from benzoyl chloride and copper cyanide, which was refluxed for 3 h in acetonitrile. The yellow brown oil was distilled under reduced pressure to give 18 ml of a colorless liquid with 92% yield. IR and NMR data clearly characterized the structure of benzoyl cyanide. Table 4-1 shows the red shift of the carbonyl absorption from 1771  $\text{cm}^{-1}$  of benzoyl chloride to 1685  $\text{cm}^{-1}$  of benzoyl cyanide. While the disappearance of C-Cl at 875  $\text{cm}^{-1}$  absorption in concomitant with the appearance of  $\text{C}\equiv\text{N}$  absorption of 2222  $\text{cm}^{-1}$  were observed (Figures A1 and A4).



**Table 4-1.** Interpretation of IR spectra of benzoyl chloride and benzoyl cyanide

Compound	wavenumber (cm <sup>-1</sup> )			
	$\nu(\text{C-H})$	$\nu(\text{C=O})$	$\nu(\text{C}\equiv\text{N})$	$\nu(\text{C-Cl})$
benzoyl chloride	3069	1771	-	875
benzoyl cyanide	3068	1685	2222	-

The 200 MHz <sup>1</sup>H NMR spectrum (Figure A5) of benzoyl cyanide in chloroform-*d* exhibited the characteristics of aromatic protons as a 1H triplet (J = 6 Hz) at  $\delta$  7.56 ppm, a 2H triplet (J = 2 Hz) at  $\delta$  7.77 ppm and a 2H doublet (J = 2 Hz) at  $\delta$  8.10 ppm.

The 50 MHz <sup>13</sup>C NMR spectrum of benzoyl cyanide in chloroform-*d* (Figure A6) showed the chemical shift of cyano carbon at 112.8 ppm.<sup>24</sup>

#### 4.1.2 Preparation of terephthaloyl cyanide

The mixture of terephthaloyl chloride and copper cyanide was refluxed for 24 h in acetonitrile. The resulting residue after solvent removal was sublimed under reduced pressure to give 10.14 g of a white crystal with 37% yield, m.p. 149.2-149.9 °C

IR and NMR data clearly confirmed the structure of terephthaloyl cyanide as follows:

In Table 4-2, the IR spectra (KBr) of terephthaloyl cyanide (Figure A10) and terephthaloyl chloride (Figure A7) is compared. There was the new absorption peak at 2231 cm<sup>-1</sup> indicating the C $\equiv$ N stretching of terephthaloyl cyanide.

**Table 4-2.** Interpretation of IR spectra of terephthaloyl chloride and terephthaloyl cyanide

Compound	wavenumber (cm <sup>-1</sup> )			
	$\nu(\text{C-H})$	$\nu(\text{C=O})$	$\nu(\text{C}\equiv\text{N})$	$\nu(\text{C-Cl})$
terephthaloyl chloride	3099	1727	-	853
terephthaloyl cyanide	3092	1687	2231	-

The 200 MHz <sup>1</sup>H NMR spectrum (Figure A11) of terephthaloyl cyanide in DMSO indicated the characteristic of aromatic protons as a singlet at 8.23 ppm (4H).

The 50 MHz <sup>13</sup>C NMR spectra of terephthaloyl cyanide (Figure A12) and terephthaloyl chloride (Figure A9) were compared. The chemical shift of carbon at 113.3 ppm assigned to the carbon of C≡N.

#### 4.2 Synthesis of 4-chloro-2,5-diphenyloxazole

4-Chloro-2,5-diphenyloxazole was prepared by one step reaction. The synthetic route started from the preparation of benzoyl cyanide and then reacting with benzaldehyde. The product was recrystallized from ethanol to give 67% yield of pure white crystals.

IR, NMR and mass spectrometry supported the structure of this compound as follows:

The IR spectrum (KBr) (Figure A13) showed the absorption bands at 3057, 1604, 1448 and 983 cm<sup>-1</sup> corresponding to C-H aromatic stretching, C=C aromatic

stretching and C-Cl stretching, respectively. The absorption band at  $1580\text{ cm}^{-1}$  is the characteristic of the -NCO ring of oxazole.

The 500 MHz  $^1\text{H}$  NMR spectrum of this compound (Figure D1) indicated a 2H multiplet at  $\delta$  8.11-8.08 ppm corresponding to the aromatic protons at positions 2'' and 6'' of benzene ring, a 2H doublet ( $J = 7\text{ Hz}$ ) at  $\delta$  7.95 ppm corresponding to the aromatic protons at positions 2' and 6' of benzene ring, a 5H multiplet at  $\delta$  7.51-7.48 belonging to the aromatic protons at positions 3'', 4'', 5'', 3' and 5' of benzene ring, and a 1H triplet ( $J = 7.5\text{ Hz}$ ) at  $\delta$  7.39 ppm belonging to the aromatic proton at position 4' of benzene ring (Figure 4.1).

In addition, the  $^1\text{H}$ - $^1\text{H}$  COSY spectrum (Figure D3) supplied the informative data to prove the actual structure of this compound.

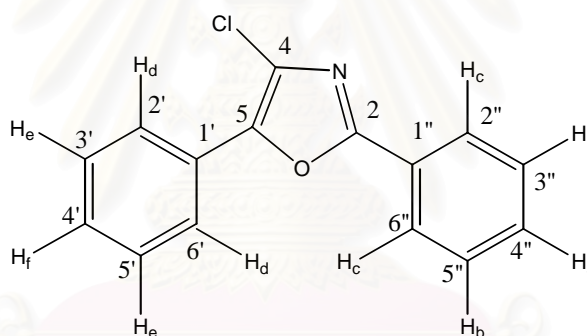


**Figure 4.1** Chemical structure of 4-chloro-2,5-diphenyloxazole with atomic numbering.

The 125 MHz  $^{13}\text{C}$  NMR spectrum of 4-chloro-2,5-diphenyloxazole (Figure D2) could be achieved by comparing with that of PPO. Firstly, the carbons of the oxazole ring in PPO could be assigned by using the phenyl group substitute effect on the C-2 and C-5 of oxazole itself.<sup>28</sup> The calculated chemical shift positions of C-2 and C-5 are 158.9 and 143.9 ppm, respectively. Moreover, the chemical shifts of each carbon of 4-chloro-2,5-diphenyloxazole was calculated comparing with Chem Draw program

(Table 4.3). It was shown that the chemical shifts from  $^{13}\text{C}$  NMR measurement and calculated were similar.

**Table 4-3.** 125 MHz  $^{13}\text{C}$  NMR chemical shifts of 4-chloro-2,5-diphenyloxazole

Position	*Calculated	Found
2	150.6	158.98
4	125.4	126.91
5	138.1	143.92
1'	136.5	126.45
2'	127.0	125.01
3'	129.0	128.83
4'	128.5	128.66
5'	129.0	128.83
6'	127.0	125.01
1''	136.5	126.40
2''	127.0	126.35
3''	129.0	128.85
4''	128.5	130.97
5''	129.0	128.85
6''	127.0	126.35

\*Calculated by Chem Draw program

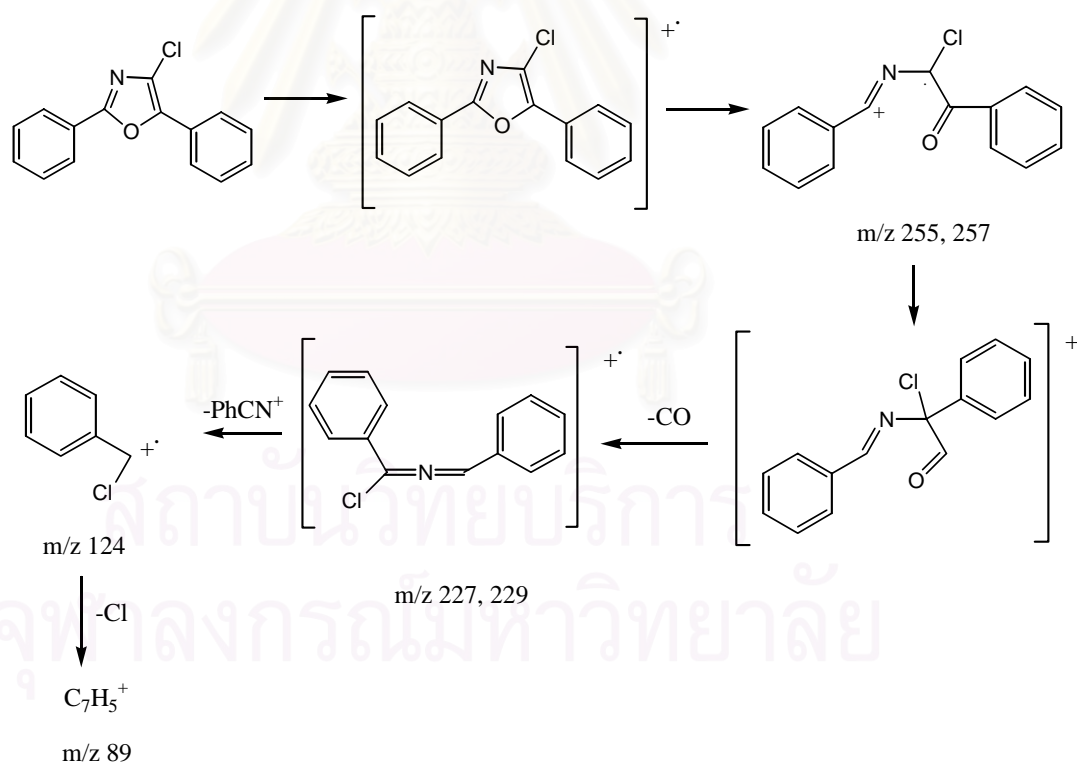
The  $^{13}\text{C}$  NMR spectra (Figure D2) showed the five peaks signals of quaternary carbon at  $\delta$  158.98, 143.92, 126.91, 126.45 and 126.40 ppm. Furthermore, the gHMQC spectra (Figure D4) and the gHMBC spectra (Figure D5) can be confirmed the structure of this compound. In Figure 4.1,  $H_a$  showed the correlation with C-2', C-6'

that the  $H_a$  displayed the long-range-coupling with  $H_e$ ,  $H_f$  of C-3', C-5' and C-4', respectively. In addition,  $H_c$  showed the correlation with C-2'', C-6'' which this proton displayed the correlation with  $H_a$  of C-4'' at  $\delta$  130.97 ppm.

The mass spectrum of this compound indicated the molecular ions at  $m/z$  255(100) and 257(34) in Table 4-4. It clearly confirmed the structure of molecule. The characteristic pattern of the peak was presented that it had a chlorine atom due to the  $M+2$  peak was about a third as large as the  $M+$  peak.

**Table 4-4.** Mass spectroscopic data of 4-chloro-2,5-diphenyloxazole (Figure A16)

Compound	$m/z$
4-chloro-2,5-diphenyloxazole	255(100), 257(34), 227(18), 192(25), 165(30), 124(10), 105(34), 89(50), 77(75)

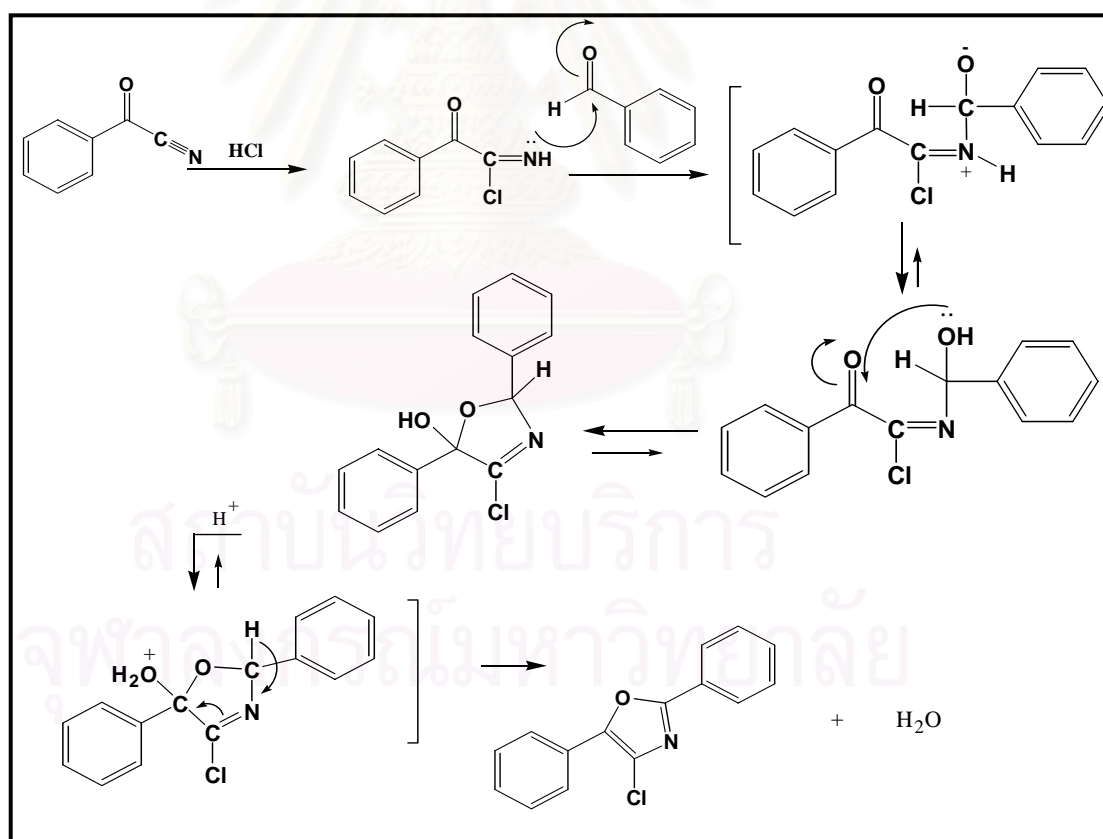


**Scheme 4.1** The fragmentation pathway of 4-chloro-2,5-diphenyloxazole

In Scheme 4.1, it showed the fragmentation pattern. The majority of oxazoles fragmentaria followed the main ring-cleavage fragmentation pattern of unsubstituted oxazole: radical cation formation, cleavage of the O-C<sub>2</sub> bond, and loss of CO, followed by loss of HCN or nitrile.<sup>30</sup>

According to the spectroscopic data, it could be concluded that the product was 4-chloro-2,5-diphenyloxazole.

The method of Ternai has been prepared using modified Fischer synthesis from the one step reaction but they did not supply very much detail. Therefore, in this study, the mechanism (Scheme 4.2) of the 4-chloro-oxazole formation is proposed. First, the addition of HCl onto the cyano group gave acylimidoyl chloride. Then, acylimidoyl chloride promptly attacked the aldehyde carbonyl carbon and reaction proceeded by the cyclization by losing water.



**Scheme 4.2** Proposed mechanism of 4-chloro-oxazole formation

However, the proposed mechanism of 4-chloro-oxazole formation is a reason for using synthesis 4-chloro-oxazolic derivatives of POPOP that terephthaloylcarboxaldehyde was used instead of benzaldehyde by reacting with benzoyl cyanide or terephthaloyl cyanide was used instead of benzoyl cyanide by reacting with benzaldehyde. While this method is shorter, it is obviously more convenient than previous report, which required several steps.<sup>31</sup>

### 4.3 Synthesis of 1,4-bis(4-chloro-5-phenyloxazol-2-yl)benzene

1,4-Bis(4-chloro-5-phenyloxazol-2-yl)benzene was prepared by using benzoyl cyanide and terephthaloylcarboxaldehyde which was used instead of benzaldehyde. When the reaction was allowed to occur for 3 days, it was observed that the product was formed as a pale yellow powder. However, TLC showed that this powder was a mixture consisting of two compounds, terephthaloylcarboxaldehyde and the new compound, compound A. Therefore, the mixture was separated by column chromatography with 5% ethyl acetate in hexane. Compound A was obtained as slightly green crystal with m.p. 142-144°C.

The IR spectrum (KBr) of compound A (Figure A31) exhibits the absorption bands at 3061, 1580, 1608, 1447 and 987  $\text{cm}^{-1}$  corresponding to C-H aromatic stretching, -NCO ring, C=C aromatic stretching and C-Cl stretching. It obviously indicated that it was an oxazole compound. Interestingly, the sharp absorption band at 2737  $\text{cm}^{-1}$  and the strong absorption at 1706  $\text{cm}^{-1}$  appear clearly in the spectrum. This absorption is the characteristic of the aldehyde. It is possible that the cyclization occurs with only one aldehydic group and thus the other one was left.  $^1\text{H}$  NMR and  $^{13}\text{C}$  NMR spectroscopy also confirmed this conclusion.



The 200 MHz  $^1\text{H}$  NMR spectrum of this compound (Figure A32) indicated a 1H singlet at  $\delta$  10.07, a 2H doublet ( $J = 7.3$  Hz) at  $\delta$  8.26, a 4H triplet ( $J = 7.3$  Hz) at  $\delta$  7.98, and a 3H multiplet at  $\delta$  7.53-7.36.

The chemical shifts of each carbon of this compound (Figure A33) were calculated using  $^{13}\text{C}$  NMR Chem Draw program (Table 4-5). It was shown that the chemical shifts from  $^{13}\text{C}$  NMR measurement and calculated were similar.



สถาบันวิทยบริการ  
จุฬาลงกรณ์มหาวิทยาลัย

**Table 4-5.** 50 MHz  $^{13}\text{C}$  NMR chemical shifts of compound A

Position	*Calculated	Found
2	150.6	157.59
4	125.4	125.25
5	138.1	137.54
1'	136.5	130.21
2'	127.0	126.50
3'	129.0	128.96
4'	128.5	127.03
5'	129.0	128.96
6'	127.0	126.50
1''	142.3	145.14
2''	127.5	126.77
3''	130.2	129.19
4''	136.7	131.33
5''	130.2	129.19
6''	127.5	126.77
7''	190.0	191.35

\*Calculated by Chem Draw program

สถาบันวิทยบริการ  
จุฬาลงกรณ์มหาวิทยาลัย

Accordingly, the structure of compound A was assigned as 4-(4-chloro-5-phenyloxazol-2-yl)-benzaldehyde (Figure 4.2).

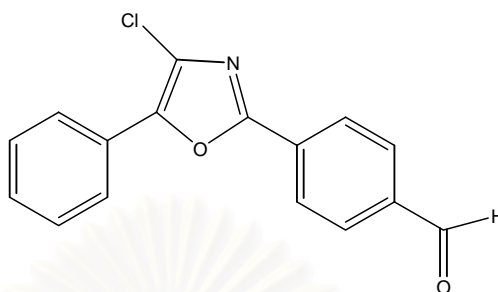
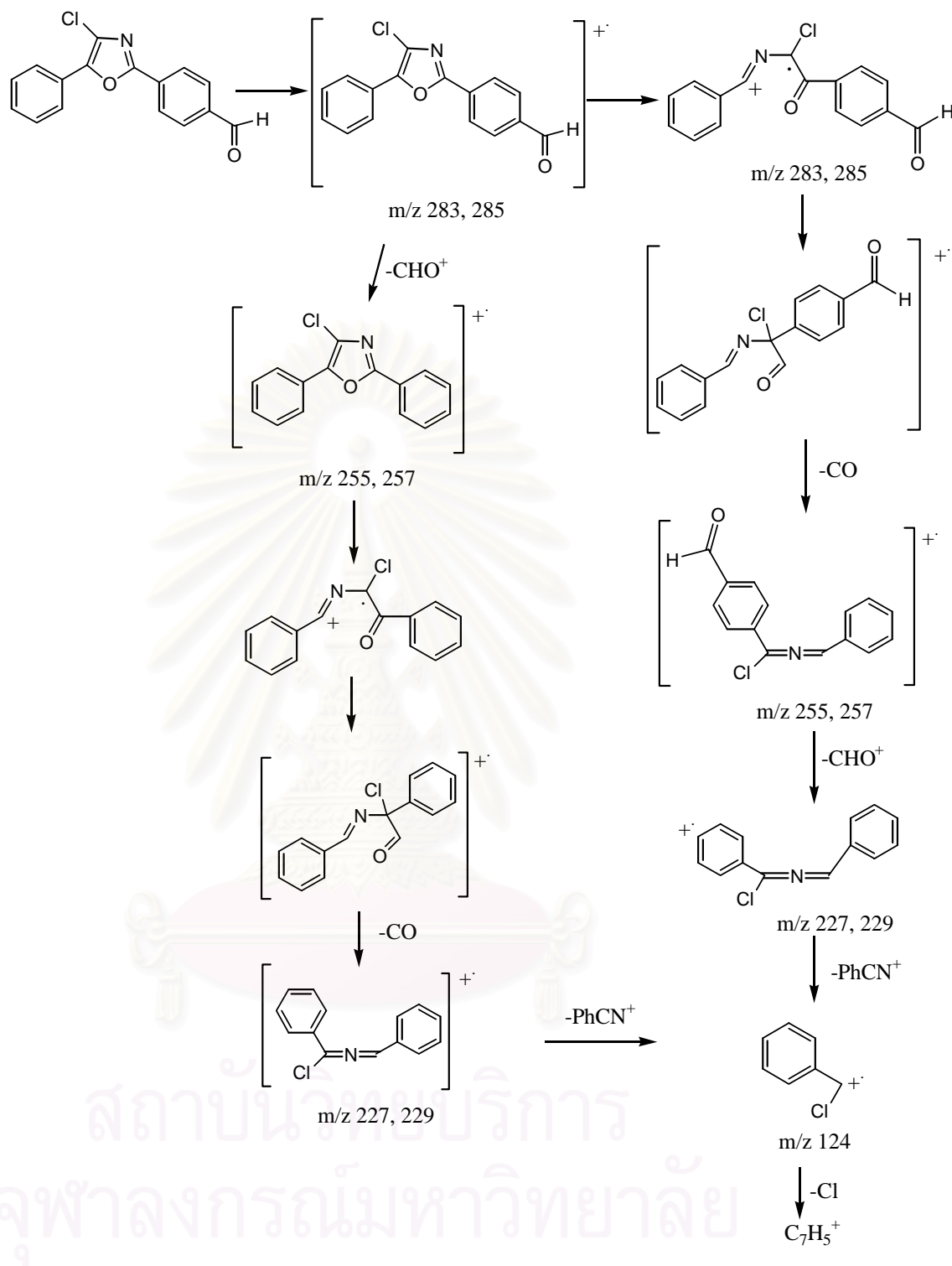


**Figure 4.2** The structure of 4-(4-chloro-5-phenyloxazol-2-yl)-benzaldehyde

**Table 4-6.** Mass spectroscopic data of 4-(4-chloro-5-phenyloxazol-2-yl)-benzaldehyde (Figure A34)

Compound	m/z
4-(4-chloro-5-phenyloxazol-2-yl)-benzaldehyde	283(100), 285(34), 255(10), 226(10), 192(10), 165(25), 124(8), 105(25), 89(15), 77(28)

The mass spectrum of this compound (Figure A34) indicated the molecular ions in Table 4-6 at m/z 283(100) and 285(34), 255(8) and 257(5) due to the fragments as shown in Scheme 4.3. These fragments appeared as a pair of the peaks with the intensity ratio of 3:1 that was the characteristic of the compound consisting of chlorine. It clearly confirmed the structure of molecule. The characteristic pattern of the peak was presented that it had a chlorine atom due to the M+2 peak was about a third as large as the M+ peak.



**Scheme 4.3** The fragmentation pathways of 4-(4-chloro-5-phenyloxazol-2-yl)-benzaldehyde

The mass spectrum thus assured that compound A was 4-(4-chloro-5-phenyloxazol-2-yl)-benzaldehyde. In order to obtain 1,4-bis(4-chloro-5-phenyloxazol-2-yl)benzene, compound B (Figure 4.3) the cyclization at the other aldehydic group must be taken place.

Apparently, the synthesis of 1,4-bis(4-chloro-5-phenyloxazol-2-yl)benzene, compound B requires a longer reaction time than 3 days. It was found that at least 7 days of the reaction was needed. The reaction gave a pale yellow of this product with 59% yield, m.p. 249-249.4 °C.

The IR spectrum (KBr) of this product (Figure A17) shows 3054, 1445, 1605, 1574 and 985  $\text{cm}^{-1}$  which are corresponding to C-H aromatic stretching, C=C aromatic stretching -NCO-ring and C-Cl stretching. The IR data conformed very well with the proposed structure of compound B.

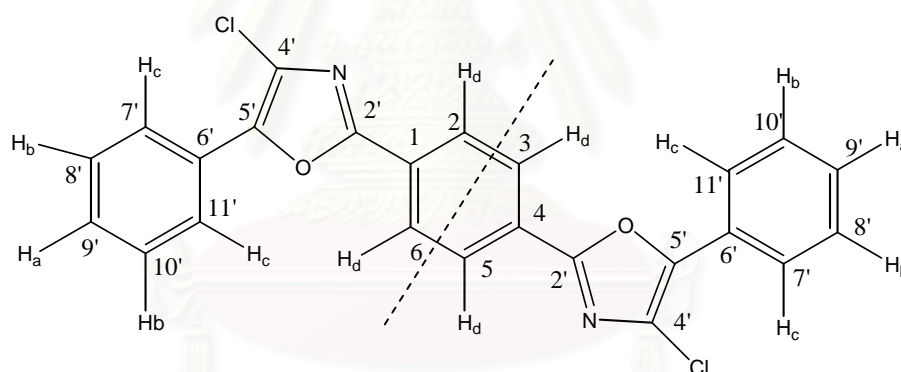


**Figure 4.3** Chemical structure of 1,4-bis(4-chloro-5-phenyloxazol-2-yl)benzene with atomic numbering.

The 500 MHz  $^1\text{H}$  NMR spectrum ( $\text{CDCl}_3$ ) of this product (Figure D6) exhibited the 4H singlet at  $\delta$  8.19 ppm corresponding to the aromatic protons at the positions 2, 3, 5 and 6 of the middle benzene ring (Figure 4.3), a 4H doublet ( $J = 7$  Hz) at  $\delta$  7.96 ppm

belonging to the aromatic protons at positions 7' and 11' of both terminal benzene rings, a 4H triplet ( $J = 7$  Hz) at  $\delta$  7.50 ppm belonging to the aromatic at positions 8' and 10' of both terminal benzene rings and a 2H triplet ( $J = 7$  Hz) at 7.40 ppm belonging to the aromatic at positions 9' of both terminal benzene rings (Table 4.7). This assignment was confirmed by the  $^1\text{H}$ - $^1\text{H}$  COSY spectra (Figure D8).

The 125 MHz  $^{13}\text{C}$  NMR spectroscopy (Figure D7) also identified this product to be 1,4-bis(4-chloro-5-phenyloxazol-2-yl)benzene. The  $^{13}\text{C}$  NMR assignments of this product are shown in Table 4-7.

The 125 MHz  $^{13}\text{C}$  NMR spectra (Figure D7) showed five signals of quaternary carbons at  $\delta$ 158.00, 144.61, 128.25, 126.81 and 126.66 ppm. While the HMQC and HMBC in Figures D9 and D10, respectively, also revealed the signals, which could be assigned as follows: the signal of  $\text{H}_d$  at  $\delta$  8.19 ppm correlated with C-2, C-3, C-5, C-6 at  $\delta$  126.76 ppm. This proton signal displayed the long-range- coupling with C-2' at  $\delta$  158.00 ppm. Meanwhile the signal of  $\text{H}_c$  was correlated with C-7', C-11' at  $\delta$  125.15 ppm and exhibited the long-range-coupling with C-5' and C-9' at  $\delta$  144.61 ppm and  $\delta$  128.96 ppm, respectively.

**Table 4-7.** NMR chemical shifts of 1,4-bis(4-chloro-5-phenyloxazol-2-yl)benzene

Position	<sup>1</sup> H NMR (ppm)		<sup>13</sup> C NMR (ppm)	
	*Calculated	Found	*Calculated	Found
1	-	-	136.5	126.66
2	7.54	8.19 (1H, s)	127.5	126.76
3	7.54	8.19 (1H, s)	127.5	126.76
4	-	-	136.5	126.66
5	7.54	8.19 (1H, s)	127.5	126.76
6	7.54	8.19 (1H, s)	127.5	126.76
2'	-	-	150.6	158.00
4'	-	-	125.4	128.25
5'	-	-	138.1	144.61
6'	-	-	136.5	126.82
7'	7.48	7.96 (2H, d)	127.0	125.15
8'	7.32	7.50 (2H, t)	129.0	128.90
9'	7.22	7.40 (2H, t)	128.5	128.96
10'	7.32	7.50 (2H, t)	129.0	128.90
11'	7.48	7.96 (2H, d)	127.0	125.15

\*Calculated by Chem Draw program

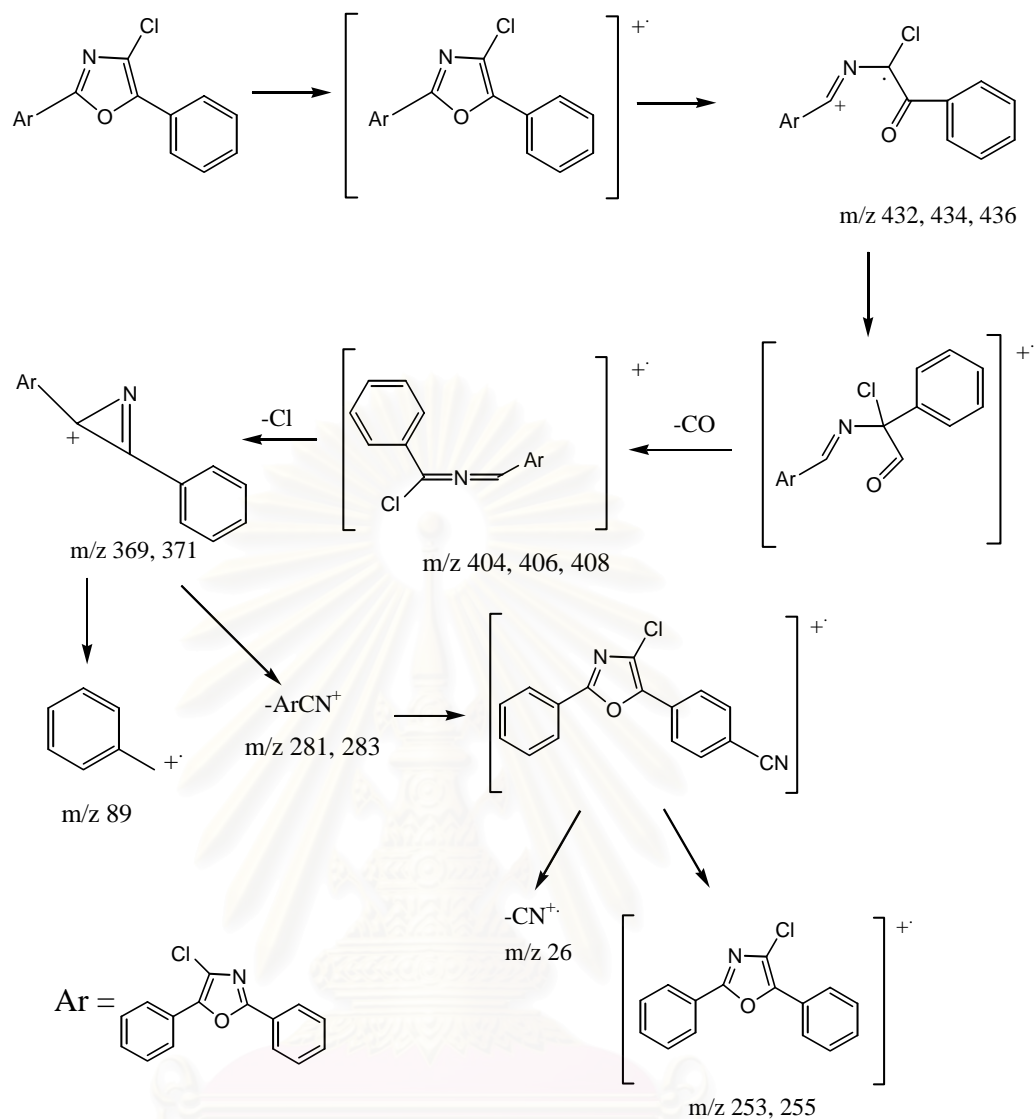
Consequently, the assignment of all the signals appeared in the NMR spectra was correct.



**Table 4-8.** Mass spectrum data of 1,4-bis(4-chloro-5-phenyloxazole-2-yl)benzene (Figure A20)

Compound	m/z
1,4-bis(4-chloro-5-phenyloxazole-2-yl)benzene	432(100), 434(82), 436(10), 369(20), 165(30), 124(10), 105(48), 89(15), 77(45)

The mass spectrum of this product also supported the proposed structure of this compound. It was indicated a molecular ion at m/z 432(100), 434(82) and 436(10) in Table 4-8. The fragmentation pattern is shown in Scheme 4.4 and the mass spectrum presented the existing of two chlorine atoms in the compound.



**Scheme 4.4** The fragmentation pattern of 1,4-bis(4-chloro-5-phenyloxazole-2-yl)benzene

Besides, the elemental analysis of compound B was performed. The result showed that compound B had C 66.59%, H 3.25%, N 6.49%. It was consistent with the calculation for  $C_{24}H_{14}Cl_2N_2O_2$ : C 66.53%, H 3.26%, N 6.47%.

The IR, NMR, Mass spectroscopy, Element analysis data concluded the structure of compound B as 1,4-bis (4-chloro-5-phenyloxazol-2-yl)benzene.

#### 4.4 Synthesis of 1,4-bis(4-chloro-2-phenyloxazol-5-yl)benzene

The synthesis of this compound started with the preparation of terephthaloyl cyanide from reaction of terephthaloyl chloride with copper cyanide. While the reaction was kept at 0°C for 3 days, it was found that the reaction could not occur the cyclization of oxazole formation. It still was the reaction mixture of the starting materials. When the reaction was allowed to occur for at least 7 days, it was observed that the product was formed as a bright yellow 52% yield, m.p. 273.5-275.5°C.

The IR spectrum (KBr) of compound C (Figure A21) showed the absorption bands at 3060, 1447, 1600, 1587, 984  $\text{cm}^{-1}$  corresponding to C-H aromatic stretching, C=C aromatic stretching, -NCO ring and C-Cl stretching.

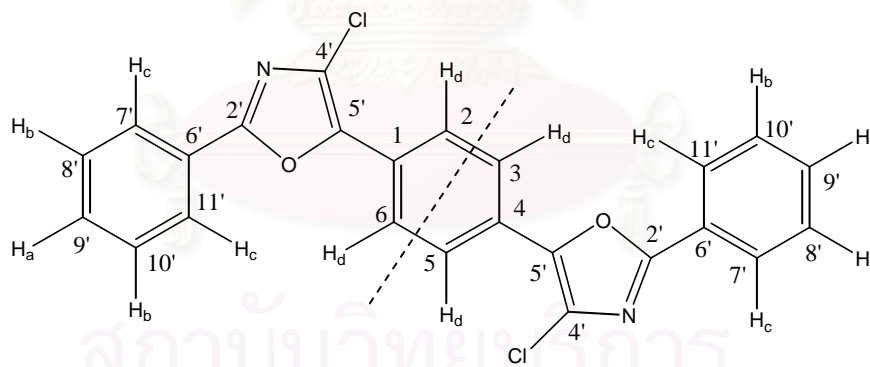


**Figure 4.4** Chemical structure of 1,4-bis(4-chloro-2-phenyloxazol-5-yl)benzene with atomic numbering.

The 500 MHz  $^1\text{H}$  NMR spectrum of this product (Figure D11) exhibited the 4H multiplet at  $\delta$  8.12-8.10 ppm corresponding to the aromatic protons at the positions 7' and 11' of both terminal benzene rings (Figure 4.4), a 4H singlet at  $\delta$  8.08 ppm corresponding to the aromatic protons at the positions 2, 3, 5 and 6 of the middle benzene ring, and a 6H multiplet at  $\delta$  7.53-7.50 ppm belonging to the aromatic protons at positions 8', 9' and 10' of both terminal benzene rings (Table 4.11). This assignment was confirmed by  $^1\text{H}$ - $^1\text{H}$  COSY spectra (Figure D13).

The 125 MHz  $^{13}\text{C}$  NMR spectroscopy also identified this product to be 1,4-bis(4-chloro-2-phenyloxazol-5-yl)benzene (Figure D12). The  $^{13}\text{C}$  NMR assignments of this product are shown in Table 4-9.

The 125 MHz  $^{13}\text{C}$  NMR spectra (Figure D12) showed five peaks of quaternary carbons at  $\delta$  159.35, 143.35, 127.33, 126.79 and 125.50 ppm. While the HMQC, and HMBC spectra in Figure D14 and D15, respectively also revealed the signals, which could be assigned as follows: the signal of  $\text{H}_d$  at  $\delta$  8.08 ppm correlated with C-2, C-3, C-5, C-6 at  $\delta$  125.23 ppm, which this proton displayed the long-range-coupling with C-2' at  $\delta$  143.35 ppm. Meanwhile the signal of  $\text{H}_c$  at  $\delta$  7.53-7.50 ppm correlated with C-7', C-11' at  $\delta$  126.47 ppm and exhibited the long-range-coupling with C-9' at  $\delta$  131.20 ppm.

**Table4-9.** NMR chemical shifts of 1,4-bis(4-chloro-2-phenyloxazol-5-yl)benzene

Position	<sup>1</sup> H NMR (ppm)		<sup>13</sup> C NMR (ppm)	
	*Calculated	Found	*Calculated	Found
1	-	-	136.5	126.79
2	7.54	8.08 (1H, s)	127.5	125.23
3	7.54	8.08 (1H, s)	127.5	125.23
4	-	-	136.5	126.79
5	7.54	8.08 (1H, s)	127.5	125.23
6	7.54	8.08 (1H, s)	127.5	125.23
2'	-	-	150.6	159.35
4'	-	-	125.4	127.33
5'	-	-	138.1	143.35
6'	-	-	136.5	125.56
7'	7.48	7.53-7.50 (2H, m)	127.0	126.47
8'	7.32	8.12-8.10 (2H, m)	129.0	128.98
9'	7.22	7.53-7.50 (2H, m)	128.5	131.20
10'	7.32	8.12-8.10 (2H, m)	129.0	128.98
11'	7.48	7.53-7.50 (2H, m)	127.0	126.47

\*Calculated by Chem Draw program

สถาบันวิทยบริการ  
จุฬาลงกรณ์มหาวิทยาลัย

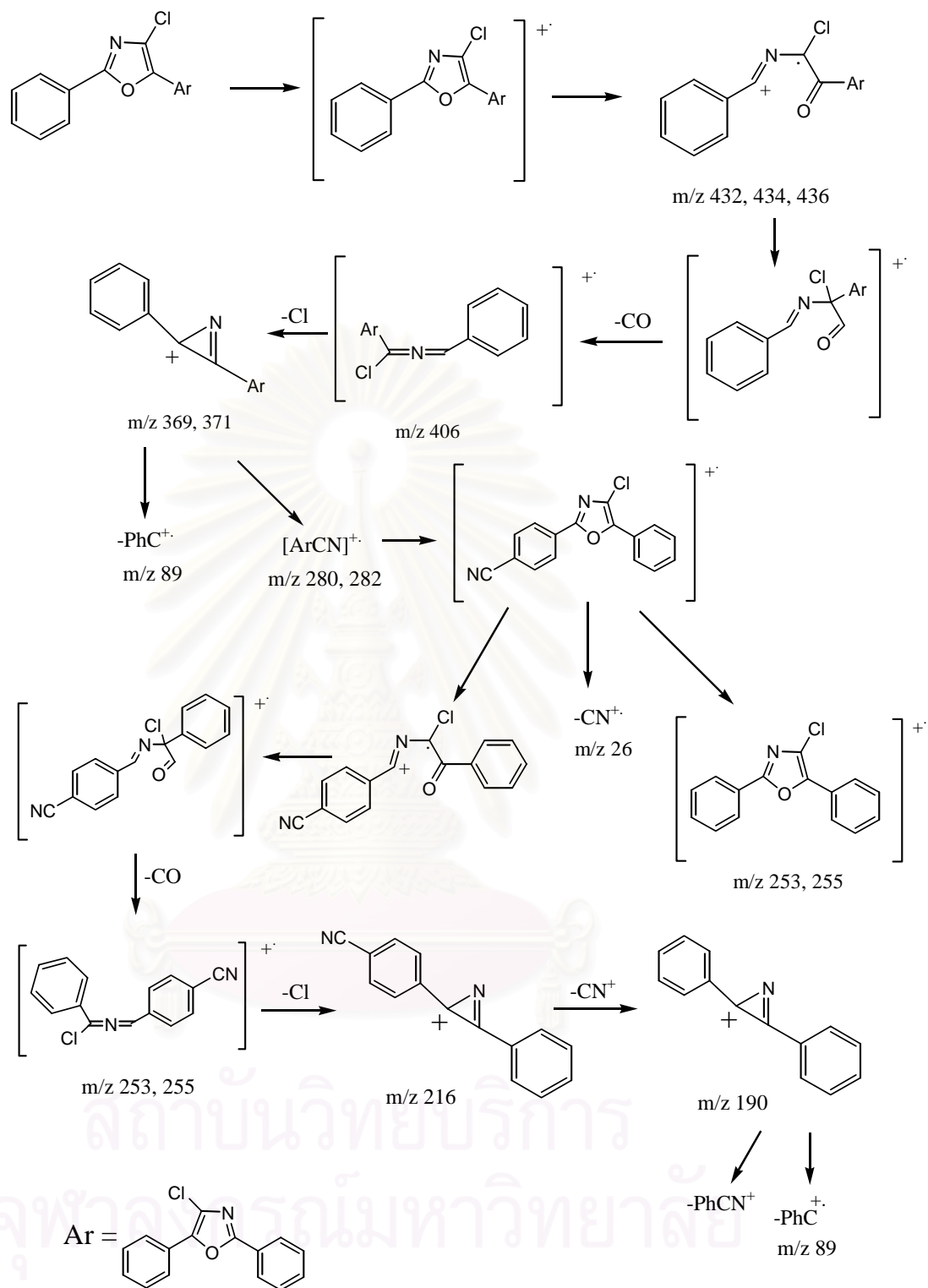
Consequently, the assignment of all the signals appeared in the NMR spectra is correct.

**Table 4-10.** Mass spectrum data of 1,4-bis(4-chloro-2-phenyloxazole-5-yl)benzene (Figure A24)

Compound	m/z
1,4-bis(4-chloro-2-phenyloxazole-5-yl)benzene	432(100), 434(65), 436(10), 369(20), 150(10), 123(20), 105(48), 89(42), 77(28)

The mass spectrum of this product also supported the proposed structure of this compound. It was indicated a molecular ion at m/z 432(100), 434(65) and 436(10) in Table 4-10. The fragments as shown in Scheme 4.5 and the mass spectrum presented the existing of two chlorine atoms in the compound.

Besides, the elemental analysis of compound C was performed. The result showed that compound C had C 66.50%, H 3.49% and N 6.39%. It was consistent with the calculation for  $C_{24}H_{14}Cl_2N_2O_2$ : C 66.53%, H 3.26%, N 6.47%. In addition, using single crystal X-ray diffraction as revealed in Table 4-11 and 4-12 and Figure 4.5 can assure this structure of molecule.



**Scheme 4.5** The fragmentation pathways of 1,4-bis(4-chloro-2-phenyloxazole-5-yl)benzene



**Table4-11.** Crystal and experimental data of 1,4-bis(4-chloro-2-phenyloxazole-5-yl)benzene

Formula	$C_{24}H_{14}Cl_2N_2O_2$
Formula weight	433.27
Temperature	293 (2) K
Wavelength, (Å)	0.71073
Crystal system	monoclinic
Space group	P21/n
Unit cell dimensions	
<i>a</i> , (Å)	8.7815(12)
<i>b</i> , (Å)	11.0432(15)
<i>c</i> , (Å)	10.2351(14)
α, (°)	90
β, (°)	97.804(2)
γ, (°)	90
Volume, (Å <sup>3</sup> )	983.4(2)
Z	2
Calculated density, (g/cm <sup>3</sup> )	1.463
Absorption coefficient (μ), (mm <sup>-1</sup> )	0.355
Reflections collected/unique	8473/2375 [ <i>R</i> (int) = 0.0294]
Refinement method	Full-matrix least-squares on <i>F</i> <sup>2</sup>
Goodness-of-fit on <i>F</i> <sup>2</sup>	1.115
Final <i>R</i> indices [ <i>I</i> > 2σ( <i>I</i> )]	<i>R</i> <sub>1</sub> = 0.0565, <i>wR</i> <sub>2</sub> = 0.1207
<i>R</i> indices (all data)	<i>R</i> <sub>1</sub> = 0.0795, <i>wR</i> <sub>2</sub> = 0.1303
Largest diff. Peak and hole	0.248 and -0.153 e.Å <sup>-3</sup>

**Table4-12.** Bond lengths (Å) and angles (°) of 1,4-bis(4-chloro-2-phenyloxazole-5-yl)benzene

---

C(1)-C(2)	1.380(3)
C(1)-C(6)	1.391(3)
C(2)-C(3)	1.363(4)
C(3)-C(4)	1.382(4)
C(4)-C(5)	1.380(4)
C(5)-C(6)	1.384(3)
C(6)-C(7)	1.461(3)
C(7)-N(1)	1.290(3)
C(7)-O(1)	1.361(3)
C(8)-C(9)	1.349(3)
C(8)-N(1)	1.374(3)
C(8)-Cl(1)	1.707(2)
C(9)-O(1)	1.383(2)
C(9)-C(10)	1.454(3)
C(10)-C(12)	1.389(3)
C(10)-C(11)	1.394(3)
C(11)-C(12)#1	1.380(3)
C(12)-C(11)#1	1.380(3)
C(2)-C(1)-C(6)	119.7(2)
C(3)-C(2)-C(1)	120.7(3)
C(2)-C(3)-C(4)	120.2(2)
C(5)-C(4)-C(3)	119.9(3)

C(4)-C(5)-C(6)	120.2(2)
C(5)-C(6)-C(1)	119.4(2)
C(5)-C(6)-C(7)	121.46(19)
C(1)-C(6)-C(7)	119.1(2)
N(1)-C(7)-O(1)	113.90(18)
N(1)-C(7)-C(6)	128.38(19)
O(1)-C(7)-C(6)	117.71(18)
C(9)-C(8)-N(1)	111.69(19)
C(9)-C(8)-Cl(1)	128.90(17)
N(1)-C(8)-Cl(1)	119.41(16)
C(8)-C(9)-O(1)	105.29(17)
C(8)-C(9)-C(10)	137.60(19)
O(1)-C(9)-C(10)	117.11(17)
C(12)-C(10)-C(11)	118.18(19)
C(12)-C(10)-C(9)	121.59(19)
C(11)-C(10)-C(9)	120.23(18)
C(12)#1-C(11)-C(10)	120.6(2)
C(11)#1-C(12)-C(10)	121.2(2)
C(7)-N(1)-C(8)	103.86(18)
C(7)-O(1)-C(9)	105.25(16)

---

Symmetry transformations used to generate equivalent atoms: #1  $-x+1, -y, -z+1$

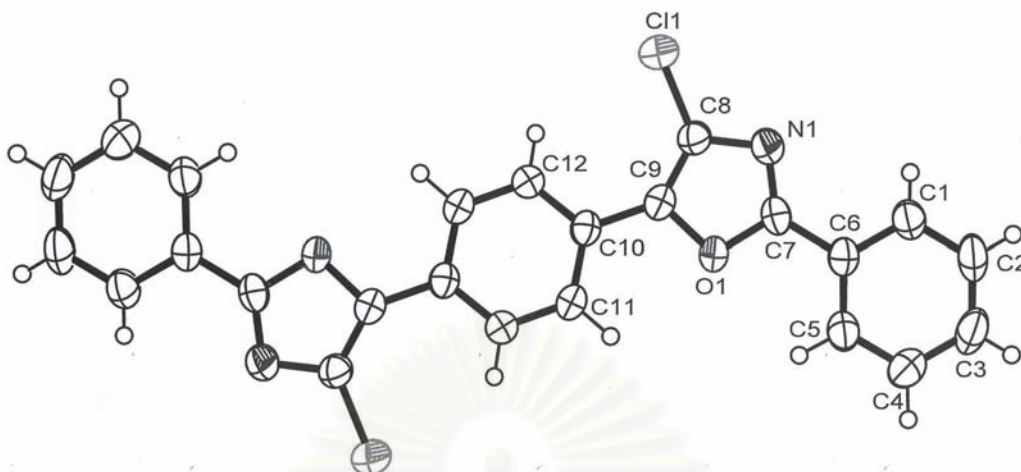


**Figure 4.5** An ORTEP drawing of 1,4-bis(4-chloro-2-phenyloxazole-5-yl)benzene, showing 50% probability displacement ellipsoids

The IR, NMR, mass spectrometry, element analysis and single crystal X-ray diffraction data supported the structure of compound C was 1,4-bis (4-chloro-2-phenyloxazol-5-yl)benzene.

#### 4.5 Reduction of 1,4-bis(4-chloro-5-phenyloxazol-2-yl)benzene to POPOP

1,4-Bis(5-phenyloxazol-2-yl)benzene was prepared by catalytic hydrogenation employing 10% Pd/C as a catalyst. The reaction mixture was stirred in a Parr hydrogenation reactor under 57.8PSI (4atm) of hydrogen at 55°C. The product can be further purified by chromatography to give 10% yield of pale yellow, presumably 1,4-bis(5-phenyloxazol-2-yl)benzene, m.p. 242-243°C.

The structure of yellow compound, presumably 1,4-bis(5-phenyloxazol-2-yl)benzene was characterized by TLC, IR and NMR data as follows:

The Rf value was 0.25 when using an aluminum plate as the absorbent and a mixture of 5% ethyl acetate in hexane.

The IR spectrum of 1,4-bis(5-phenyloxazol-2-yl)benzene displayed in Figure A25. The spectrum can be observed the absorption bands at 3099, 1485 and 1583  $\text{cm}^{-1}$  corresponding to C-H aromatic stretching, C=C aromatic stretching and the -NCO-ring, respectively.

The 200 MHz  $^1\text{H}$  NMR spectrum of 1,4-bis(5-phenyloxazol-2-yl)benzene (Figure A26) indicated a 4H singlet at  $\delta$  8.20 ppm, a 4H doublet ( $J = 3.5$  Hz) at  $\delta$  7.71 ppm, a 8H multiplet at  $\delta$  7.51-7.30 ppm.

The chemical shifts of carbon NMR occurred at  $\delta$  160.45, 151.76, 129.01, 128.69, 127.81, 126.64, 124.32 and 123.82 ppm (Figure A 27) in Table 4-11 can be assured that this product was 1,4-bis(5-phenyloxazol-2-yl)benzene.

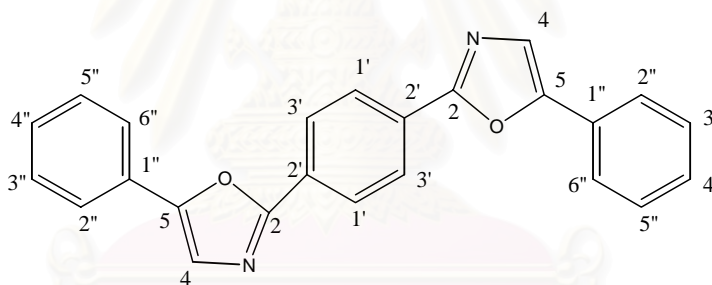


**Figure 4.6** Chemical structure of 1,4-bis(5-phenyloxazol-2-yl)benzene with atomic numbering.

**Table 4-13.** NMR chemical shifts of 1,4-bis(5-phenyloxazol-2-yl)benzene

Position	<sup>1</sup> H NMR (ppm)		<sup>13</sup> C NMR (ppm)	
	*Calculated	Found	*Calculated	Found
1	-	-	-	-
2	-	-	150.6	160.45
3	-	-	-	-
4	7.09	7.51-7.30 (2H, m)	125.4	123.82
5	-	-	138.1	151.76
1'	7.54	8.2 (2H, s)	127.5	126.64
2'	-	-	136.5	129.01
3'	7.54	8.2 (2H, s)	127.5	126.64
1''	-	-	136.5	129.01
2''	7.48	7.71 (2H, d)	127.0	124.32
3''	7.32	7.51-7.30 (2H, m)	129.0	128.69
4''	7.22	7.51-7.30 (2H, m)	128.5	127.81
5''	7.32	7.51-7.30 (2H, m)	129.0	128.69
6''	7.48	7.71 (2H, d)	127.0	124.32

\*Calculated by Chem Draw program

สถาบันวิทยบริการ  
จุฬาลงกรณ์มหาวิทยาลัย

#### 4.6 The Larger molecules of the oxazole containing compounds

The cyclization of 0.092 g (0.5 mmol) terephthaloyl cyanide and 0.101 g (0.75 mmol) terephthacarboxaldehyde gave the yellow powder 0.0280 g. In this synthesis, it was found that this product could be partly dissolved in organic solvent such as chloroform, THF, DMSO. Therefore, it cannot find the clearly molecular weight.

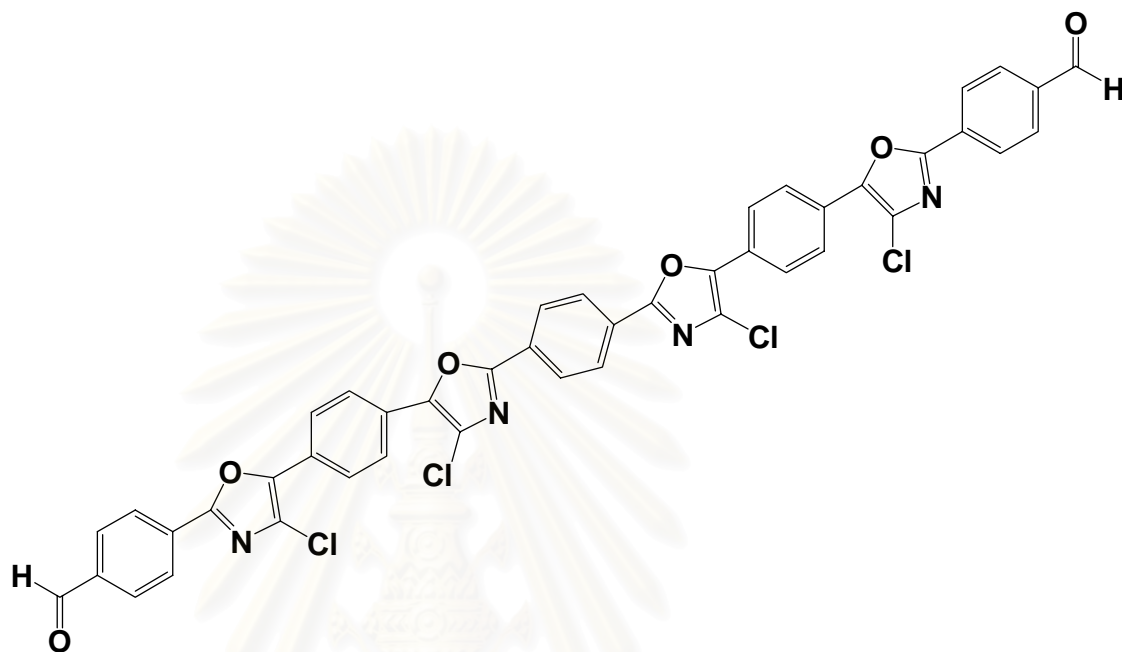
The IR spectrum (KBr) of this product (Figure A28) exhibited the absorption bands at 1580, 1610, 1417 and 987  $\text{cm}^{-1}$  corresponding to  $-\text{NCO}$  ring,  $\text{C}=\text{C}$  aromatic stretching and  $\text{C}-\text{Cl}$  stretching. It obviously indicated that it was an oxazole compound. Interestingly, the sharp absorbance band at 2854  $\text{cm}^{-1}$  and the absorbance at 1720  $\text{cm}^{-1}$  appeared clearly in the spectrum. These absorbance bands are the characteristic of the aldehyde.  $^1\text{H}$  NMR and  $^{13}\text{C}$  NMR spectroscopy confirmed the conclusion.

The 200 MHz  $^1\text{H}$  NMR spectrum of this compound (Figure A29) partly dissolved in chloroform-*d* to indicate a 2H singlet at  $\delta$  10.12 ppm and a 20H multiplet at  $\delta$  8.28-7.99 ppm. Moreover, it could be observed the peak area of  $^1\text{H}$  NMR that the ratio of these peak 2:20 corresponding to the proton of aldehyde and the protons of aromatic group.

The  $^{13}\text{C}$  NMR spectrum of this compound (Figure A30) showed the chemical shifts positions of carbon of compound [11]. The chemical shift of carbon occurred at  $\delta$  191.32 ppm corresponding to the carbon of aldehyde and the chemical shift at  $\delta$  137.78, 130.97, 130.21, 126.99 and 124.86 ppm belonging to the carbon of aromatic group.



Accordingly, this compound was postulated as the oligomer with the following structure.



สถาบันวิทยบริการ  
จุฬาลงกรณ์มหาวิทยาลัย

## **Part II: Optical property**

In this study, the new oxazole containing compounds were investigated the optical property such as UV-vis and fluorescence spectra data.

### **4.7 The results of UV-Absorption analysis**

The oxazole containing compounds have been successfully synthesized that were investigated by UV-Absorption. In this study, these compounds were dissolved various the solvents as dichloromethane, tetrahydrofuran, and n-butanol. They were found that the effect of polarity of the solvent is not so large. As the results of, the extinction coefficient,  $\epsilon$ , of each sample is calculated similarly. Therefore, in discussions, all of these results will be described by using dichloromethane solvent.

The  $\lambda_{\max}$  and  $\log \epsilon_{\max}$  of 4-chloro-2,5-diphenyloxazole, 2,5-diphenyloxazole, 1,4-bis(4-chloro-5-phenyloxazol-2-yl)benzene, 1,4-bis(4-chloro-2-phenyloxazol-5-yl)benzene, and 1,4-bis(4-chloro-5-phenyloxazol-2-yl)benzene in this work are shown in Table 4-14.

**Table 4-14.**  $\lambda_{\max}$  and  $\log \epsilon_{\max}$  of 4-chloro-2,5-diphenyloxazole, 2,5-diphenyloxazole, 1,4-bis(4-chloro-5-phenyloxazol-2-yl)benzene, 1,4-bis(4-chloro-2-phenyloxazol-5-yl)benzene, and 1,4-bis(4-chloro-5-phenyloxazol-2-yl)benzene in dichloromethane.

<b>Oxazole</b>	<b><math>\lambda_{\max}</math> (nm)</b>	<b><math>\log \epsilon_{\max}</math></b>
4-chloro-2,5-diphenyloxazole	310	4.50
2,5-diphenyloxazole	306	4.62
1,4-bis(4-chloro-5-phenyloxazol-2-yl)benzene	369	4.78
1,4-bis(4-chloro-2-phenyloxazol-5-yl)benzene	363	4.62
1,4-bis(5-phenyloxazol-2-yl)benzene	361	4.85

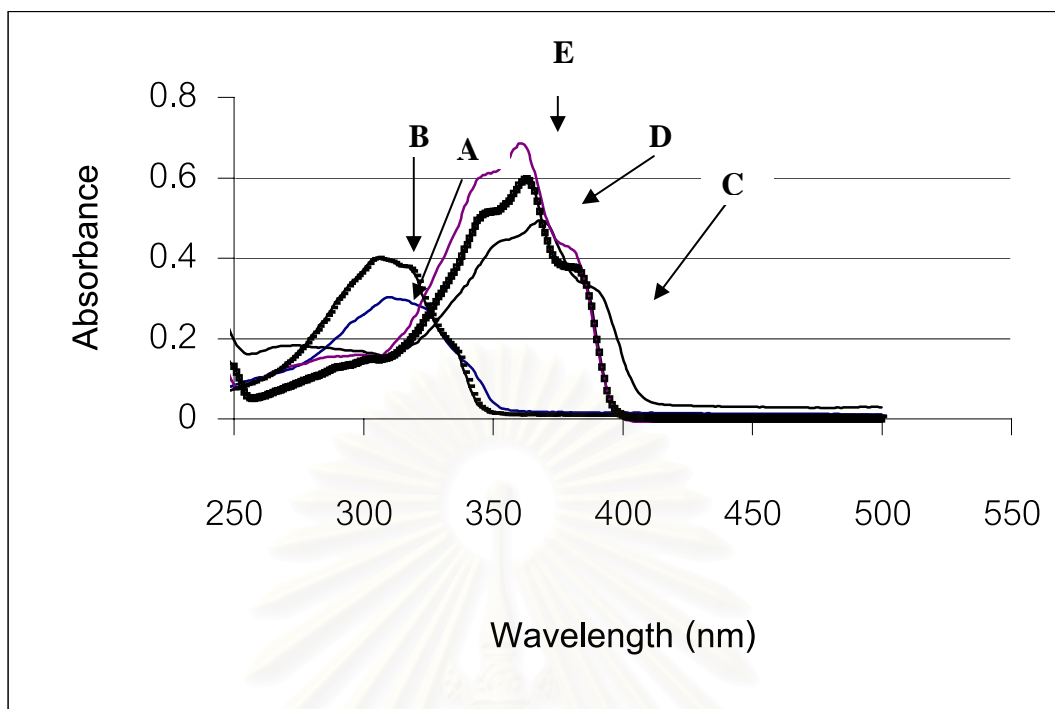


**Figure 4.7** The UV-absorption spectra of the oxazole containing compounds in dichloromethane

- A) 4-chloro-2,5-diphenyloxazole at  $9.9 \times 10^{-6}$  M
- B) 2,5-diphenyloxazole at  $9.9 \times 10^{-6}$  M
- C) 1,4-bis(4-chloro-5-phenyloxazol-2-yl)benzene at  $10 \times 10^{-6}$  M
- D) 1,4-bis(4-chloro-2-phenyloxazol-5-yl)benzene at  $10 \times 10^{-6}$  M
- E) 1,4-bis(5-phenyloxazol-2-yl)benzene at  $10 \times 10^{-6}$  M

In Figure 4.7, the UV-absorption spectra of the oxazole containing compounds in dichloromethane were compared in the same concentration. It was found that 4-chloro-2,5-diphenyloxazole and 2,5-diphenyloxazole were absorbed at 0.303 and 0.401, respectively. While 1,4-bis(4-chloro-5-phenyloxazol-2-yl)benzene, 1,4-bis(4-chloro-2-phenyloxazol-5-yl)benzene and 1,4-bis(5-phenyloxazol-2-yl)benzene were absorbed at 0.543, 0.628 and 0.685, respectively. It showed that not only the chlorine atom but the

high long conjugations also have an effect with the absorption bands. The high long conjugation causes the absorption band to shift towards longer wavelengths. The observation that 1,4-bis(4-chloro-5-phenyloxazol-2-yl)benzene, 1,4-bis(4-chloro-2-phenyloxazol-5-yl)benzene and 1,4-bis(5-phenyloxazol-2-yl)benzene absorb at  $\lambda_{\max}$  369 nm,  $\lambda_{\max}$  363 nm and  $\lambda_{\max}$  361 nm which are higher than 4-chloro-2,5-diphenyloxazole, can be attributed to the extended conjugation.

#### 4.8 The results of Fluorescence analysis

The UV absorption and fluorescence emission properties of these compounds in dilute solution were studied. Dichloromethane was found to be satisfactory with its UV cutoff at 230 nm. Some of emission light can be re-absorbed by the sample if the wavelength of the emission light is overlapped with that of the absorption spectrum. If the concentration is high, a part of emission light will be absorbed by the solution. Therefore, in this study, they were presented in very low concentration. When the concentration is low, almost of the emission light is not absorbed by the solution.

##### 4.8.1 Fluorescence analysis of 4-chloro-2,5-diphenyloxazole

The fluorescence of 4-chloro-2,5-diphenyloxazole in dichloromethane solvent at the concentration of  $0.91 \times 10^{-6}$  M (Figure 4.8) exhibits the excitation wavelength at 310 nm. The fluorescence emission spectra of 4-chloro-2,5-diphenyloxazole shows band at  $\lambda_{\max}$  372 nm which is the mirror images of the corresponding absorption spectra. The fluorescence quantum yield gave 0.10 in Figure C2.

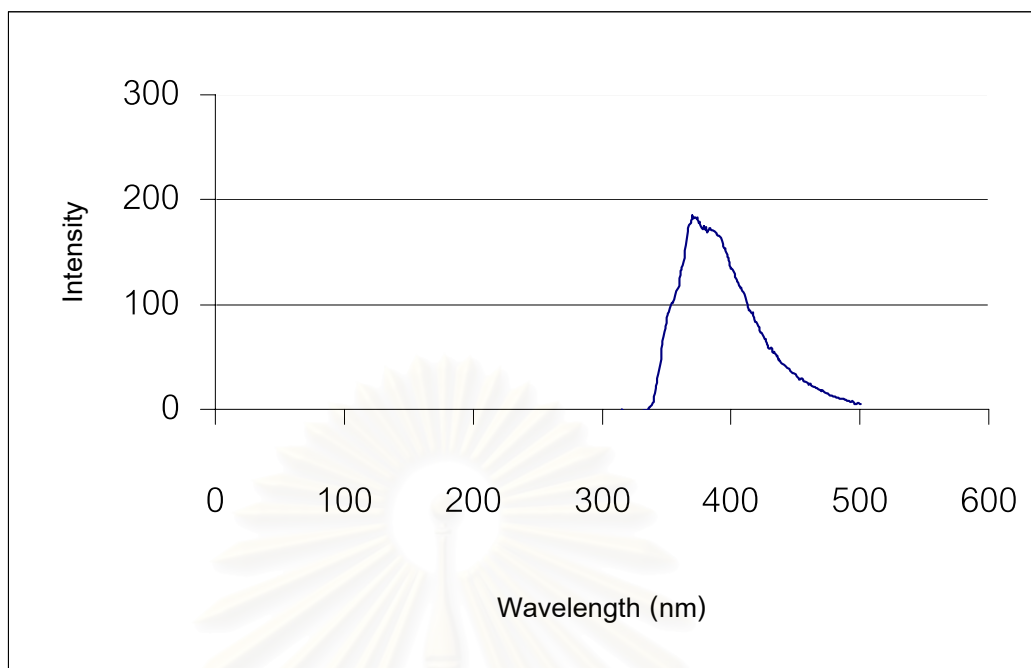


**Figure 4.8** The emission spectra of 4-chloro-2,5-diphenyloxazole in dichloromethane at the concentration  $0.91 \times 10^{-6}$  M,  $\lambda_{\text{ex}}$  310 nm

#### 4.8.2 Fluorescence analysis of 2,5-diphenyloxazole

The fluorescence of 2,5-diphenyloxazole in dichloromethane at  $0.91 \times 10^{-6}$  M in Figure 4.9 exhibited the excitation wavelength at 306 nm. The fluorescence emission spectra of 2,5-diphenyloxazole shows band at  $\lambda_{\text{max}}$  363 nm, which is the mirror images of the corresponding absorption spectra. The fluorescence quantum yield gave 0.15 in Figure C8.

สถาบันวิทยบริการ  
จุฬาลงกรณ์มหาวิทยาลัย

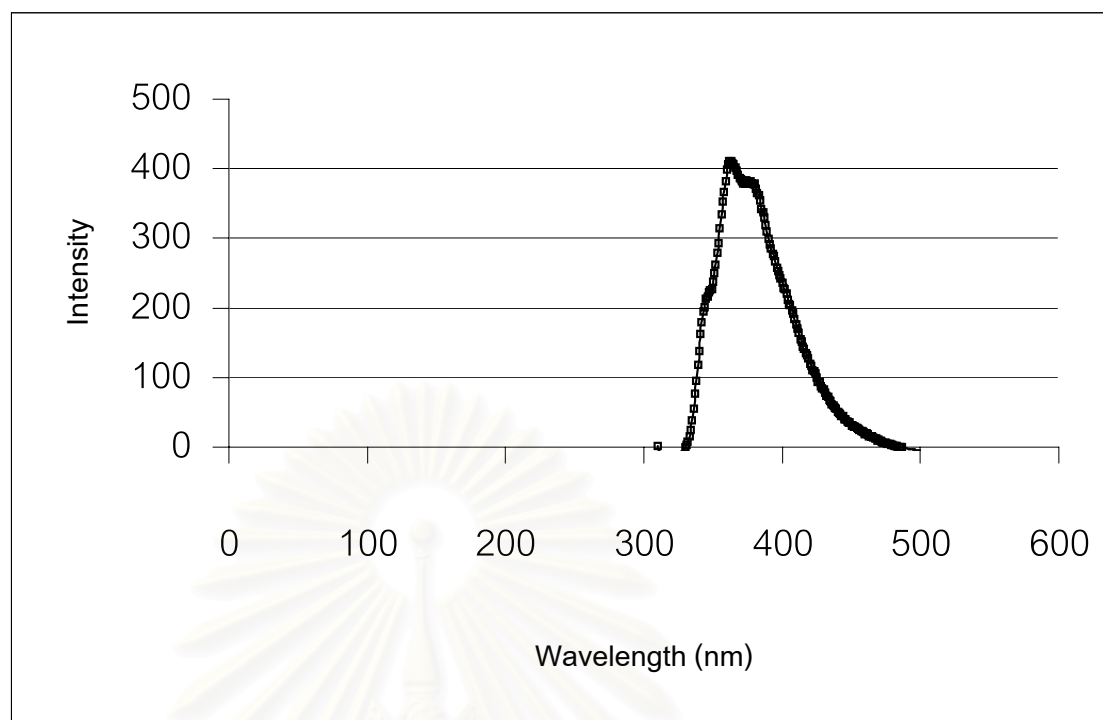


**Figure 4.9** The emission spectra of 2,5-diphenyloxazole in dichloromethane at the concentration  $0.91 \times 10^{-6}$  M,  $\lambda_{\text{ex}}$  306 nm

#### 4.8.3 Fluorescence analysis of 1,4-bis(4-chloro-5-phenyloxazol-2-yl)benzene

The fluorescence of 1,4-bis(4-chloro-5-phenyloxazol-2-yl)benzene in dichloromethane solvent at the concentration  $0.5 \times 10^{-6}$  M in Figure 4.10 exhibits the excitation wavelength at 369 nm. The fluorescence emission spectra of 1,4-bis(4-chloro-5-phenyloxazol-2-yl)benzene shows band at  $\lambda_{\text{max}}$  429 nm, which is the mirror images of the corresponding absorption spectra. The fluorescence quantum yield gave 0.17 in Figure C5.

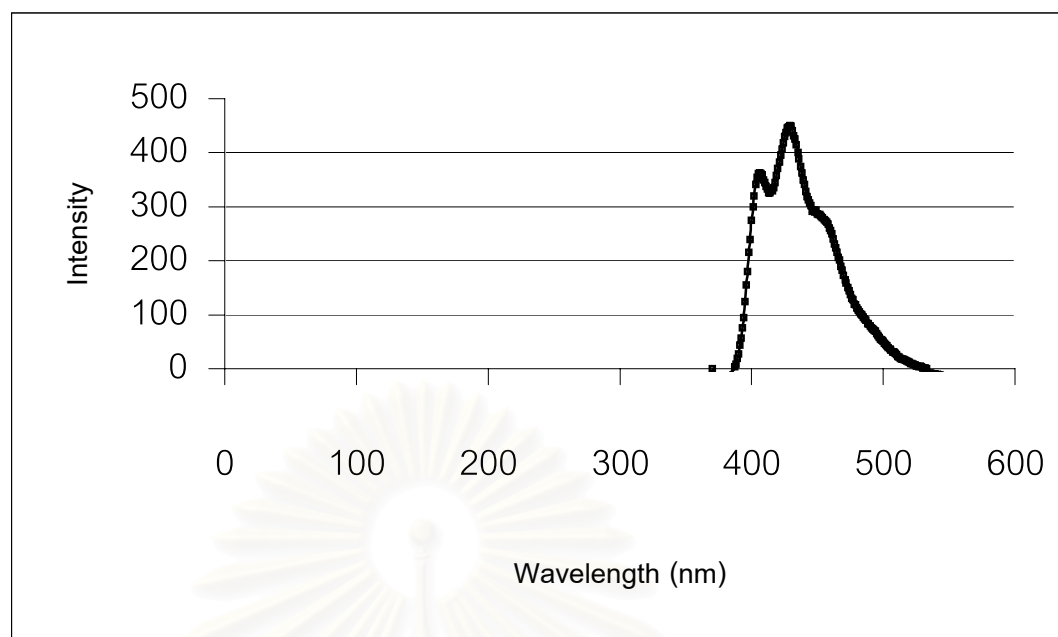


**Figure 4.10** The emission spectra of 1,4-bis(4-chloro-5-phenyloxazol-2-yl)benzene in dichloromethane at the concentration  $0.5 \times 10^{-6} \text{ M}$ ,  $\lambda_{\text{ex}}$  369 nm

#### 4.8.4 Fluorescence analysis of 1,4-bis(4-chloro-2-phenyloxazol-5-yl)benzene

The fluorescence of 1,4-bis(4-chloro-2-phenyloxazol-5-yl)benzene in dichloromethane solvent at the concentration  $0.5 \times 10^{-6} \text{ M}$  in Figure 4.11 exhibited the excitation wavelength at 363 nm. The fluorescence emission spectra of 1,4-bis(4-chloro-2-phenyloxazol-5-yl)benzene shows band at  $\lambda_{\text{max}}$  417 nm, which is the mirror images of the corresponding absorption spectra. The fluorescence quantum yield gave 0.10 in Figure C6.



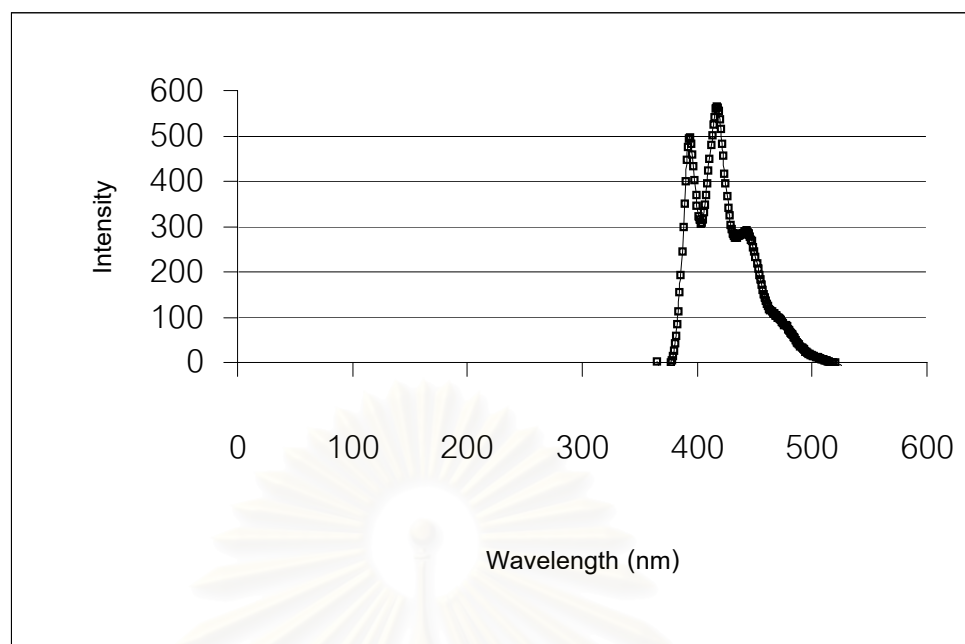


**Figure 4.11** The emission spectra of 1,4-bis(4-chloro-2-phenyloxazol-5-yl)benzene in dichloromethane at the concentration  $0.5 \times 10^{-6}$  M,  $\lambda_{\text{ex}}$  363 nm

#### 4.8.5 Fluorescence analysis of 1,4-bis(5-phenyloxazol-2-yl)benzene

The fluorescence of 1,4-bis(5-phenyloxazol-2-yl)benzene in dichloromethane solvent exhibits the excitation wavelength at 361nm. The fluorescence emission spectra of 1,4-bis(5-phenyloxazol-2-yl)benzene shows band at  $\lambda_{\text{max}}$  419 nm (Figure 4.12). It can be calculated the fluorescence quantum yield 0.22 in Figure C10.

สถาบันวิทยบริการ  
จุฬาลงกรณ์มหาวิทยาลัย

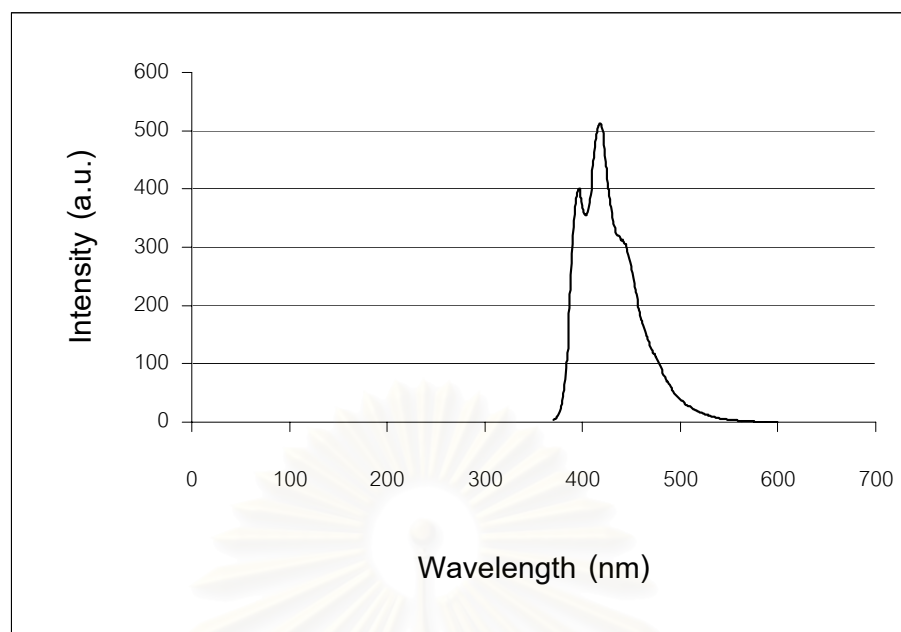


**Figure 4.12** The emission spectra of 1,4-bis(5-phenyloxazol-2-yl)benzene in dichloromethane at the concentration  $0.5 \times 10^{-6} \text{ M}$ ,  $\lambda_{\text{ex}} 361 \text{ nm}$

#### 4.8.6 Comparison the fluorescence emission spectra

The fluorescence emission spectra of 4-chloro-2,5-diphenyloxazole, 2,5-diphenyloxazole, 1,4-bis(4-chloro-5-phenyloxazol-2-yl)benzene, and 1,4-bis(4-chloro-2-phenyloxazol-5-yl)benzene were compared at the low concentration solution by absorbance should be lower than 0.05. Comparison the fluorescence emission spectra are shown in Figure 4.13.

สถาบันวิทยบริการ  
จุฬาลงกรณ์มหาวิทยาลัย

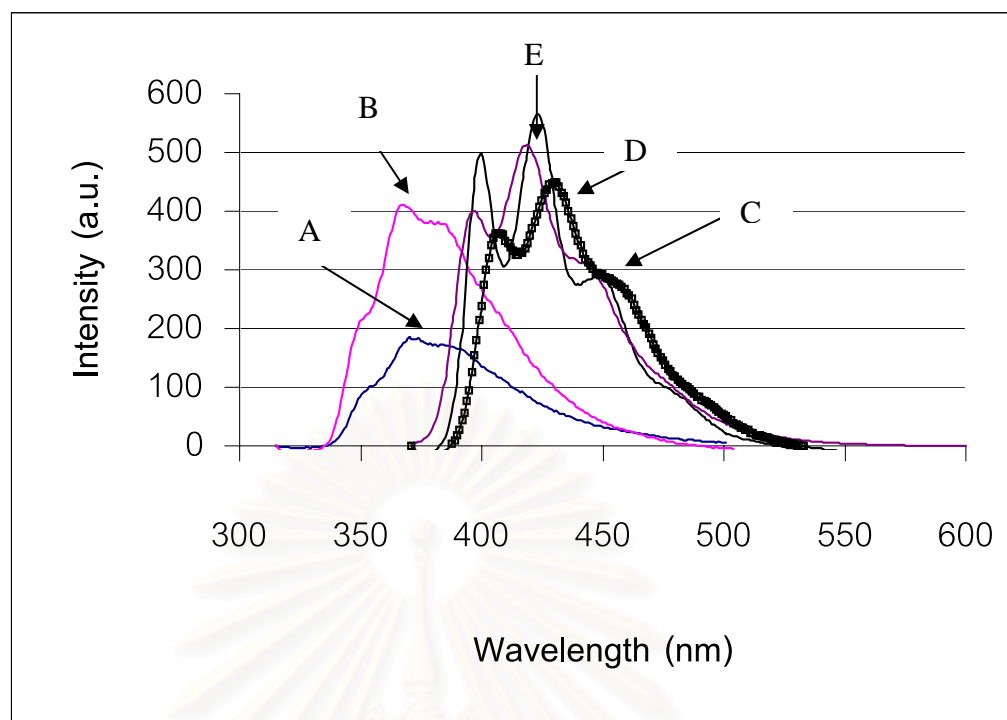


**Figure 4.13** The fluorescence emission spectra in dichloromethane solvent

- A) 4-chloro-2,5-diphenyloxazole at  $0.91 \times 10^{-6}$  M,  $\lambda_{em} = 372$  nm,  $\lambda_{ex} = 310$  nm.  
 B) 2,5-diphenyloxazole at  $0.91 \times 10^{-6}$  M,  $\lambda_{em} = 363$  nm,  $\lambda_{ex} = 306$  nm.  
 C) 1,4-bis(4-chloro-5-phenyloxazol-2-yl)benzene at  $0.5 \times 10^{-6}$  M,  $\lambda_{em} = 423$  nm,  $\lambda_{ex} = 369$  nm.  
 D) 1,4-bis(4-chloro-2-phenyloxazol-5-yl)benzene at  $0.5 \times 10^{-6}$  M,  $\lambda_{em} = 417$  nm,  $\lambda_{ex} = 363$  nm.  
 E) 1,4-bis(5-phenyloxazol-2-yl)benzene at  $0.5 \times 10^{-6}$  M,  $\lambda_{em} = 419$  nm,  $\lambda_{ex} = 361$  nm.

The spectra indicate that the bathochromic shifts are seen when increasing the long conjugation in the structure as a result of extended conjugation with the double bond. The absorption/ fluorescence evidently is due to  $\pi\pi^*$  transition.

Moreover, the compounds were investigated at various concentrations of the solution. It was found that all the compounds in high concentration do not have any excimer due to they do not appear the new emission band in longer wavelength. When the excimer emission is occurred, new emission band will be observed in the longer wavelength region. The emission bands of these compounds are the mirror images of the absorption bands.

In Table4-15 and Table4-16 concluded the results of the optical property.

**Table 4-15** The results of UV-Absorption analysis

Oxazole	Solvent								
	THF			Dichloromethane			<i>n</i> -Butanol		
	$\lambda_{\max}$	$\epsilon$	$\log \epsilon$	$\lambda_{\max}$	$\epsilon$	$\log \epsilon$	$\lambda_{\max}$	$\epsilon$	$\log \epsilon$
4-chloro-2,5-diphenyl oxazole	308	33572	4.53	310	31933	4.50	-	-	-
PPO	305	49483	4.69	306	41421	4.62	-	-	-
1,4-bis(4-chloro-5-phenyl oxazol-2-yl)benzene	368	74514	4.87	369	60578	4.78	368	38595	4.59
1,4-bis(4-chloro-2-phenyl oxazol-5-yl)benzene	363	79082	4.90	363	41852	4.62	362	22849	4.36
POPOP	361	72232	4.86	361	70654	4.85	361	32561	4.51

**Table 4-16** The results of fluorescence analysis

Oxazole	Solvent								
	THF			Dichloromethane			<i>n</i> -Butanol		
	$\lambda_{ex}$	$\lambda_{em}$	$\phi$	$\lambda_{ex}$	$\lambda_{em}$	$\phi$	$\lambda_{ex}$	$\lambda_{em}$	$\phi$
4-chloro-2,5-diphenyl oxazole	308	369	0.14	310	372	0.10	-	-	-
PPO	306	362	0.18	306	363	0.15	-	-	-
1,4-bis(4-chloro-5-phenyloxazol-2-yl)benzene	367	425	0.33	369	429	0.17	368	423	0.17
1,4-bis(4-chloro-2-phenyloxazol-5-yl)benzene	363	417	0.21	363	417	0.10	362	415	0.22
POPOP	362	417	0.18	361	419	0.22	359	418	0.23

It was found that 4-chloro-2,5-diphenyloxazole has similar the fluorescence quantum yield to PPO. While 1,4-bis(4-chloro-5-phenyloxazol-2-yl)benzene and 1,4-bis(4-chloro-2-phenyloxazol-5-yl)benzene exhibited the fluorescence quantum yield in the same range as POPOP. Therefore, It has probably useful for all the same applications. Especially, 1,4-bis(4-chloro-5-phenyloxazol-2-yl)benzene and 1,4-bis(4-chloro-2-phenyloxazol-5-yl)benzene gave the fluorescence quantum yields higher than 4-chloro-2,5-diphenyloxazole. It has probably efficiency in the utilization than 2,5-diphenyloxazole, PPO as well.

## CHAPTER V

### CONCLUSION AND SUGGESTION

#### 5.1 Conclusion

Two new oxazole containing compounds, 1,4-bis(4-chloro-5-phenyloxazol-2-yl)benzene (59%yield) and 1,4-bis(4-chloro-2-phenyloxazol-5-yl)benzene (52%yield), have been successfully synthesized with reasonable yields *via* one step cyclization of the benzoyl cyanide and terephthacarboxaldehyde, and terephthaloyl cyanide and benzaldehyde, respectively. The products could be separated and purified easily. The confirmation of their structures was unambiguously determined by the spectroscopic techniques.

The preliminary attempt to remove chlorine atoms from 1,4-bis(4-chloro-5-phenyloxazol-2-yl)benzene by catalytic hydrogenation employing 10% Pd/C as catalyst gave 1,4-bis(5-phenyloxazol-2-yl)benzene or POPOP. Though the conversion of 1,4-bis(4-chloro-5-phenyloxazol-2-yl)benzene to POPOP was in 10%yield by this method, it showed that POPOP could be synthesized more easily *via* one step cyclization and catalytic hydrogenation comparing to the other routes reported by other research groups. It could also be concluded that the oligomer with oxazole containing backbone would presumably be synthesized *via* this method.

The UV absorption and the fluorescence emission of these compounds were dependent on the solvent. 4-Chloro-2,5-diphenyloxazole has similar optical property to

PPO. Similarly, 1,4-bis(4-chloro-5-phenyloxazol-2-yl)benzene and 1,4-bis(4-chloro-2-phenyloxazol-5-yl)benzene exhibit the optical property in the same range as POPOP.

## 5.2 Proposal for future work

1. Dechlorination of 1,4-bis(4-chloro-5-phenyloxazol-2-yl)benzene should be studied. It will open the new way for POPOP production commercially.
2. The molecular structure of the polymer with oxazole containing backbone should be designed in such a way that its solubility can be improved.



สถาบันวิทยบริการ  
จุฬาลงกรณ์มหาวิทยาลัย



## REFERENCES

1. Edwin, D.; Bransome, J.R. *Physics of the liquid scintillation process*, Liquid Scintillation Counting, Massachusetts Institute of Technology: Academic press, **1970**.
2. Turchi, I.J.; Dewar, M.J.S. "The Chemistry of Oxazole" *Chemical Reviews* **1975**, *74(4)*, 389.
3. Urban, M.W.; Provder, T. *Multidimensional Spectroscopy of Polymers* *Vibrational, NMR, and Fluorescence Techniques*, ACS, Washington, DC **1995**, *Chapter 20*, 356.
4. Hercules, D.M. *Theory of Luminescence Processes*, Fluorescence and Phosphorescence analysis, Principles and Applications, *Chapter 1*, 23.
5. Hercules, D.M. *Fluorescence and Phosphorescence of Organic Molecules*, Fluorescence and Phosphorescence analysis, Principles and Applications, *Chapter 3*, 81.
6. Thommes, G.A.; Leininger, E. "The spectrofluorometric determination of anthracene, fluorine and phenanthrene in mixtures" *Talanta* **1961**, *7*, 181.
7. McClure, D.S. "Triplet-Singlet Transitions in Organic Molecules. Lifetime measurements of the triplet state" *J. Chem. Phys.* **1949**, *17*, 905.
8. Heckman, R.C. "Phosphorescence studies of some heterocyclic and related organic compounds" *J. Mol. Spectry.* **1958**, *2*, 27.
9. Furst, M., Kallmann, H. "Fluorescent behavior of solutions containing more than one solvent" *J. Chem. Phys.* **1955**, *23*, 607.
10. Heller, A. "Structural requirements of organic liquid scintillators" *J. Chem. Phys.* **1961**, *35*, 1980.

11. Giacovazzo, C. (ed). *Fundamentals of crystallography* IUCR texts on crystallography 2. Oxford U.K. : Oxford University Press, **1992**.
12. Clegg, W. *Crystal structure Determination*. Oxford New York.: Yokyo Oxford University Press, **1988**.
13. Koritsanszky, T.S.; Ceppens P. "Chemical Applications of X-ray Charge Density Analysis" *Chem. Rev.* **2001**, *101*, 1583.
14. Fischer, E. "Synthesis of 2,5-diphenyloxazole" *Ber.* **1896**, *26*, 205.
15. Robinson, R. "A New Synthesis of Oxazole Derivatives" *J. Chem. Soc.* **1909**, *95*, 2167.
16. Ternai, B.; Lakhan, R. "A General Synthesis of 2,5-Diaryl-4-chloro (or Bromo) oxazoles" *J. Het. Chem.* **1973**, *38*, 2407.
17. Pei, Q.; Yang, Y. "1,3,4-Oxadiazole-Containing Polymers as Electron-Injection and Blue Electroluminescent Materials in Polymer Light-Emitting Diodes" *Chem. Mater* **1995**, *7*, 1568.
18. Sutherland, A.J.; Clapham, B.; Richards, A.; Wood, M. "Synthesis and scintillating efficiencies of 4-functionalised-2,5-diphenyloxazoles" *Tetrahedron Lett.* **1997**, *38*, 9061.
19. Clapham, B.; Sutherland, A.J. "Synthesis and evaluation of a scintillant-containing solid support for use in combinatorial chemistry" *Tetrahedron Lett.* **2000**, *41*, 2253.
20. Diwu, Z.J.; Zhang, C.L.; Klaubert, D.H.; Haugland, R.P. "Fluorescent molecular probes VI The spectral properties and potential biological applications of water-soluble Dapoxyl TM sulfonic acid" *J. Photochem. Photobiol.* **2000**, *13(1-3)*, 95.

21. Hay, J.N.; Hamerton, I.; Jones, J.R.; Shin, Y.L. "Covalent Incorporation of 2,5-Diphenyloxazole in Sol-Gel Matrices and Their Application in Radioanalytical Chemistry" *Chem. Mater.* **2000**, *12*, 568.
22. Doroshenko, A.O. "Spin-Orbit Interaction and Structural Relaxation of the 1,2-bis-(5-phenyloxazolyl-2)-benzene Molecule in the Excited State" *Russian Journal of Physical Chemistry.* **2000**, *74(5)*, 773.
23. Megelski, S.; Lieb, A.; Pauchard, M.; Drechsler A.; Glaus S.; Debus, C.; Meixner, A.J.; Calzaferri, G. "Orientation of Fluorescent Dyes in the Nano Channels of Zeolite L" *J. Phys. Chem. B* **2001**, *105*, 25.
24. Oakwood, T. S.; Weisgerber, C. A. "Benzoyl Cyanide" *Organic Syntheses Collective Volume 3*, 112.
25. Miyamoto, K.; Yamaguchi, S.; Hanafusa, T. "New Approaches to Tetracyanoquinodimethane" *Bull. Chem. Soc. Jpn.* **1989**, *62*, 3036.
26. Kerdesky, F. A. J.; Seif, L. S. "Catalytic hydrogenation of halothiazoles" *Synthetic communications* **1995**, *25(24)*, 4081.
27. <http://www.jyhoriba.co.uk>
28. Melhuish, W. H. "Quantum efficiencies of fluorescence of organic substances: effect of solvent and concentration of the fluorescent solute" *J. Phys. Chem.* **1961**, *65*, 229.
29. Stothers, J. B. *Carbon-13 NMR Spectroscopy*. New York: Academic press, **1972**, 197.
30. Palmer, D. C. *Oxazoles: Synthesis, Reactions, And Spectroscopy Part A*. John Wiley & Sons, Inc., **2003**, 403.
31. Hayes, F.N.; Rogers, B.S.; Ott, D.G. "2,5-Diaryloxazoles and 2,5-Diaryl-1,3,4-oxadiazoles" *J. Am. Chem. Soc.* **1955**, *77*, 1850.



## Appendix A

สถาบันวิทยบริการ  
จุฬาลงกรณ์มหาวิทยาลัย

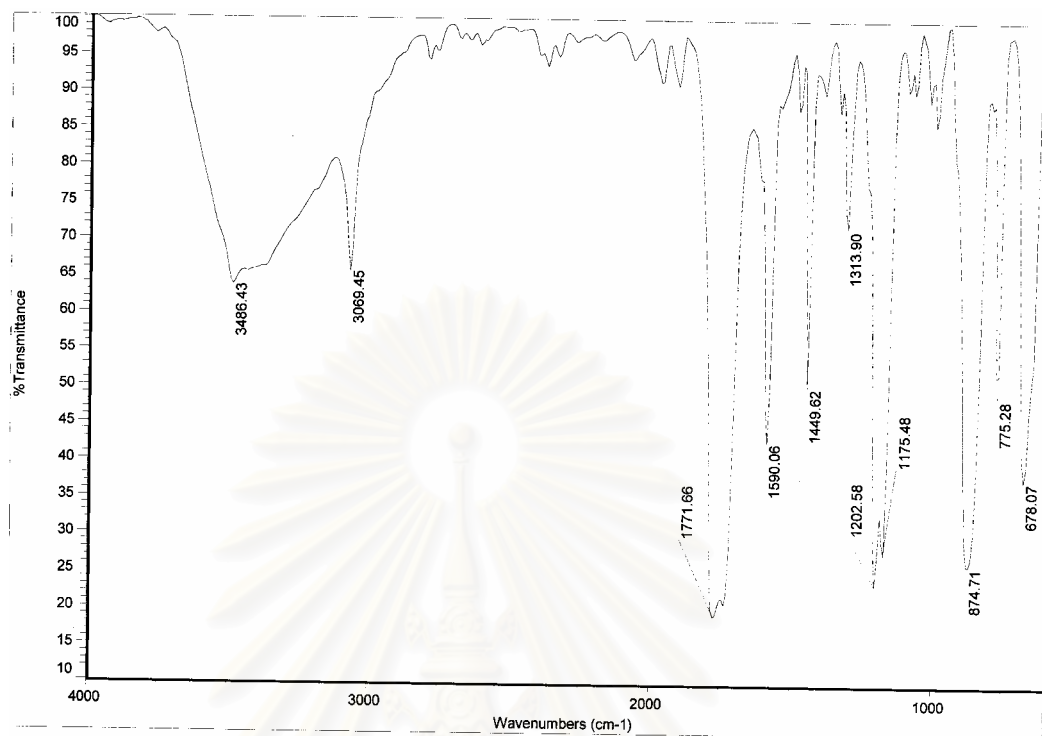


Figure A1 : IR spectrum of benzoyl chloride

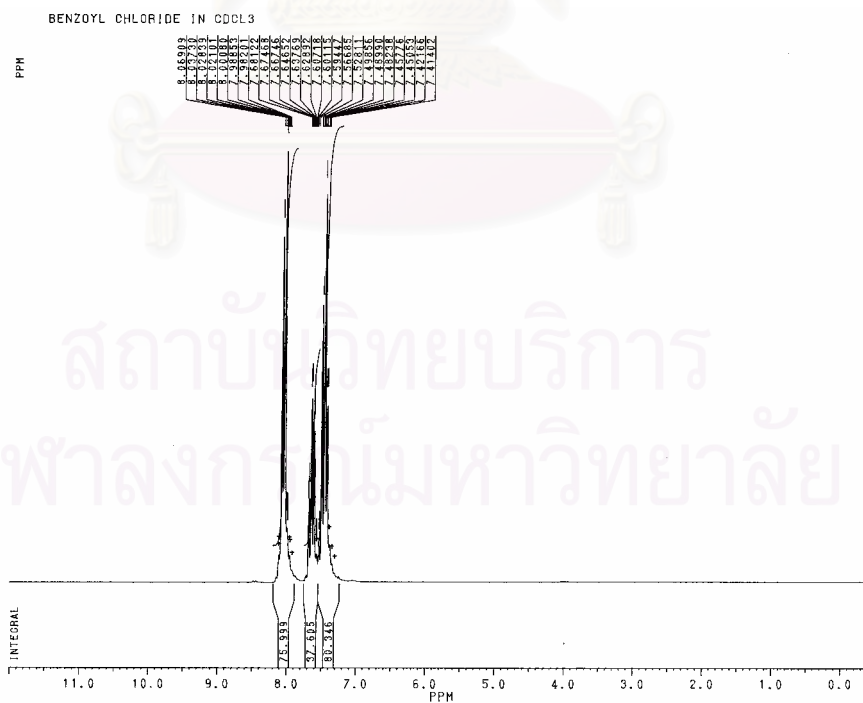


Figure A2 : 200 MHz <sup>1</sup>H NMR spectrum of benzoyl chloride (CDCl<sub>3</sub>)

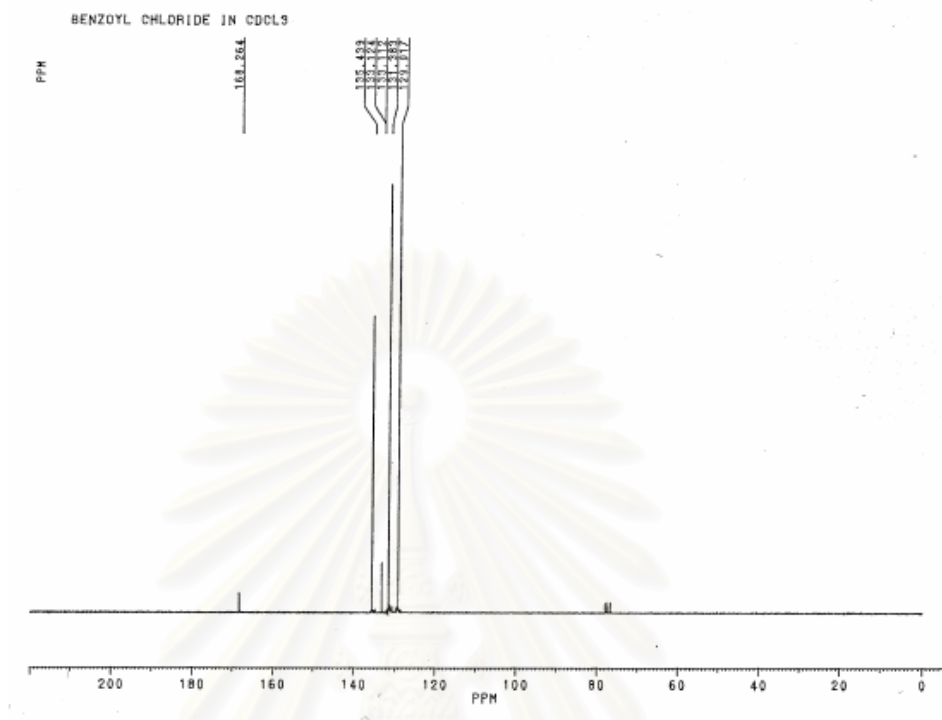


Figure A3 : 50 MHz  $^{13}\text{C}$  NMR spectrum of benzoyl chloride ( $\text{CDCl}_3$ )

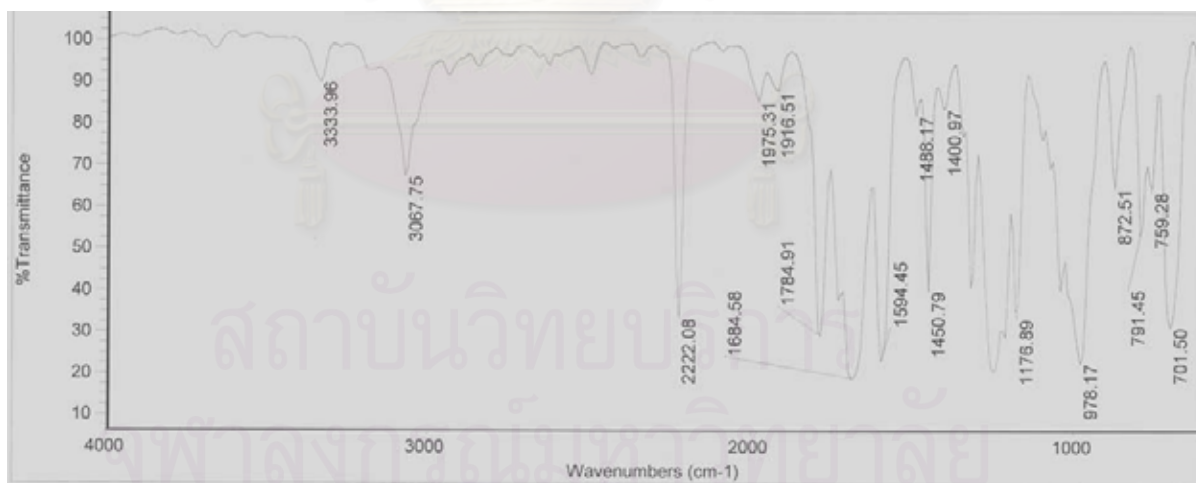


Figure A4 : IR spectrum of benzoyl cyanide





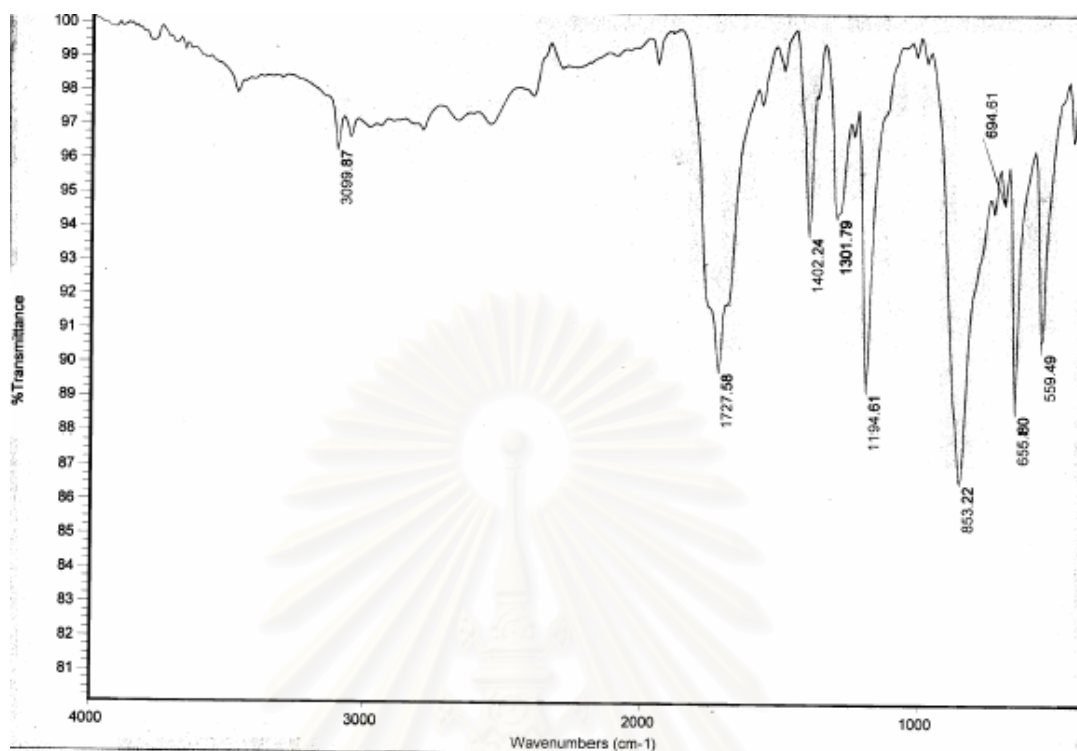


Figure A7 : IR spectrum of terephthaloyl chloride (KBr pellet)

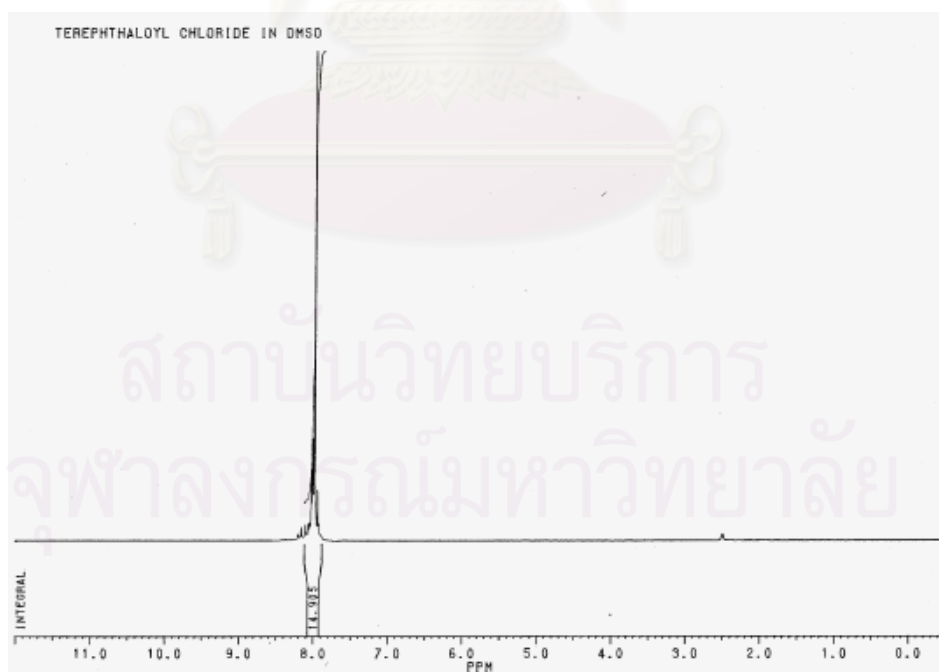


Figure A8 : 200 MHz <sup>1</sup>H NMR spectrum of terephthaloyl chloride (DMSO)



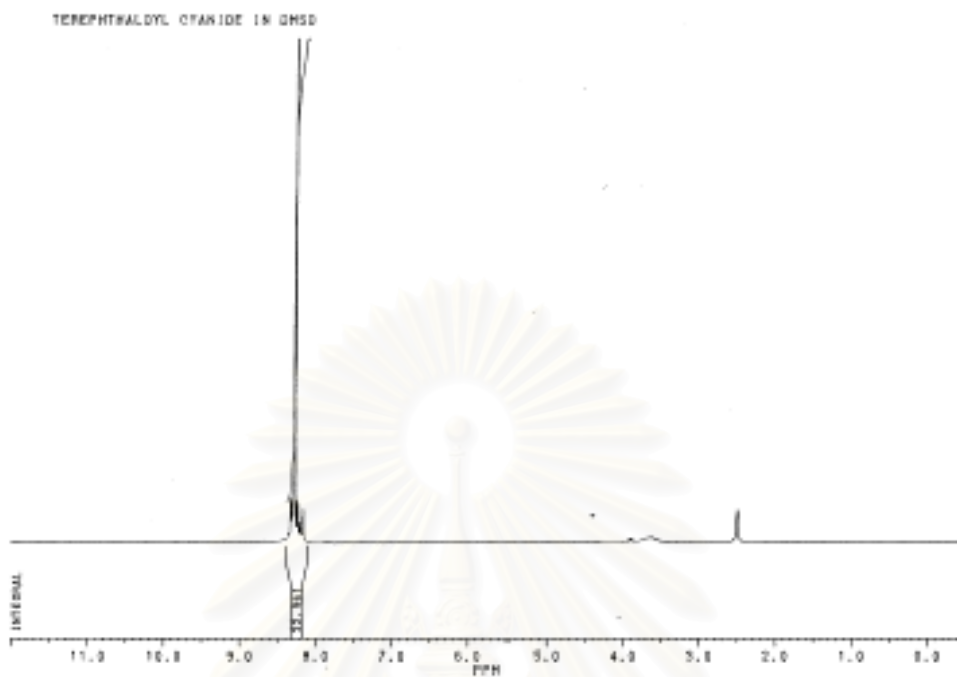


Figure A11 : 200 MHz  $^1\text{H}$  NMR spectrum of terephthaloyl cyanide (DMSO)

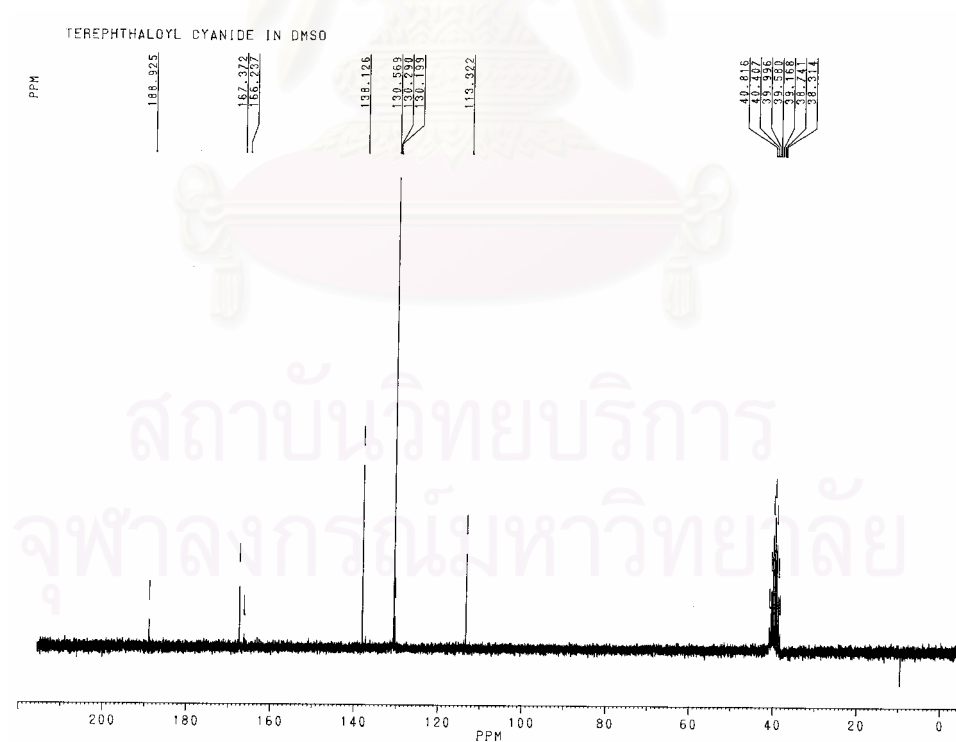


Figure A12 : 50 MHz  $^{13}\text{C}$  NMR spectrum of terephthaloyl cyanide (DMSO)

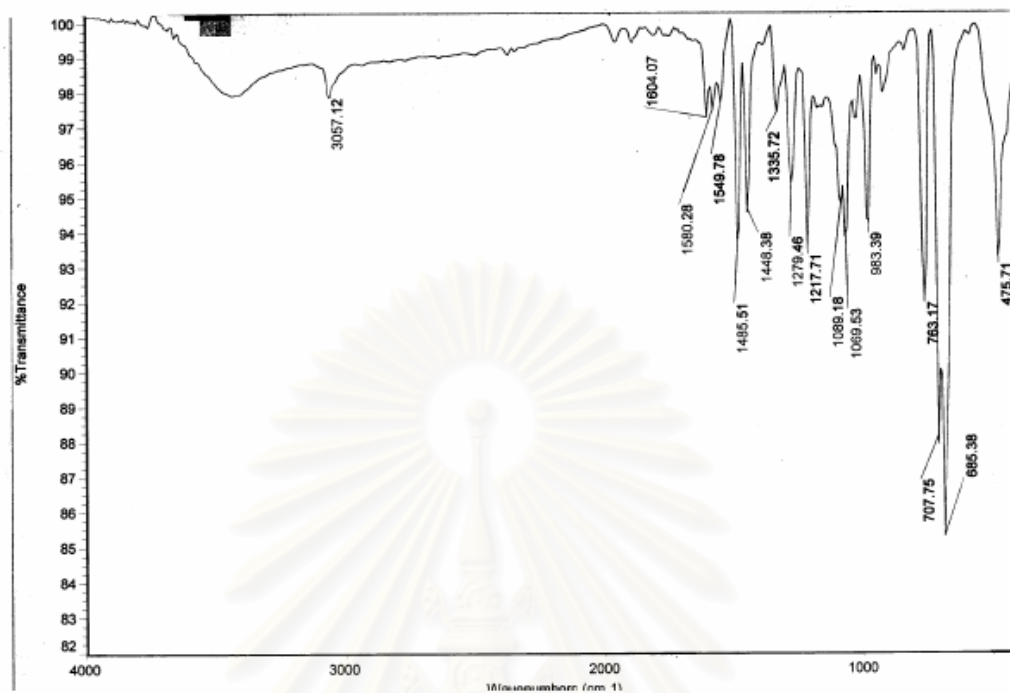


Figure A13 : IR spectrum of 4-chloro-2,5-diphenyloxazole (KBr pellet)

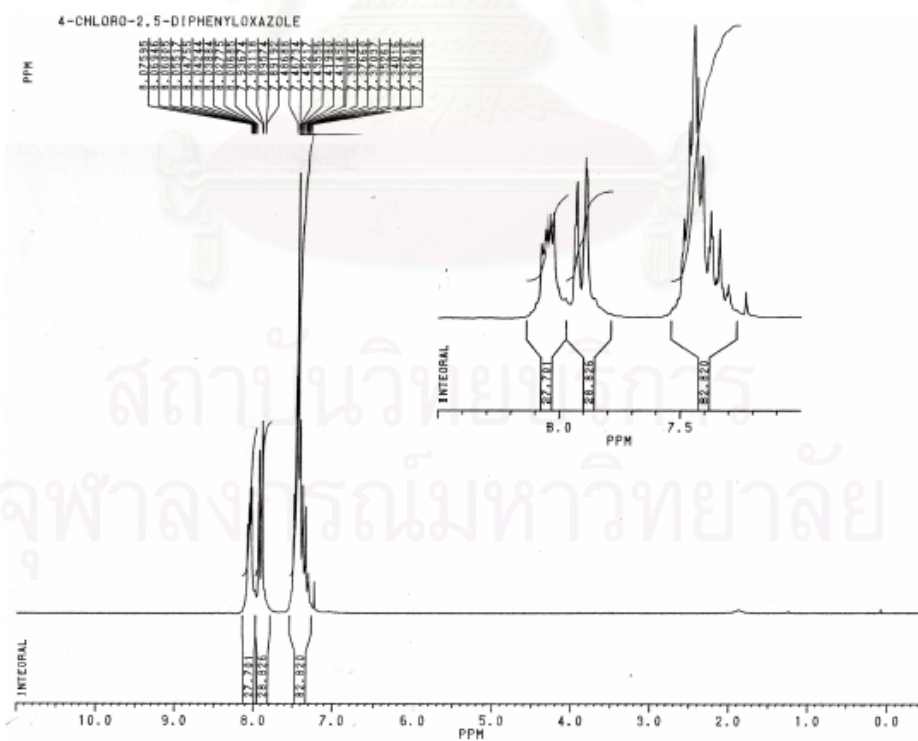


Figure A14 : 200 MHz  $^1\text{H}$  NMR spectrum of 4-chloro-2,5-diphenyloxazole ( $\text{CDCl}_3$ )

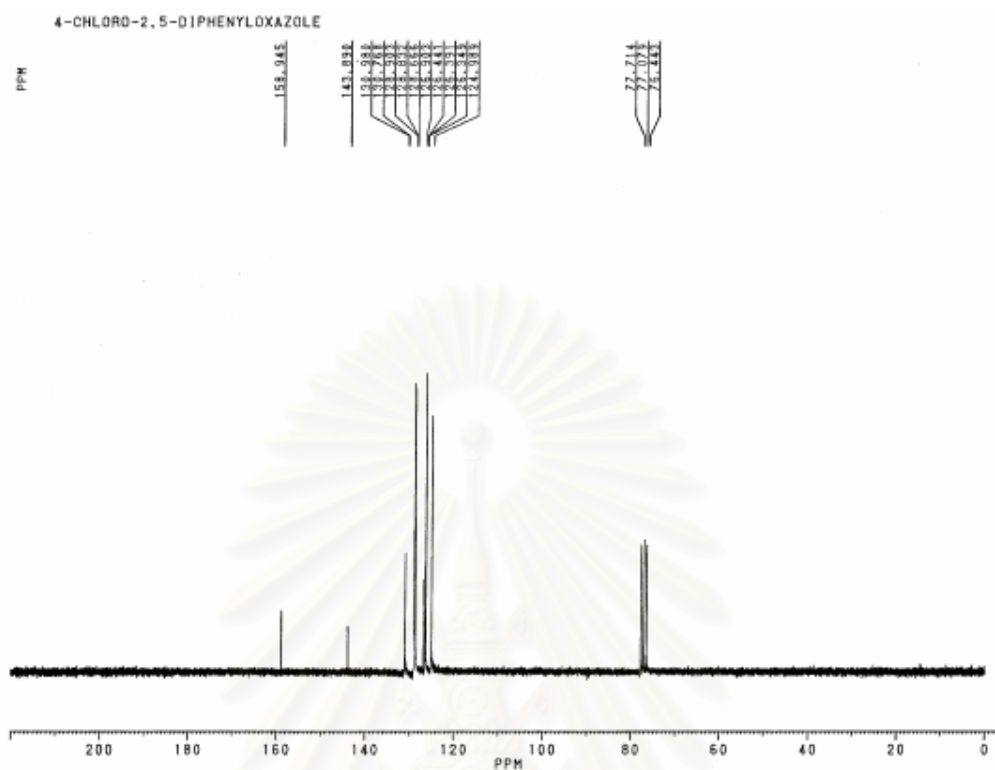


Figure A15 : 50 MHz  $^{13}\text{C}$  NMR spectrum of 4-chloro-2,5-diphenyloxazole ( $\text{CDCl}_3$ )

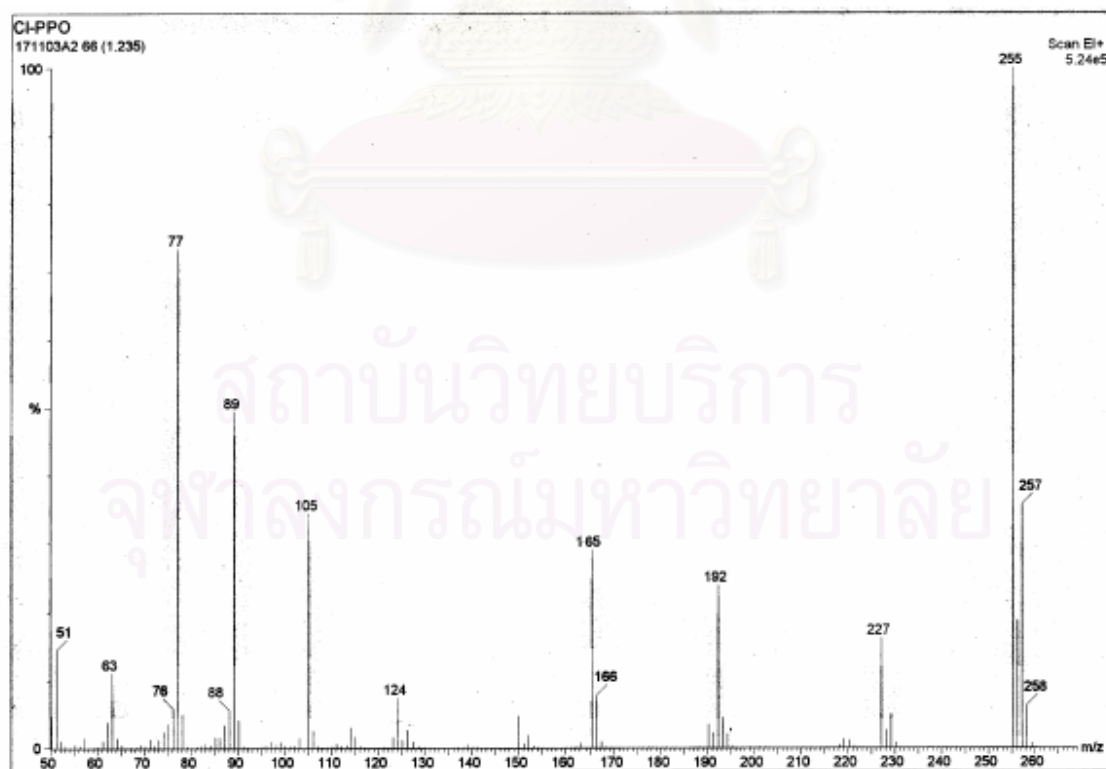


Figure A16 : Mass spectrum of 4-chloro-2,5-diphenyloxazole

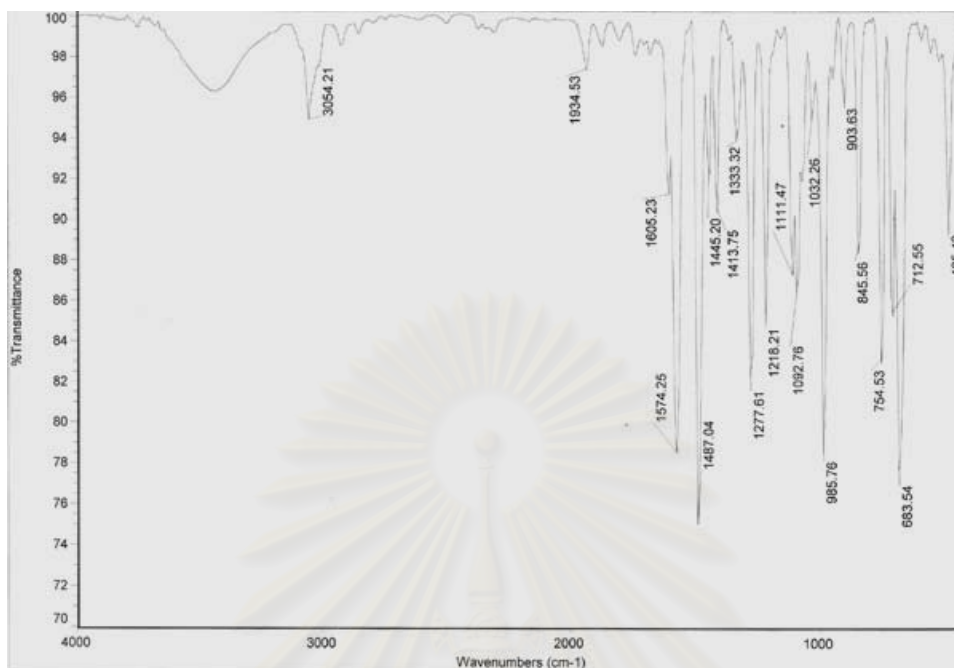


Figure A17 : IR spectrum of 1,4-bis(4-chloro-5-phenyloxazol-2-yl)benzene (KBr pellet)

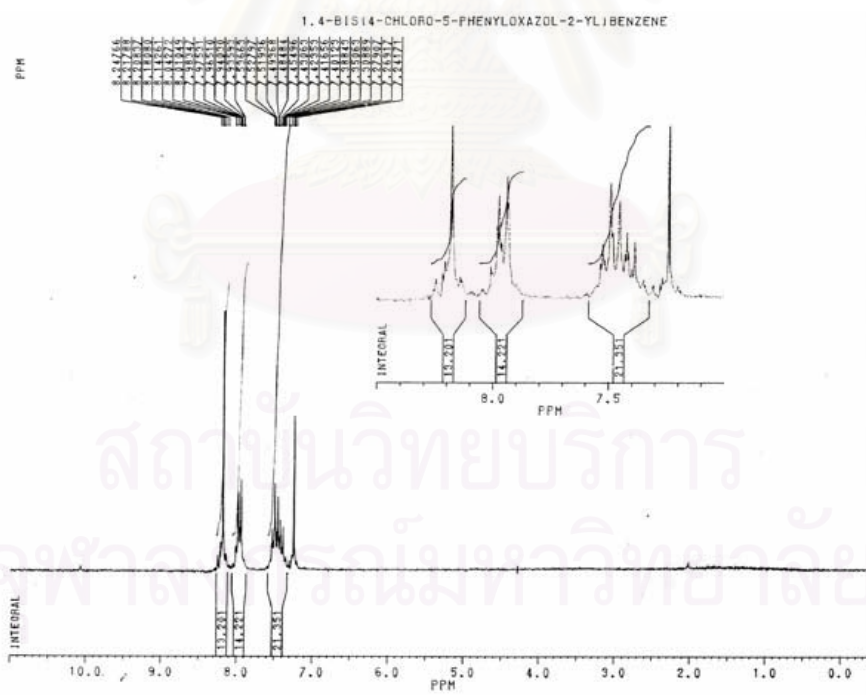


Figure A18: 200 MHz <sup>1</sup>H NMR spectrum of 1,4-bis(4-chloro-5-phenyloxazol-2-yl)benzene (CDCl<sub>3</sub>)





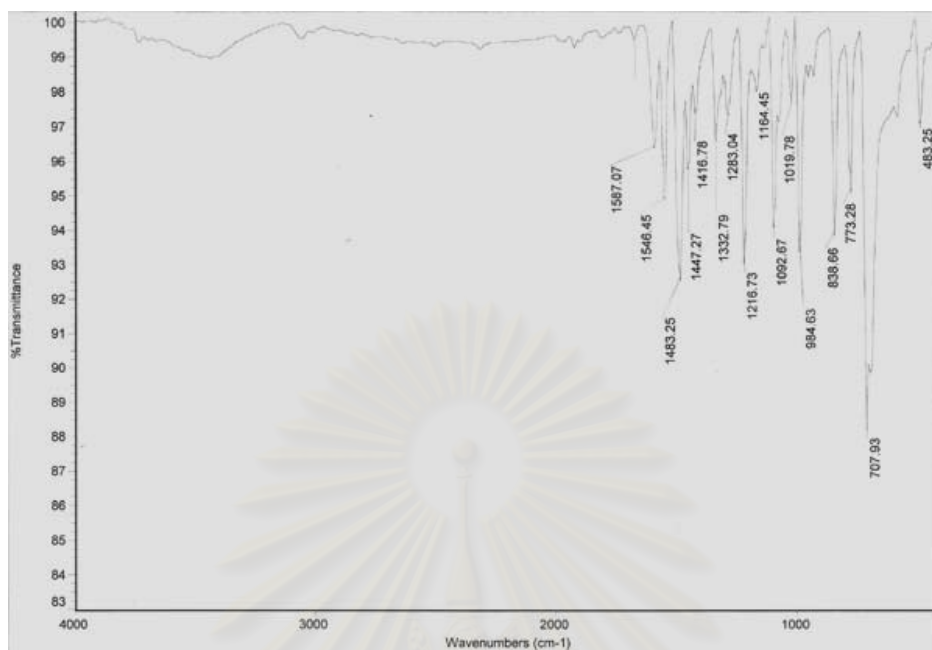


Figure A21 : IR spectrum of 1,4-bis(4-chloro-2-phenyloxazol-5-yl)benzene (KBr pellet)

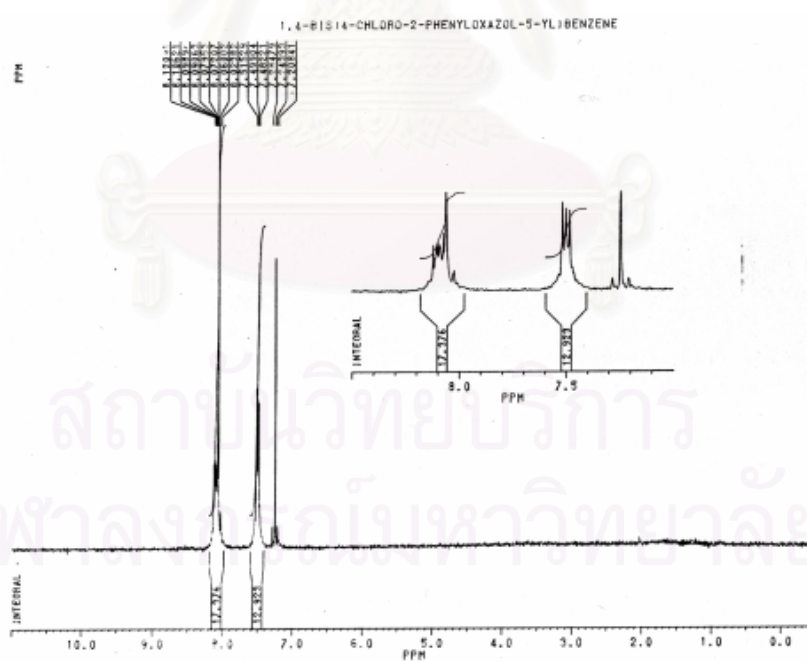


Figure A22 : 200 MHz  $^1\text{H}$  NMR spectrum of 1,4-bis(4-chloro-2-phenyloxazol-5-yl)benzene ( $\text{CDCl}_3$ )

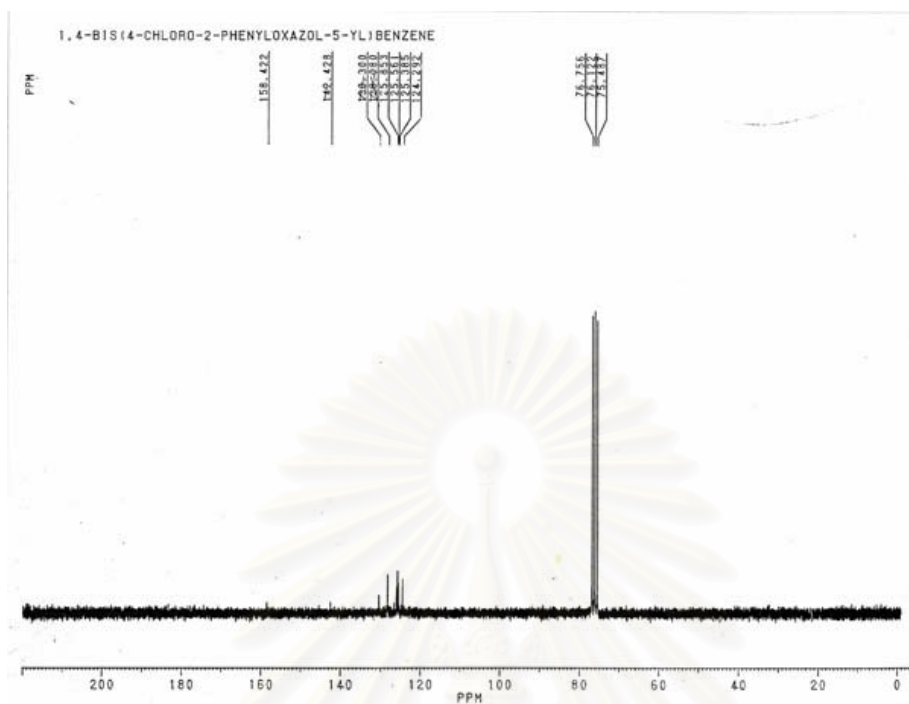


Figure A23 : 50 MHz  $^{13}\text{C}$  NMR spectrum of 1,4-bis(4-chloro-2-phenyloxazol-5-yl)benzene ( $\text{CDCl}_3$ )

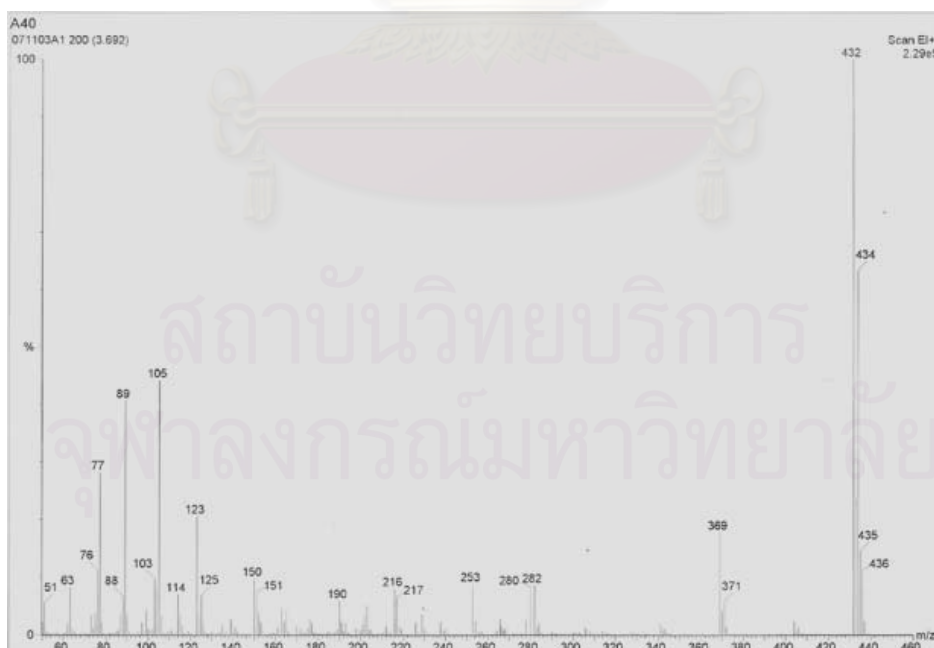


Figure A24 : Mass spectrum of 1,4-bis(4-chloro-2-phenyloxazol-5-yl)benzene

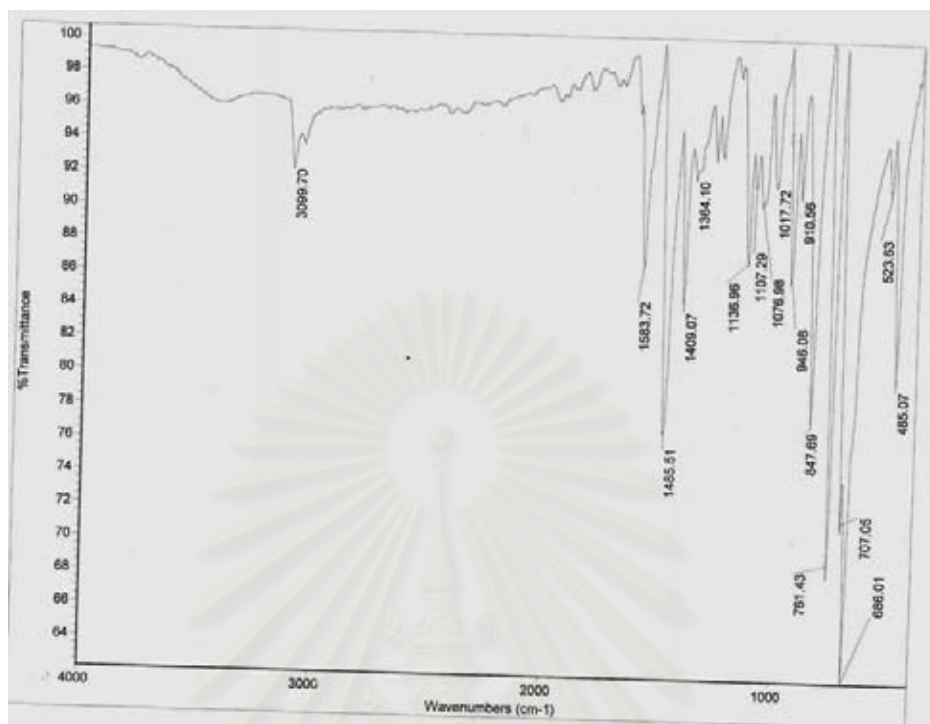


Figure A25 : IR spectrum of 1,4-bis(5-phenyloxazol-2-yl)benzene (KBr pellet)

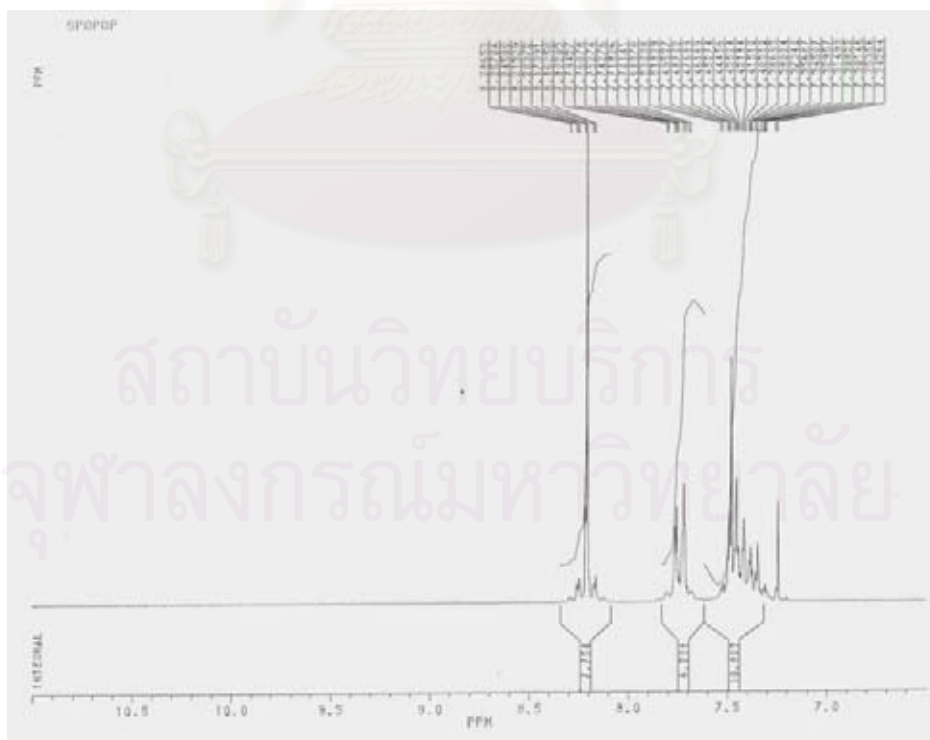


Figure A26 : 200 MHz <sup>1</sup>H NMR spectrum of 1,4-bis(5-phenyloxazol-2-yl)benzene (CDCl<sub>3</sub>)

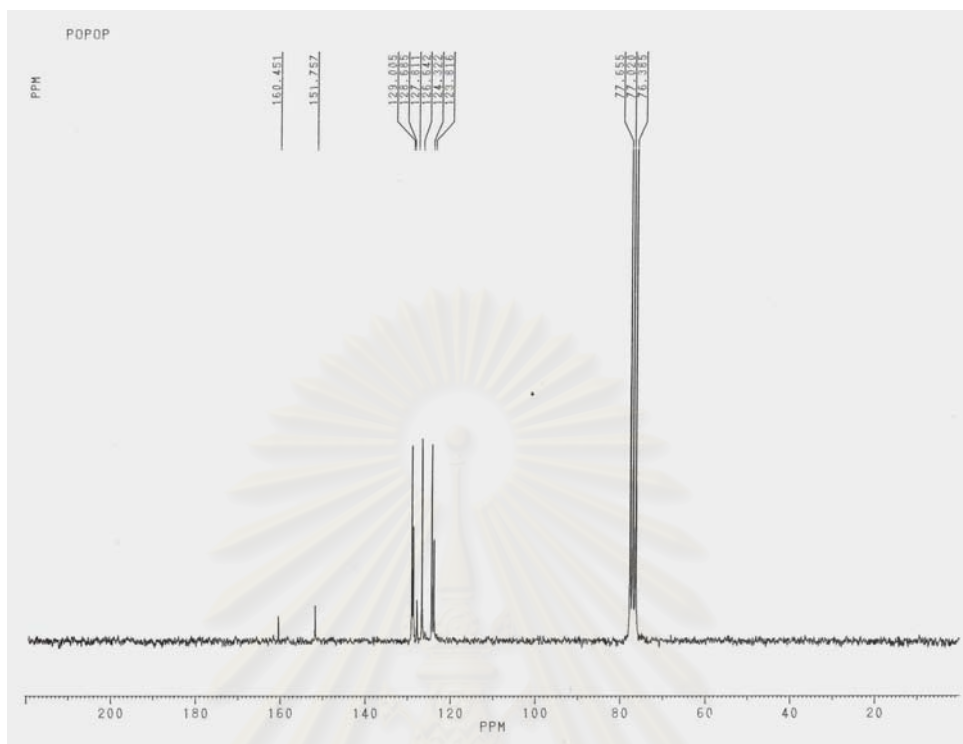


Figure A27 : 50 MHz  $^{13}\text{C}$  NMR spectrum of 1,4-bis(5-phenyloxazol-2-yl)benzene ( $\text{CDCl}_3$ )

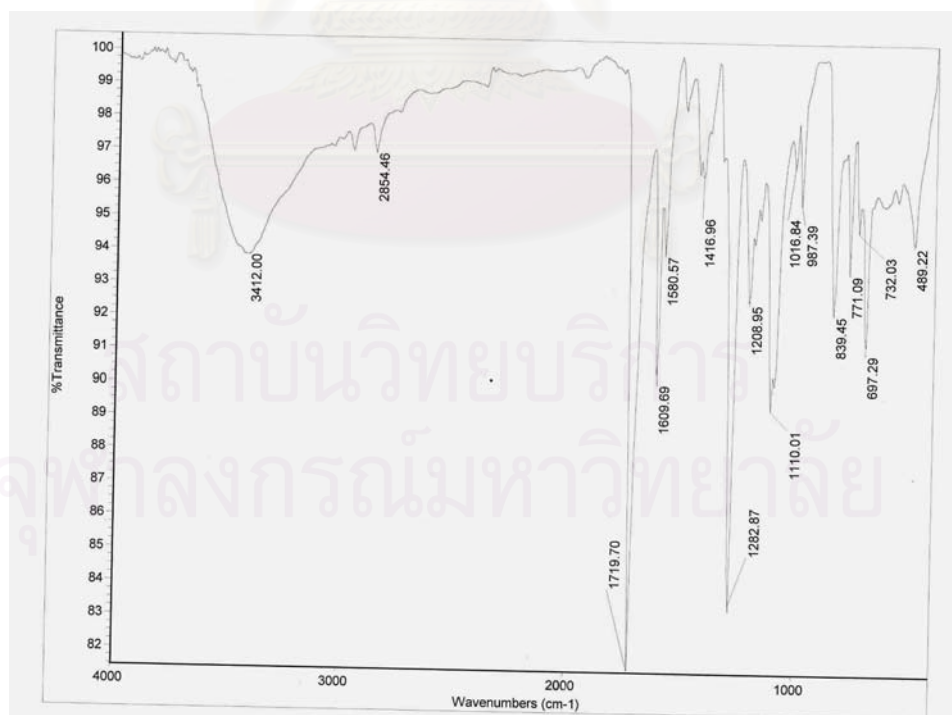


Figure A28 : IR spectrum of Oligomer [11] (KBr pellet)

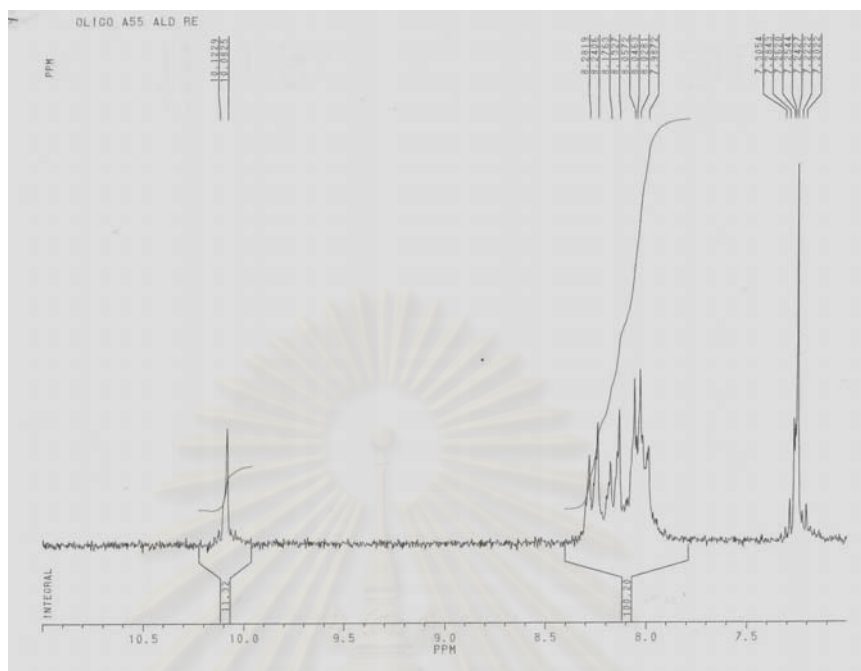


Figure A29 : 200 MHz  $^1\text{H}$  NMR spectrum of Oligomer [11] ( $\text{CDCl}_3$ )

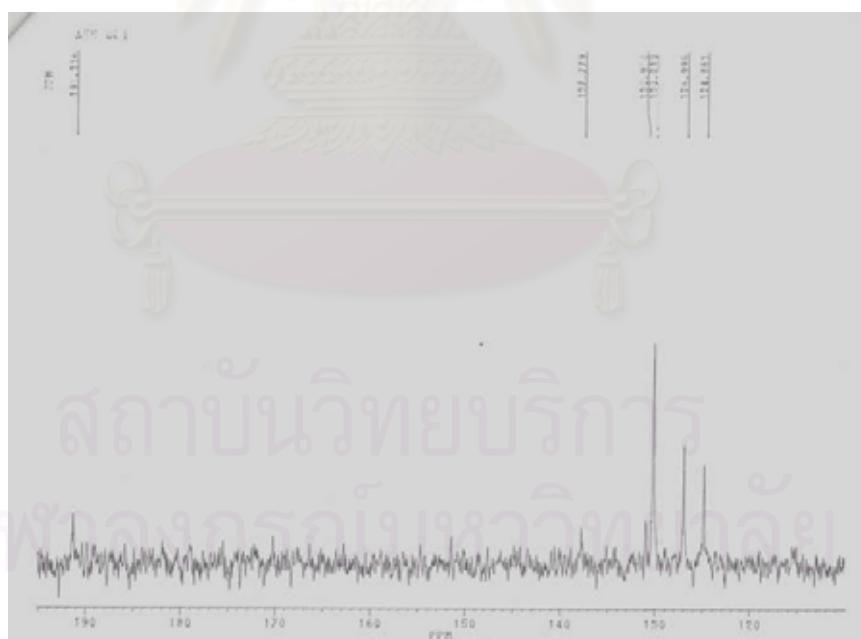


Figure A30 : 50 MHz  $^{13}\text{C}$  NMR spectrum of Oligomer [11] ( $\text{CDCl}_3$ )

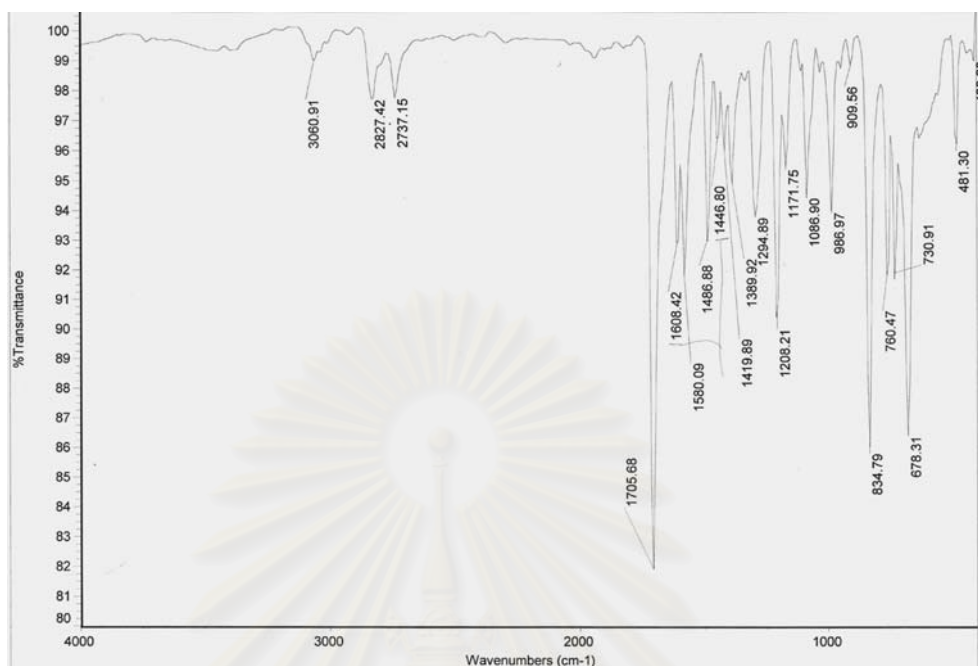


Figure A31 : IR spectrum of 4-(4-chloro-5-phenyloxazol-2-yl)-benzaldehyde[12] (KBr)

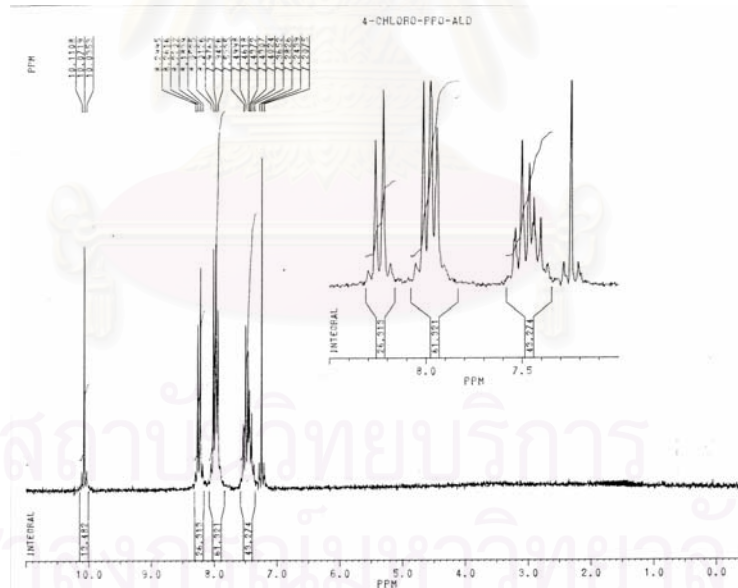
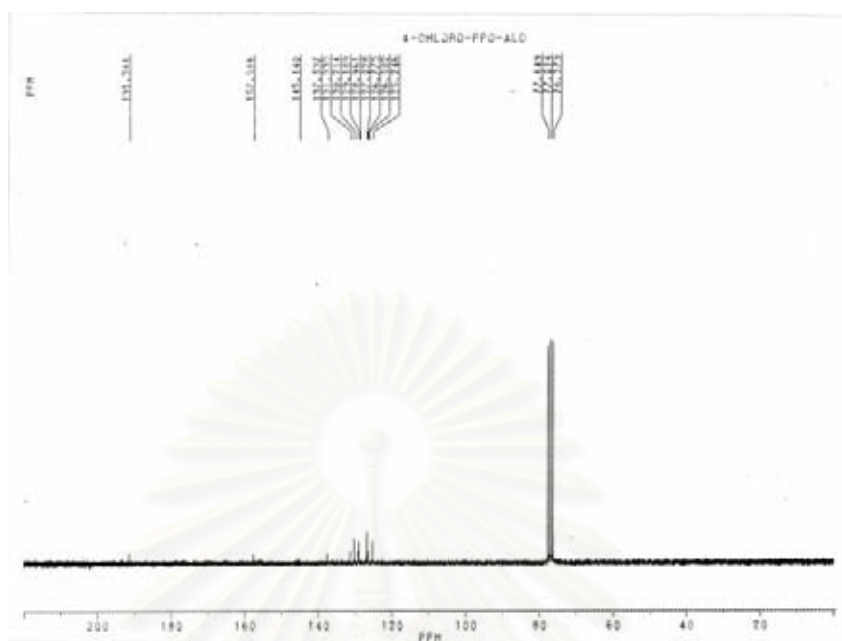
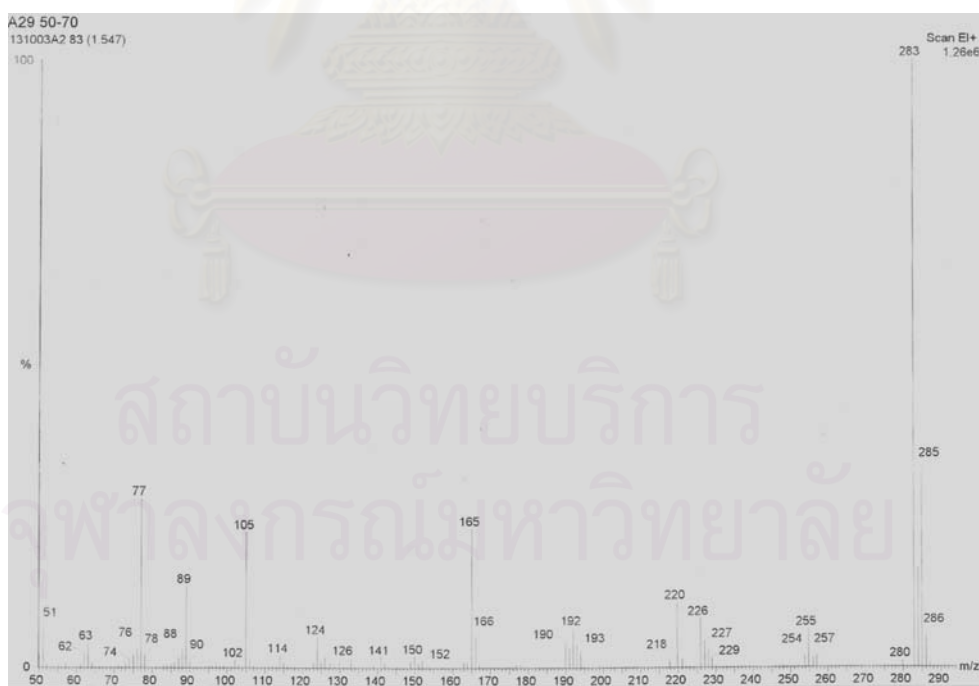


Figure A32 : 200 MHz  $^1\text{H}$  NMR spectrum of 4-(4-chloro-5-phenyloxazol-2-yl)-benzaldehyde[12] ( $\text{CDCl}_3$ )



**Figure A33** : 50MHz <sup>13</sup>C NMR spectrum of 4-(4-chloro-5-phenyloxazol-2-yl)-benzaldehyde[12]  
(CDCl<sub>3</sub>)



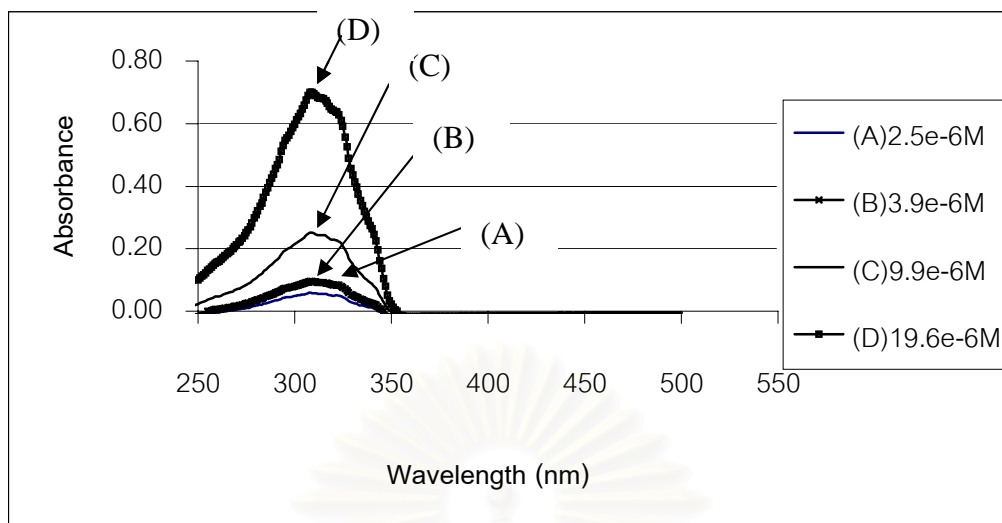
**Figure A34** : Mass spectrum of 4-(4-chloro-5-phenyloxazol-2-yl)-benzaldehyde[12]



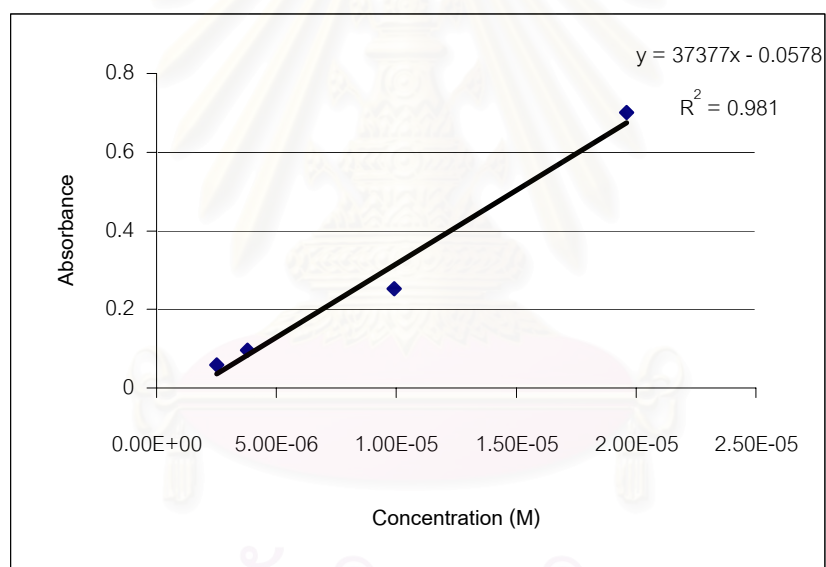


Appendix B

สถาบันวิทยบริการ  
จุฬาลงกรณ์มหาวิทยาลัย



(a)

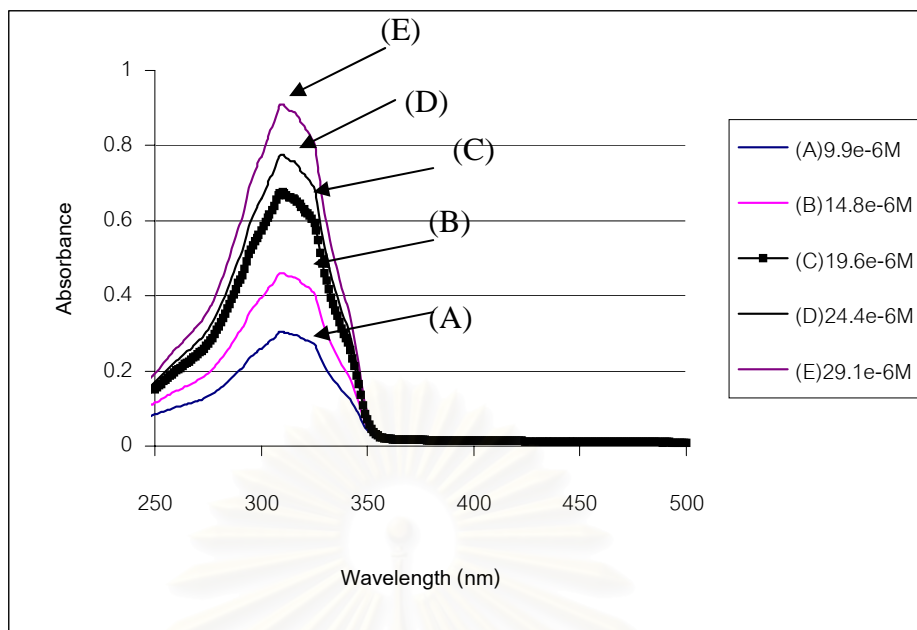


(b)

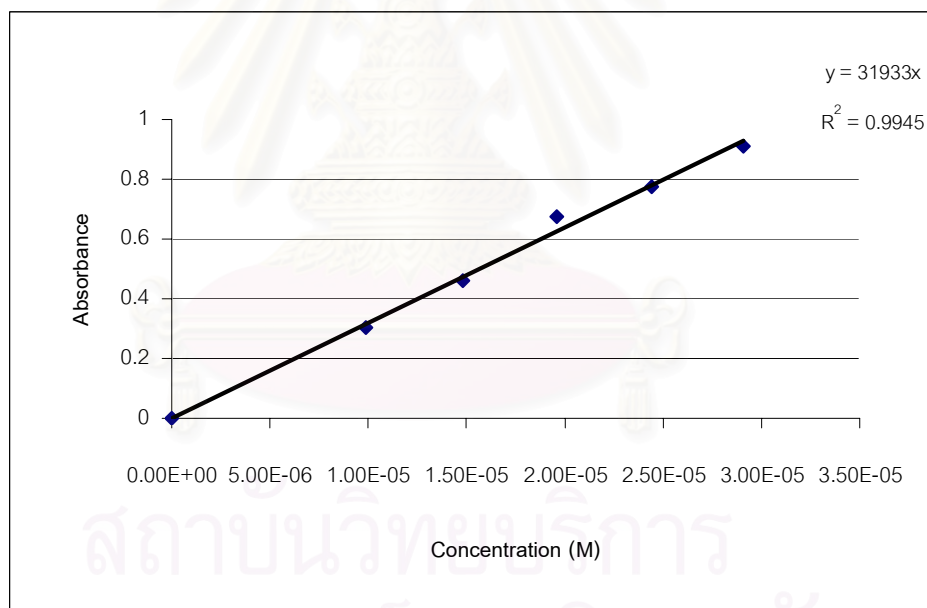
**Figure B1** (a) UV absorption spectra of 4-chloro-2,5-diphenyloxazole[6] in THF

(b) Calibration curve of [6] between Absorbance and Concentration (M) in THF,

$\lambda_{\text{ex}} = 308 \text{ nm}$ .

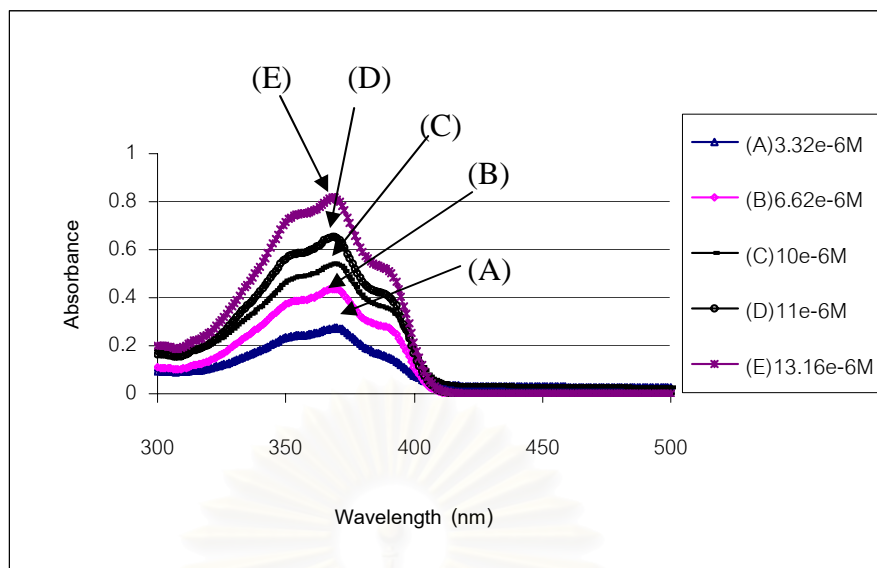


(a)

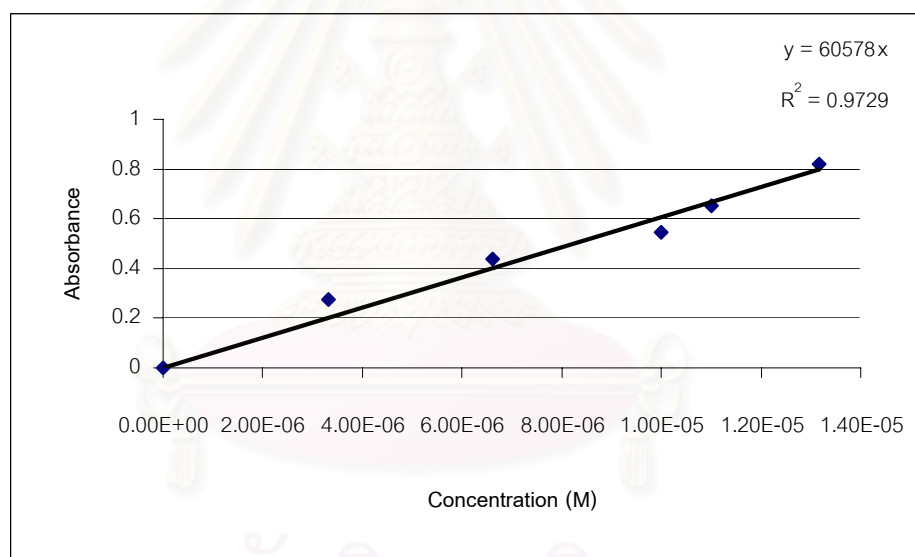


(b)

**Figure B2** (a) UV absorption spectra of 4-chloro-2,5-diphenyloxazole[6] in dichloromethane, (b) Calibration curve of [6] between Absorbance and Concentration (M) in dichloromethane,  $\lambda_{\text{ex}} = 310 \text{ nm}$ .



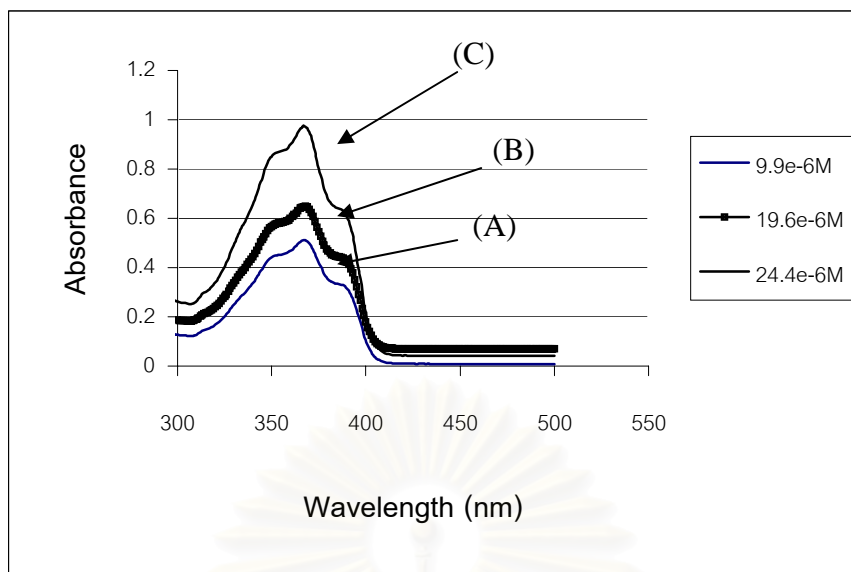
(a)



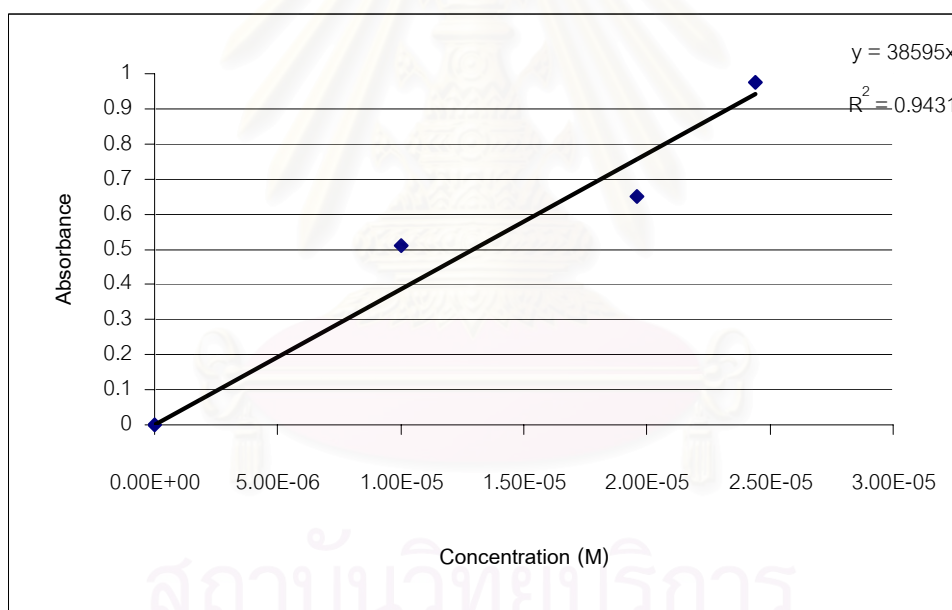
(b)

**Figure B3** (a) UV absorption spectra of 1,4-bis(4-chloro-5-phenyloxazol-2-yl)benzene [8] in dichloromethane

(b) Calibration curve of [8] between Absorbance and Concentration (M) in dichloromethane,  $\lambda_{\text{ex}} = 369$  nm.



(a)

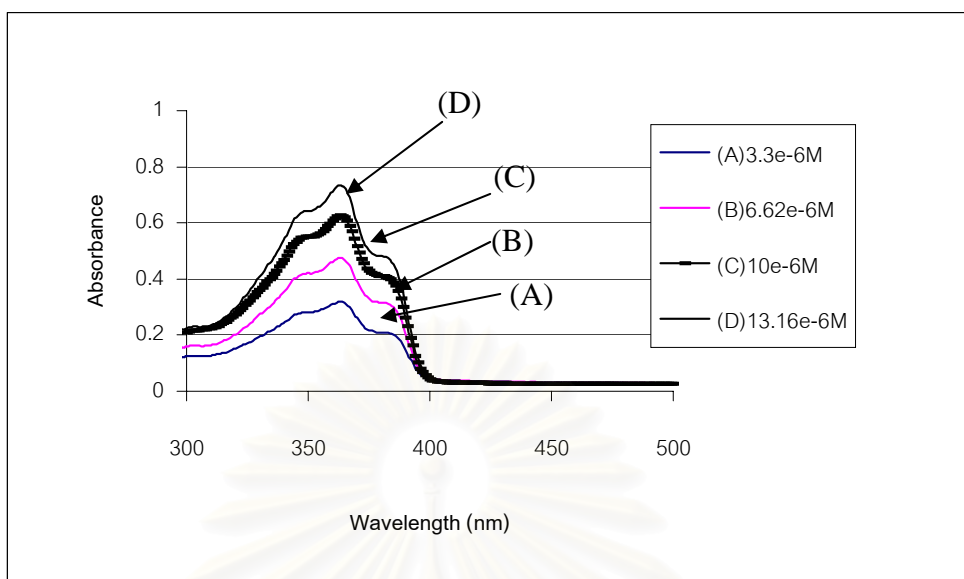


(b)

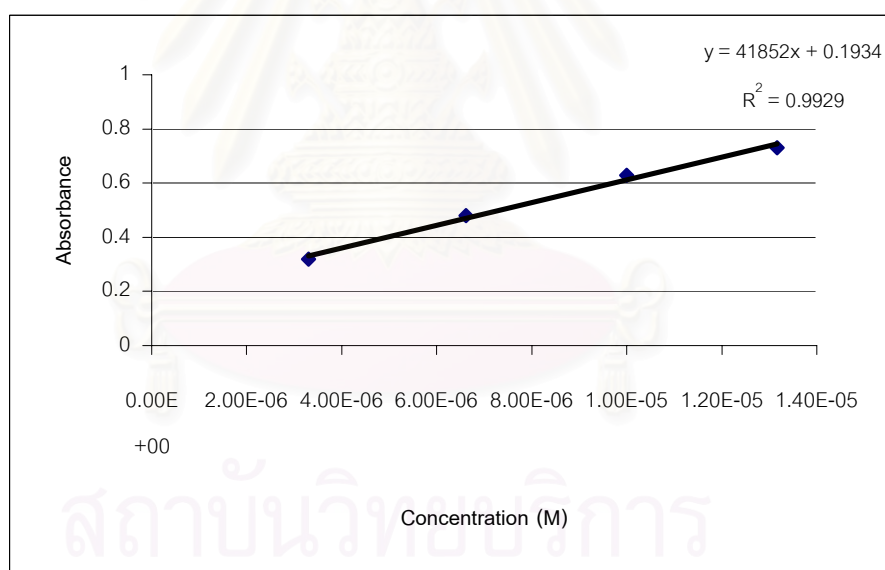
**Figure B4** (a) UV absorption spectra of 1,4-bis(4-chloro-5-phenyloxazol-2-yl)benzene **[8]** in *n*-butanol

(b) Calibration curve of **[8]** between Absorbance and Concentration (M) in *n*-butanol,

$\lambda_{\text{ex}} = 368 \text{ nm}$ .

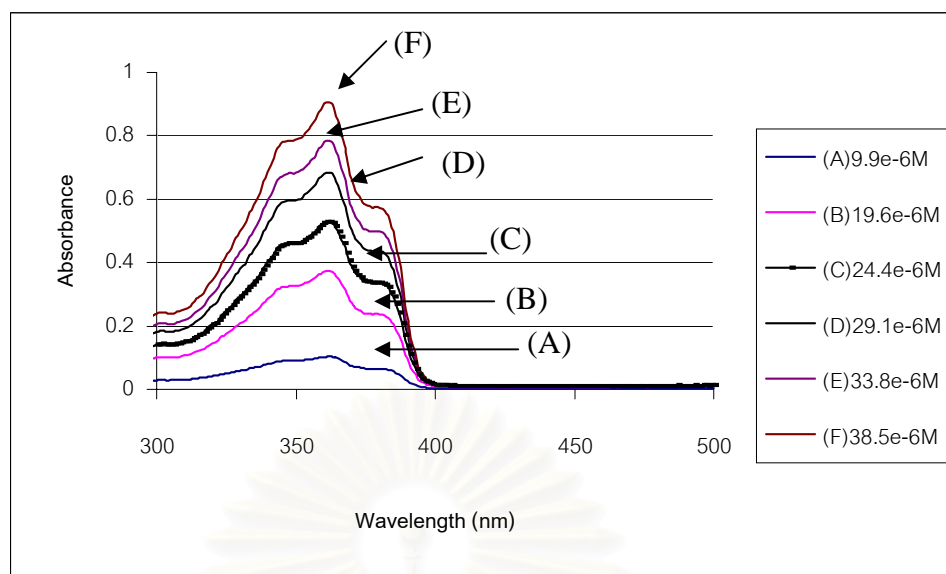


(a)

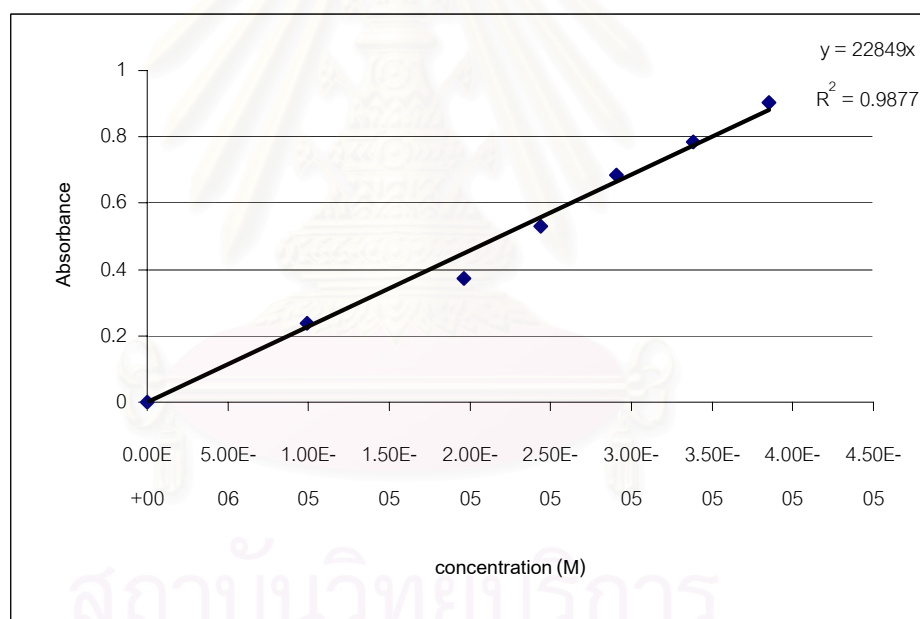


(b)

**Figure B5** (a) UV absorption spectra of 1,4-bis(4-chloro-2-phenyloxazol-5-yl)benzene [9] in dichloromethane  
 (b) Calibration curve of [9] between Absorbance and Concentration (M) in dichloromethane,  $\lambda_{\text{ex}} = 363$  nm.



(a)

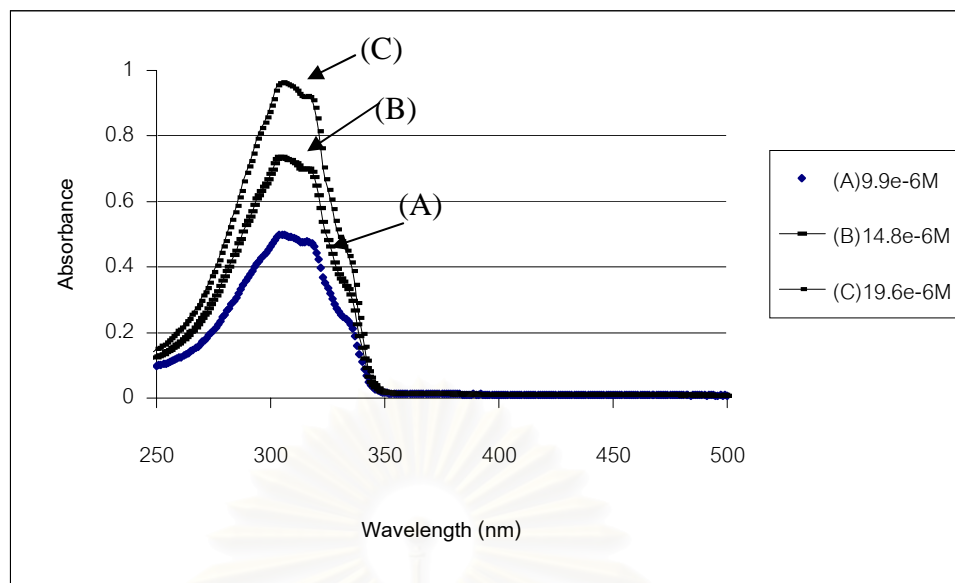


(b)

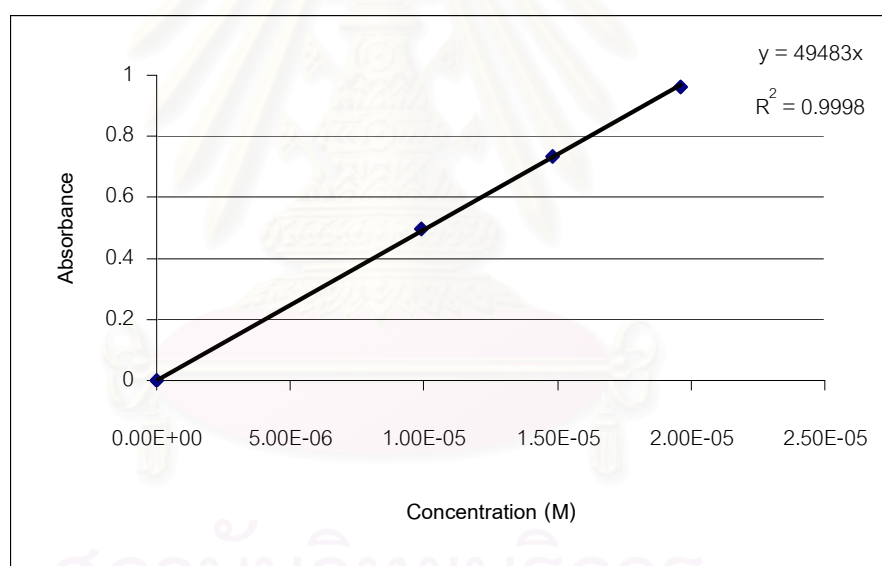
**Figure B6** (a) UV absorption spectra of 1,4-bis(4-chloro-2-phenyloxazol-5-yl)benzene [9] in *n*-butanol

(b) Calibration curve of [9] between Absorbance and Concentration (M) in *n*-butanol,  $\lambda_{\text{ex}} = 362$  nm.





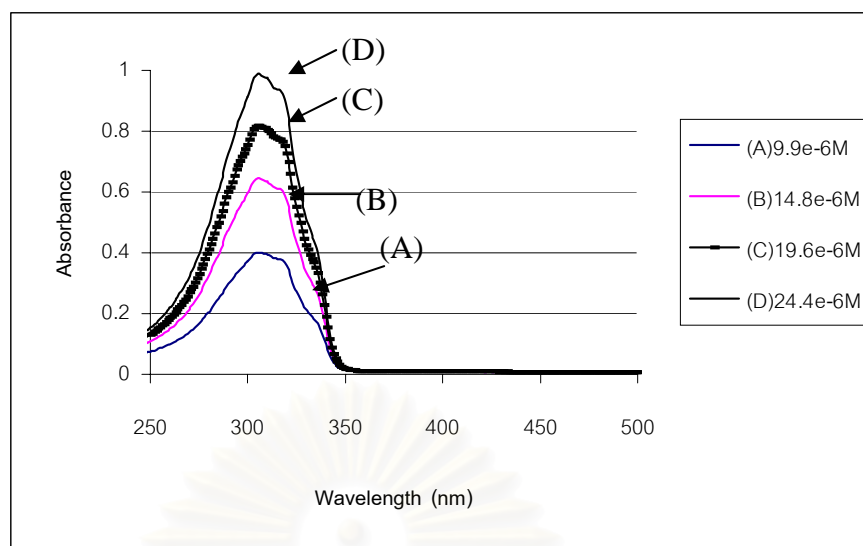
(a)



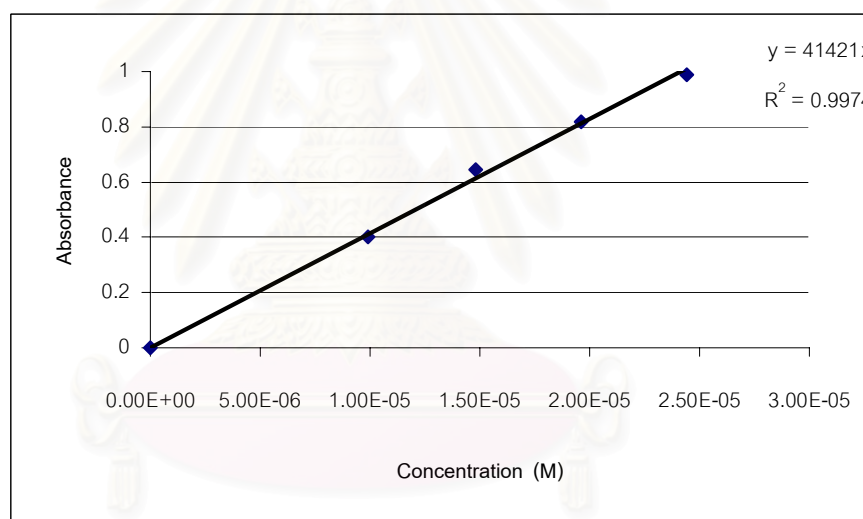
(b)

**Figure B7** (a) UV absorption spectra of 2,5-diphenyloxazole in THF

(b) Calibration curve of 2,5-diphenyloxazole between Absorbance and Concentration (M) in THF,  $\lambda_{\text{ex}} = 305 \text{ nm}$ .



(a)

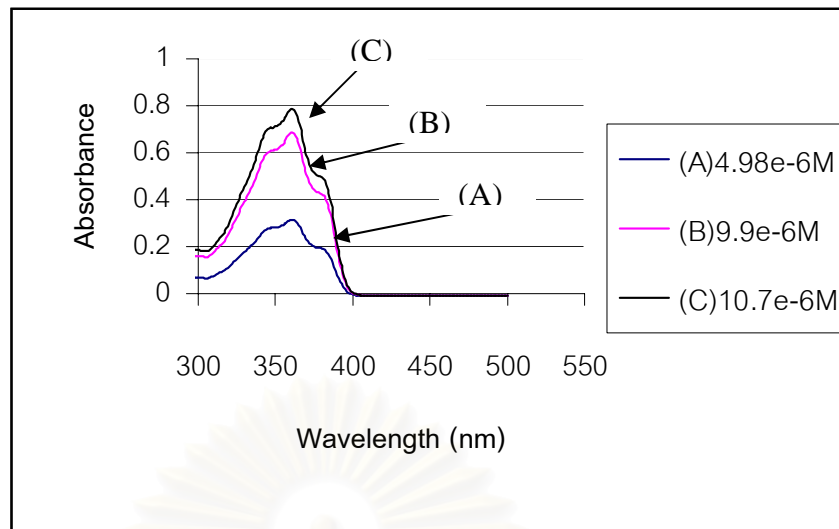


(b)

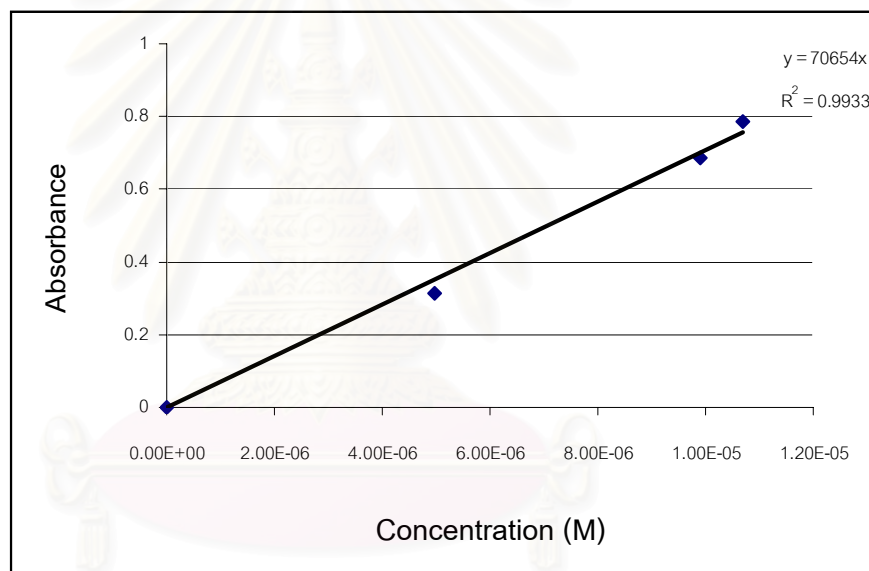
**Figure B8** (a) UV absorption spectra of 2,5-diphenyloxazole in dichloromethane

(b) Calibration curve of 2,5-diphenyloxazole between Absorbance and

Concentration (M) in dichloromethane,  $\lambda_{\text{ex}} = 306 \text{ nm}$ .



(a)

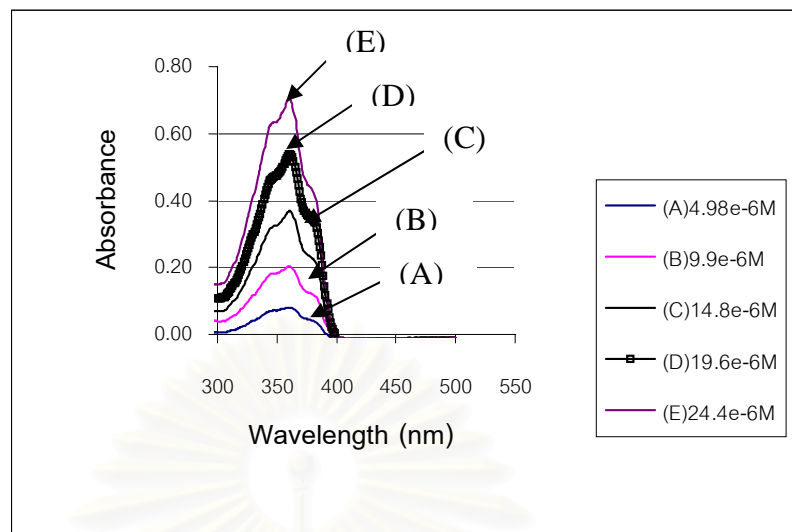


(b)

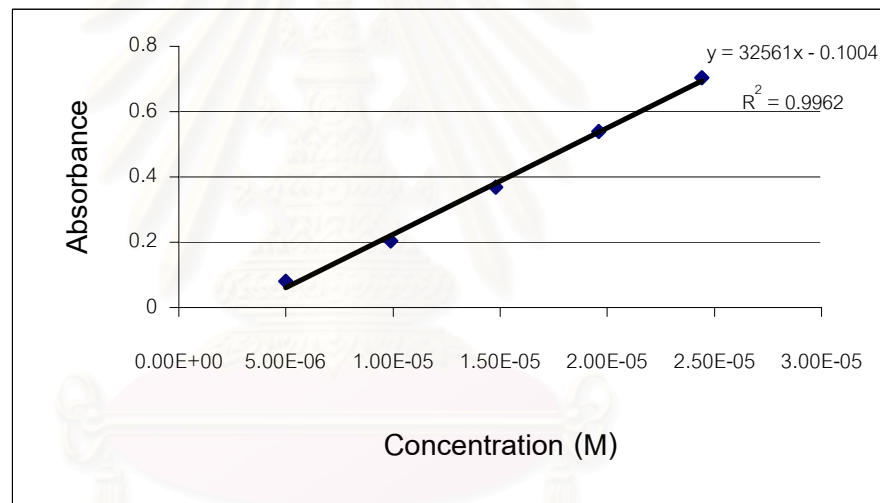
**Figure B9** (a) UV absorption spectra of POPOP in dichloromethane

(b) Calibration curve of POPOP between Absorbance and Concentration (M)

in dichloromethane,  $\lambda_{\text{ex}} = 361 \text{ nm}$ .



(a)

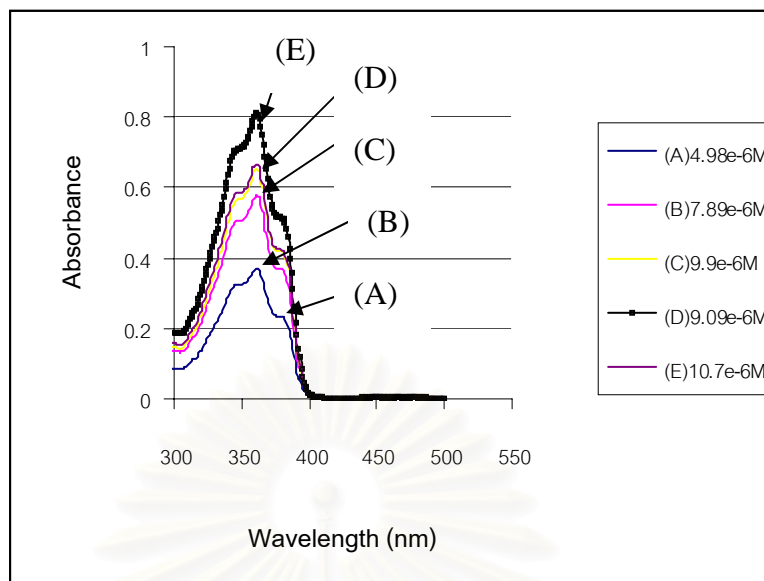


(b)

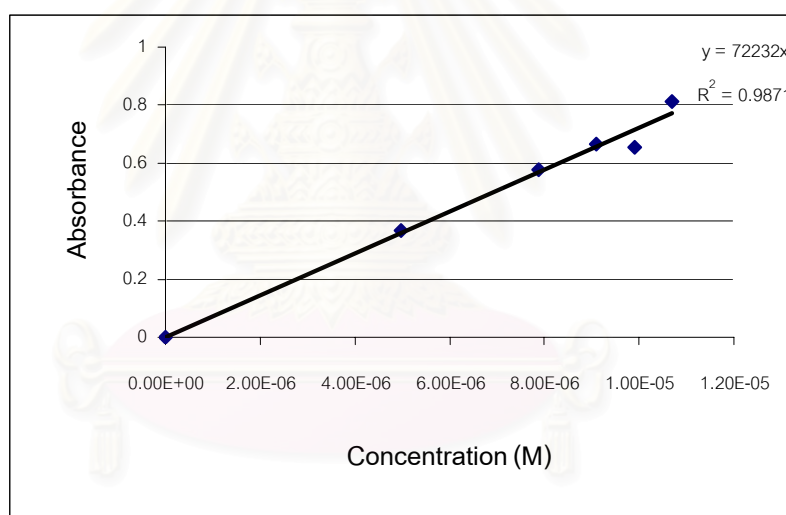
**Figure B10** (a) UV absorption spectra of POPOP in *n*-butanol

(b) Calibration curve of POPOP between Absorbance and Concentration (M)

in *n*-butanol,  $\lambda_{\text{ex}} = 361 \text{ nm}$ .



(a)

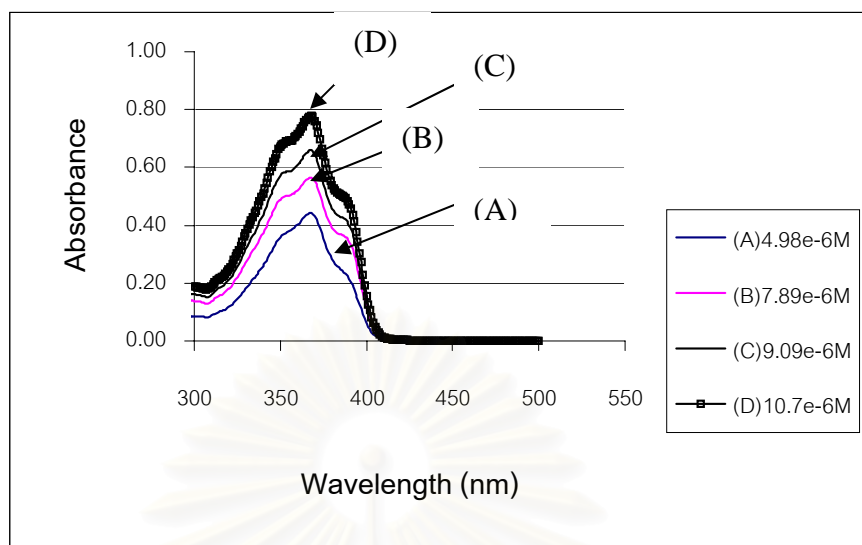


(b)

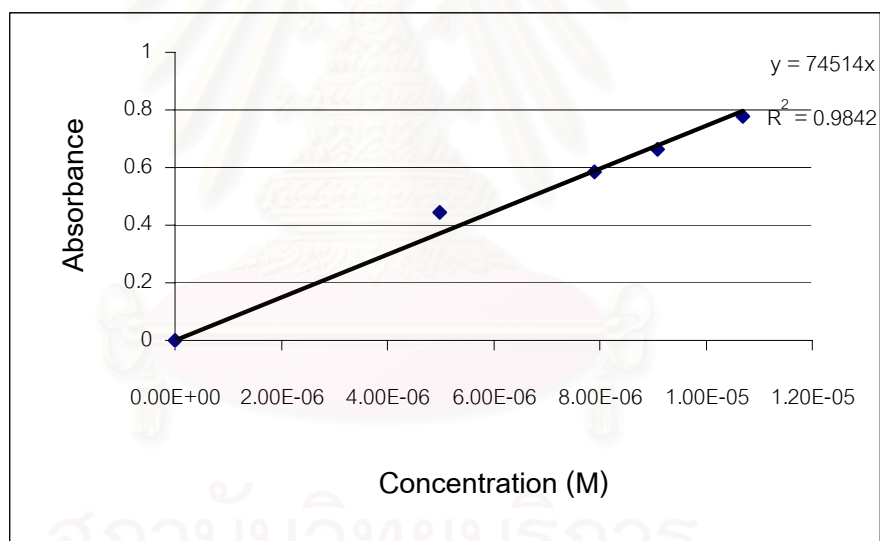
**Figure B11** (a) UV absorption spectra of POPOP in THF

(b) Calibration curve of POPOP between Absorbance and Concentration (M)

in THF,  $\lambda_{\text{ex}} = 361 \text{ nm}$ .



(a)

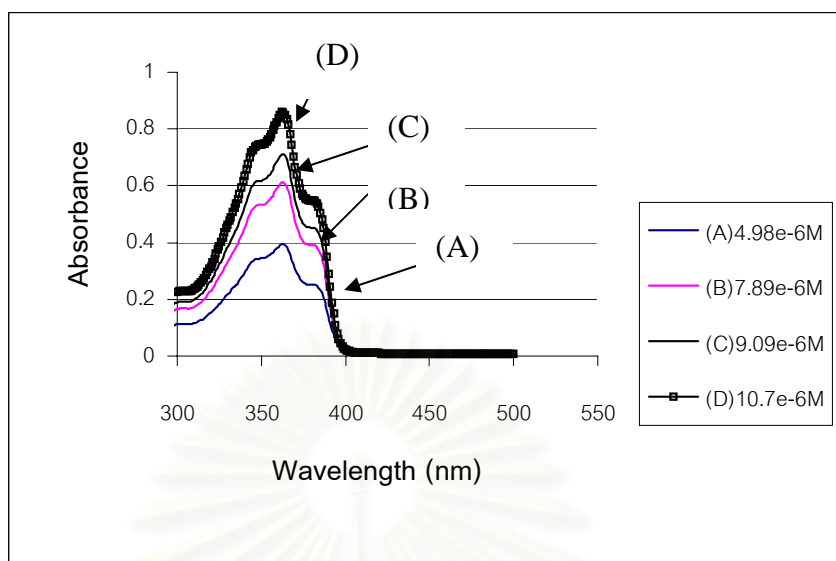


(b)

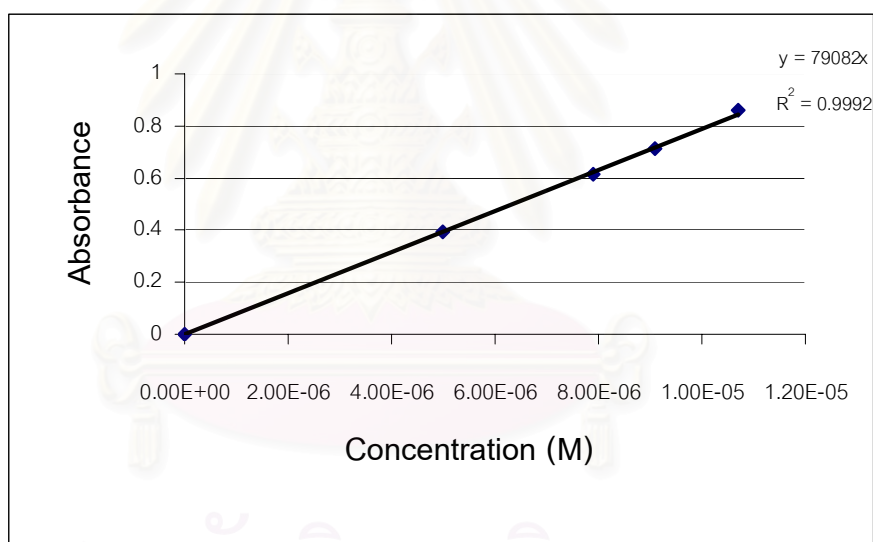
**Figure B12** (a) UV absorption spectra of 1,4-bis(4-chloro-5-phenyloxazol-2-yl)benzene [8] in THF

(b) Calibration curve of [8] between Absorbance and Concentration (M) in THF,

$$\lambda_{\text{ex}} = 368 \text{ nm.}$$



(a)



(b)

**Figure B13** (a) UV absorption spectra of 1,4-bis(4-chloro-2-phenyloxazol-5-yl)benzene [9] in THF

(b) Calibration curve of [9] between Absorbance and Concentration (M) in THF,  $\lambda_{\text{ex}} = 363 \text{ nm}$ .



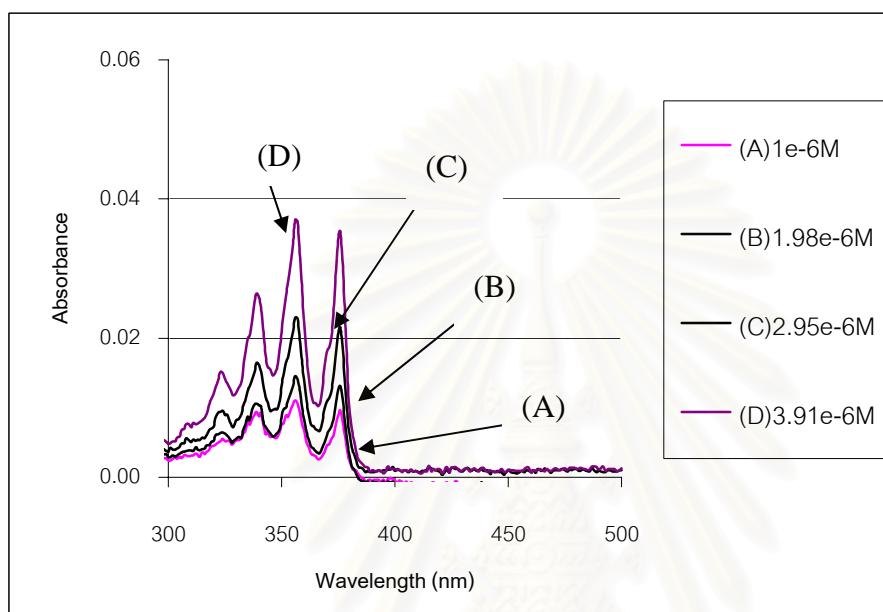
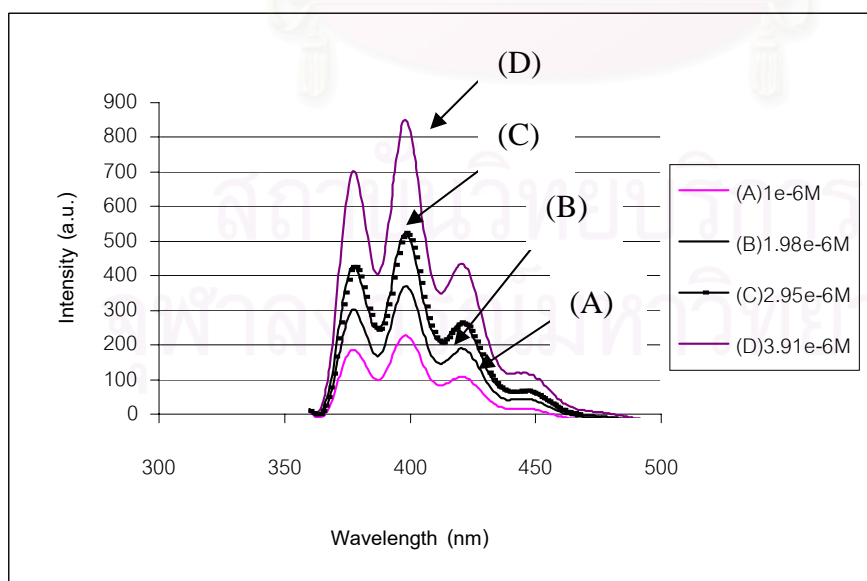


Appendix C

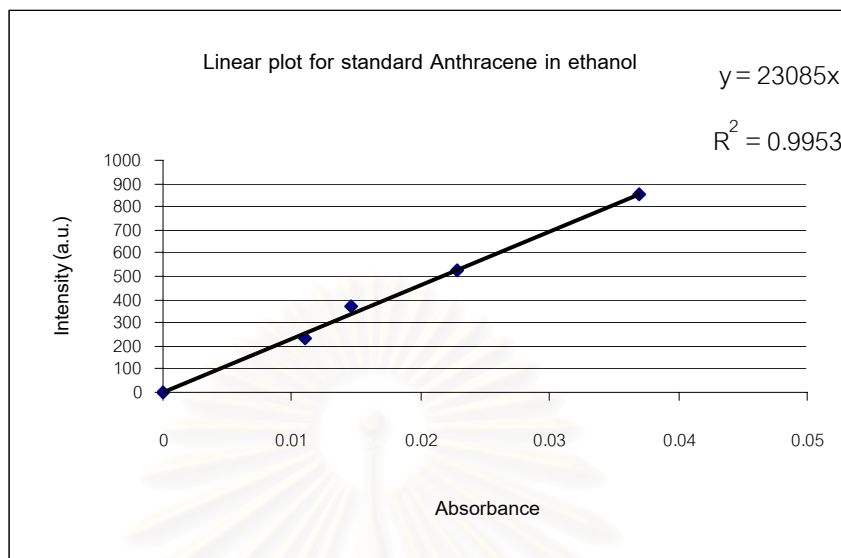
สถาบันวิทยบริการ  
จุฬาลงกรณ์มหาวิทยาลัย

Figure C1. Data Fluorescence Spectrum of Standard Anthracene in Ethanol

## 1. Fluorescence Spectrum

1.1 Excitation spectra,  $\lambda_{\text{ex}} = 356 \text{ nm}$ 1.2 Emission spectra,  $\lambda_{\text{em}} = 398 \text{ nm}$ 

## 1.3 Linear plot for Anthracene in Ethanol between Intensity vs Absorbance



Slope = 23085

While;

$$\phi_x = \frac{\phi_{st} [\text{slope}_x] [\eta_x^2]}{[\text{slope}_{st}] [\eta_{st}^2]}$$

as x = ethanol

st = ethanol

(Lit. = 0.27 Emission range 360-480 nm) *J.Phys.Chem*,1961,65,229

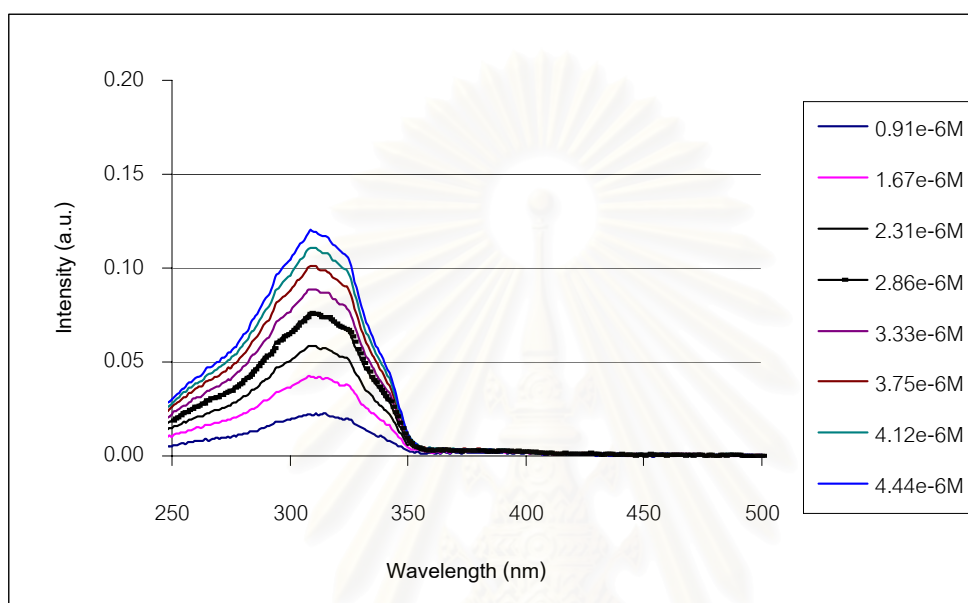
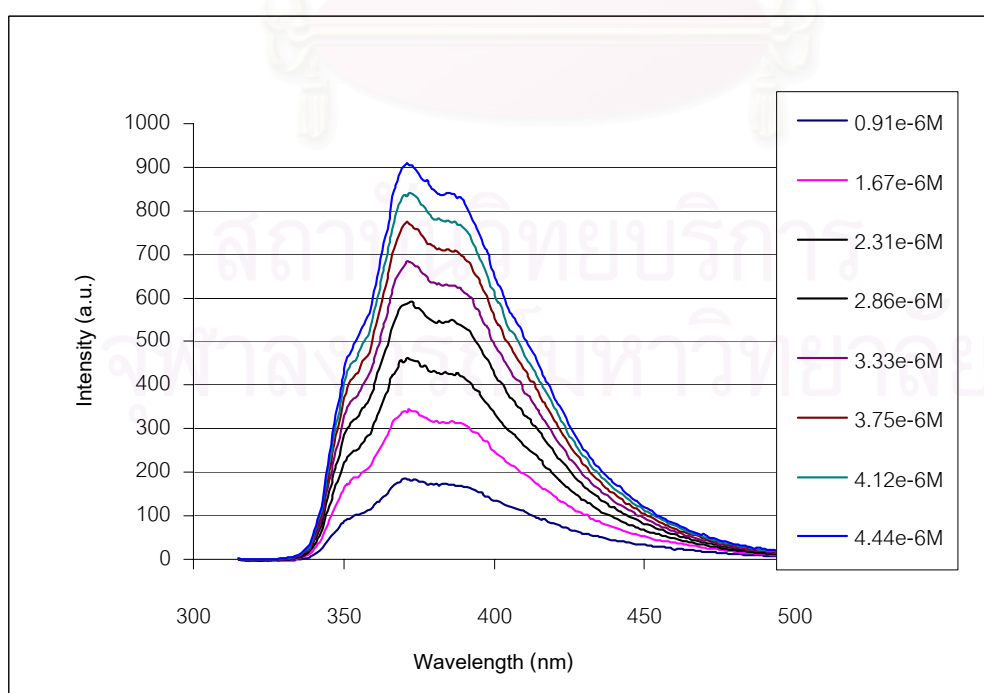
$$= 0.27 [23085] [1.3594^2]$$

$$\frac{[23085] [1.3594^2]}{[23085] [1.3594^2]}$$

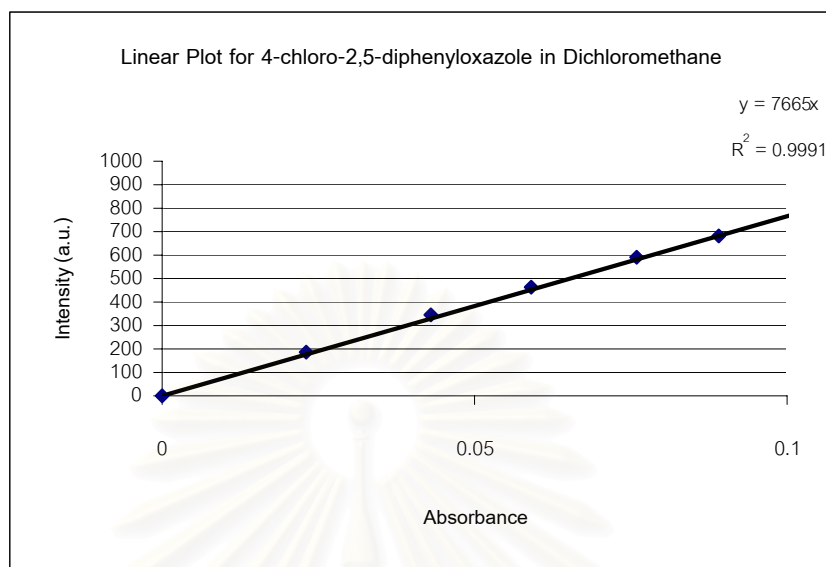
$$= 0.27$$

Figure C2. Data Fluorescence Spectrum of 4-Chloro-2,5-diphenyloxazole in dichloromethane

## 1. Fluorescence Spectrum

1.1 Excitation spectra,  $\lambda_{\text{ex}} = 310 \text{ nm}$ 1.2 Emission spectra,  $\lambda_{\text{em}} = 371 \text{ nm}$ 

## 1.3 Linear plot for 4-chloro-2,5-diphenyloxazole between Intensity vs Absorbance



Slope = 7665

While;

$$\phi_x = \frac{\phi_{st} [\text{slope}_x] [\eta_x^2]}{[\text{slope}_{st}] [\eta_{st}^2]}$$

as x = dichloromethane

st = ethanol

$$= 0.27 [7665] [1.4246^2]$$

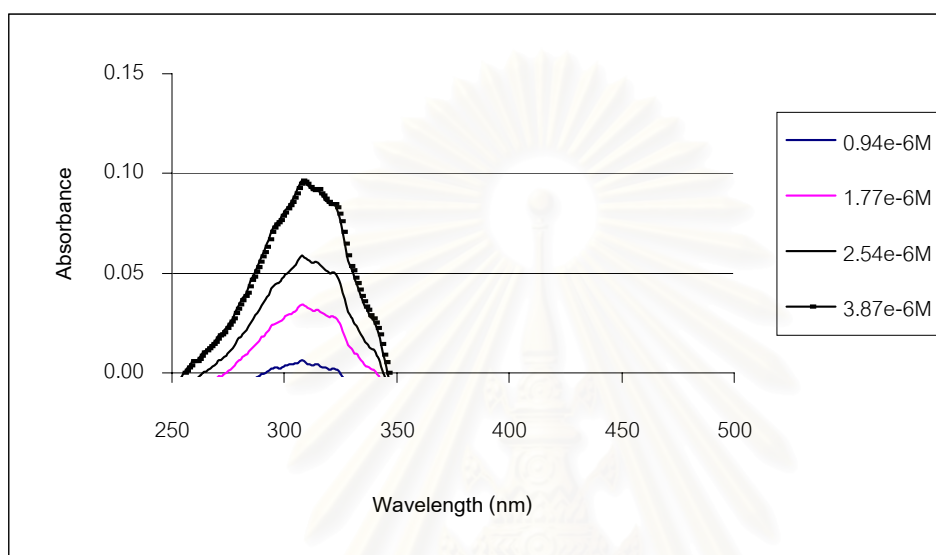
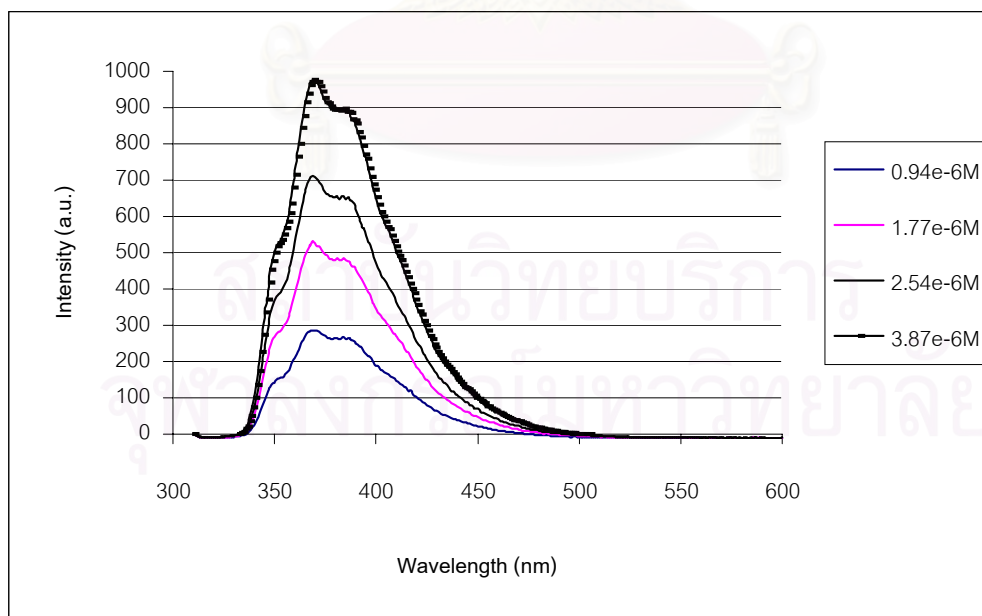
$$\frac{[23085] [1.3594^2]}{[23085] [1.3594^2]}$$

$$= 0.098 = 0.10$$

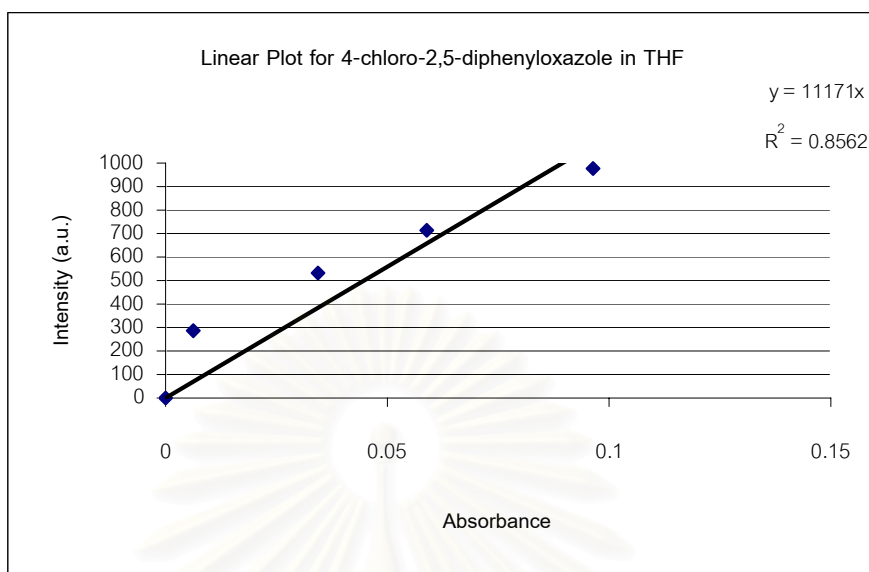
สถาบันวิทยบริการ  
จุฬาลงกรณ์มหาวิทยาลัย

Figure C3. Data Fluorescence Spectrum of 4-Chloro-2,5-diphenyloxazole in THF

## 1. Fluorescence Spectrum

1.1 Excitation spectra,  $\lambda_{\text{ex}} = 307 \text{ nm}$ 1.2 Emission spectra,  $\lambda_{\text{em}} = 369 \text{ nm}$ 

## 1.3 Linear plot for 4-chloro-2,5-diphenyloxazole between Intensity vs Absorbance



Slope = 11171

While;

$$\phi_x = \frac{\phi_{st} [\text{slope}_x] [\eta_x^2]}{[\text{slope}_{st}] [\eta_{st}^2]}$$

as x = THF

st = ethanol

$$= \frac{0.27 [11171] [1.4072^2]}{[23085] [1.3594^2]}$$

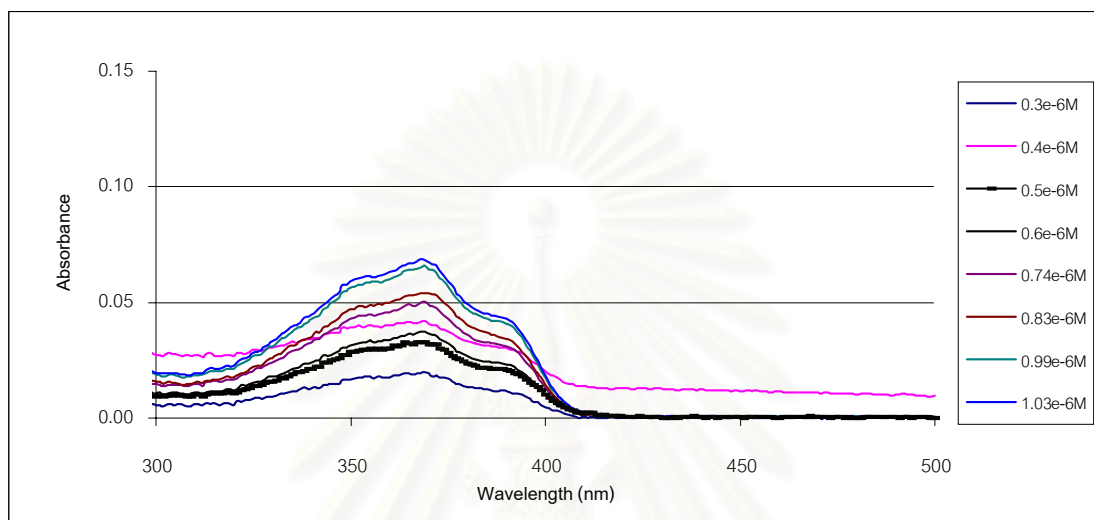
$$= 0.14$$



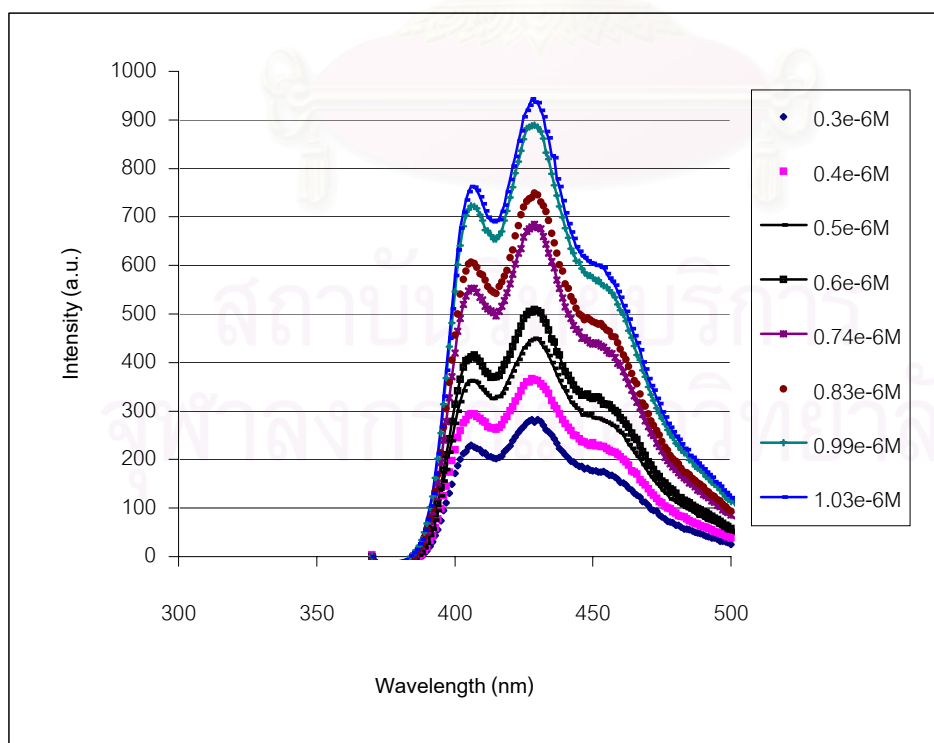
Figure C4. Data Fluorescence Spectrum of 1,4-bis(4-chloro-5-phenyloxazol-2-yl)benzene in dichloromethane

## 2. Fluorescence Spectrum

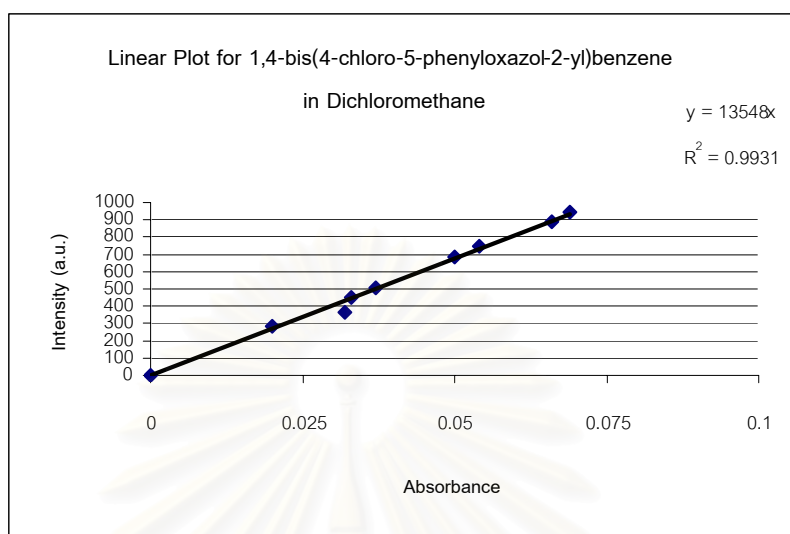
### 2.1 UV in flu $\lambda_{\text{ex}} = 368 \text{ nm}$



### 2.2 Fluorescence $\lambda_{\text{em}} = 428 \text{ nm}$



2.3 Linear plot for 1,4-bis(4-chloro-5-phenyloxazol-2-yl)benzene between Intensity vs Absorbance



Slope = 13548

While;

$$\phi_x = \frac{\phi_{st} [\text{slope}_x] [\eta_x^2]}{[\text{slope}_{st}] [\eta_{st}^2]}$$

as x = dichloromethane

st = ethanol

$$= 0.27 [13548] [1.4246^2]$$

$$\frac{[23085] [1.3594^2]}{[23085] [1.3594^2]}$$

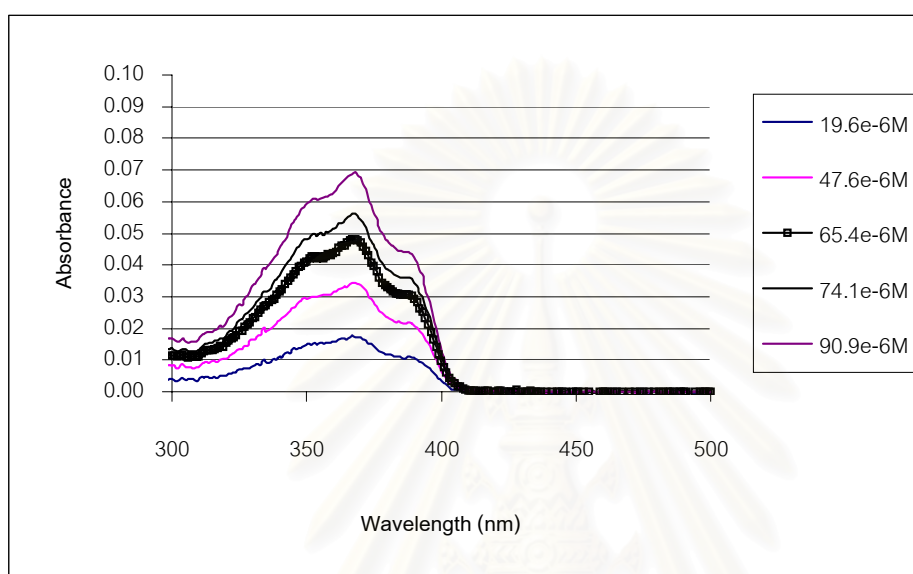
$$= 0.17$$

สถาบันวิทยบริการ  
จุฬาลงกรณ์มหาวิทยาลัย

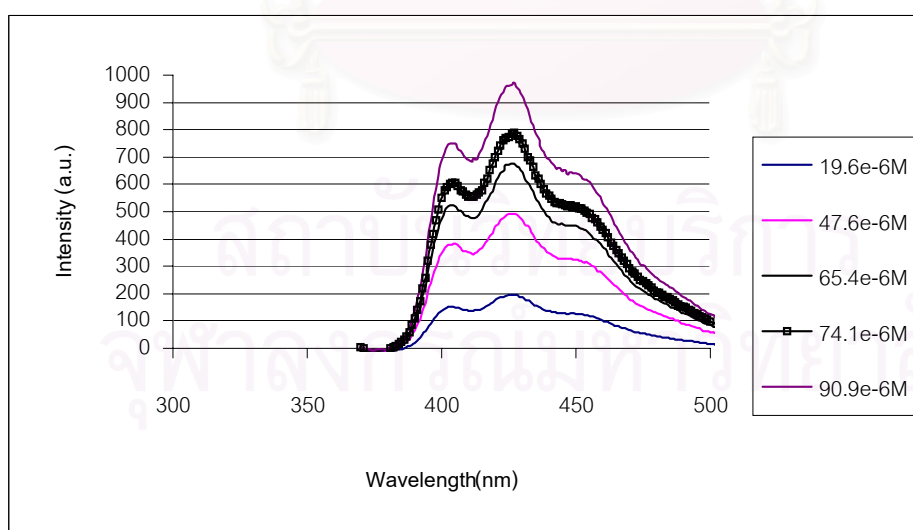
Figure C5. Data Fluorescence Spectrum of 1,4-bis(4-chloro-5-phenyloxazol-2-yl)benzene in *n*-butanol

## 1. Fluorescence Spectrum

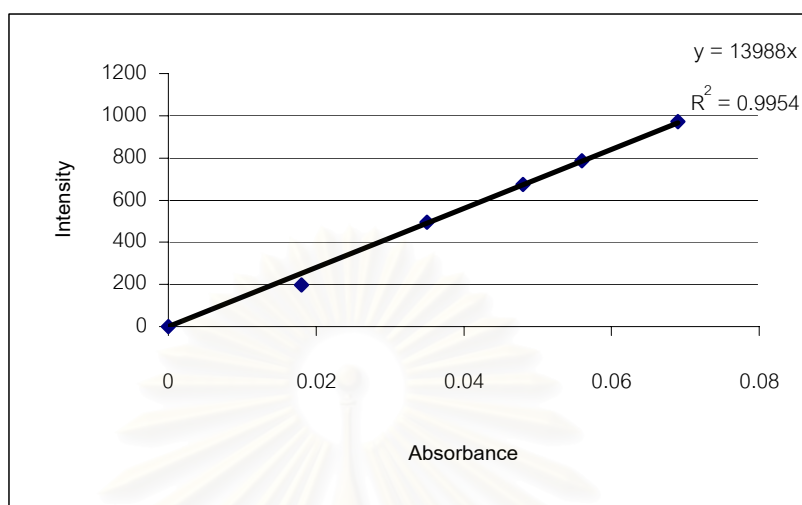
### 1.1 Excitation spectra, $\lambda_{\text{ex}} = 368 \text{ nm}$



### 1.2 Emission spectra, $\lambda_{\text{em}} = 423 \text{ nm}$



1.3 Linear plot for 1,4-bis(4-chloro-5-phenyloxazol-2-yl)benzene between Intensity vs Absorbance



Slope = 13988

While;

$$\phi_x = \frac{\phi_{st} [\text{slope}_x] [\eta_x^2]}{[\text{slope}_{st}] [\eta_{st}^2]}$$

as x = *n*-butanol

st = ethanol

$$= 0.27 [13988] [1.4246^2]$$

$$\frac{[23085] [1.3594^2]}{[23085] [1.3594^2]}$$

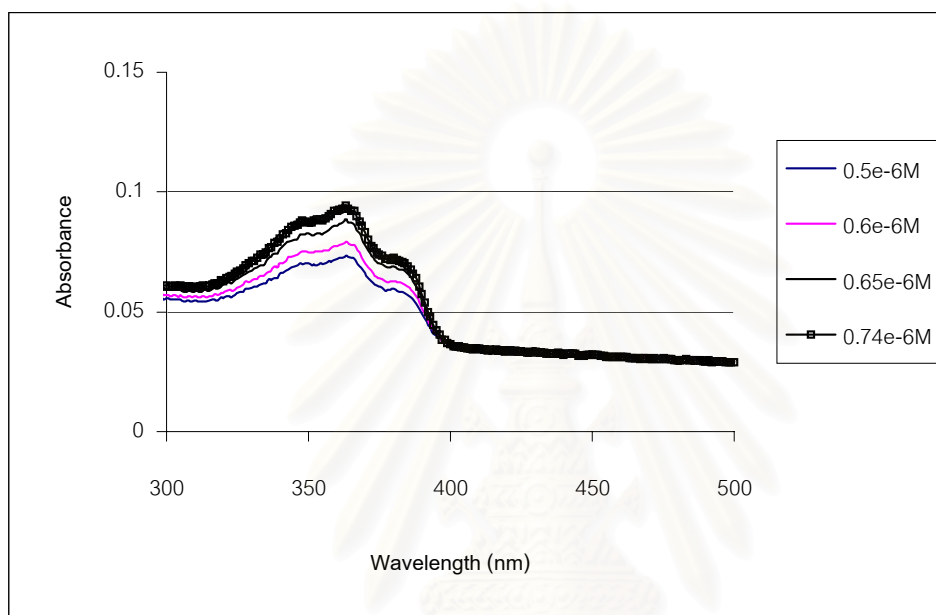
$$= 0.18$$

สถาบันวิทยบริการ  
จุฬาลงกรณ์มหาวิทยาลัย

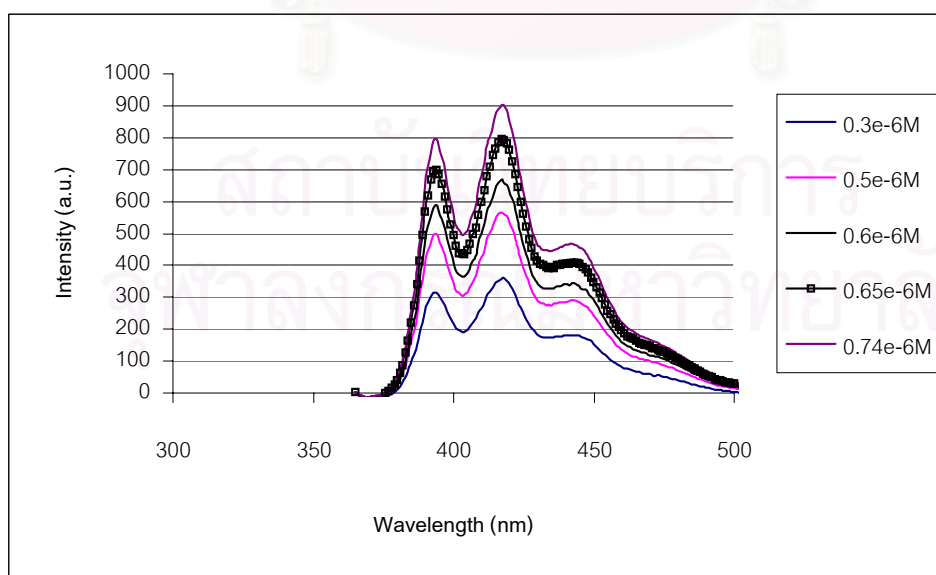
Figure C6. Data Fluorescence Spectrum of 1,4-bis(4-chloro-2-phenyloxazol-5-yl)benzene in dichloromethane

## 1. Fluorescence Spectrum

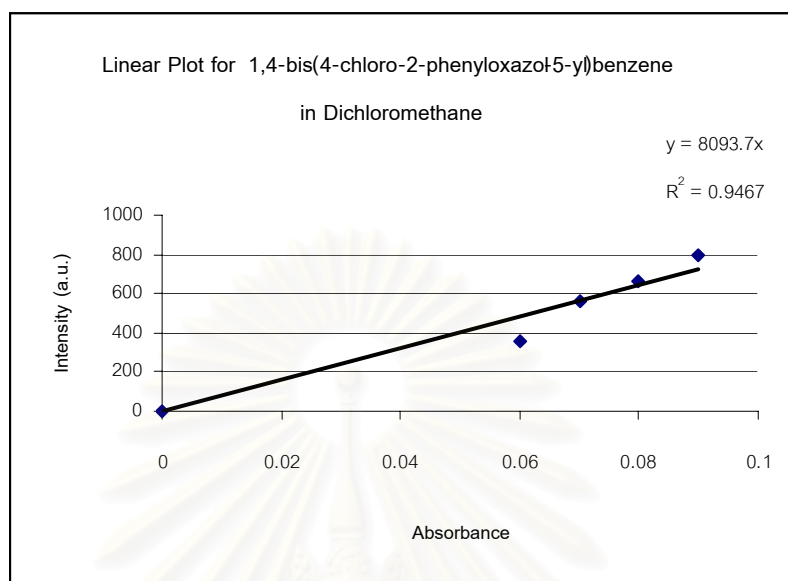
### 1.1 Excitation spectra, $\lambda_{\text{ex}} = 363 \text{ nm}$



### 1.2 Emission spectra, $\lambda_{\text{em}} = 416 \text{ nm}$



1.3 Linear plot for 1,4-bis(4-chloro-5-phenyloxazol-2-yl)benzene between Intensity vs Absorbance



Slope = 8093.7

While;

$$\phi_x = \frac{\phi_{st} [\text{slope}_x] [\eta_x^2]}{[\text{slope}_{st}] [\eta_{st}^2]}$$

as x = dichloromethane

st = ethanol

$$= 0.27 [8093.7] [1.4246^2]$$

$$= \frac{[23085] [1.3594^2]}{[23085] [1.3594^2]}$$

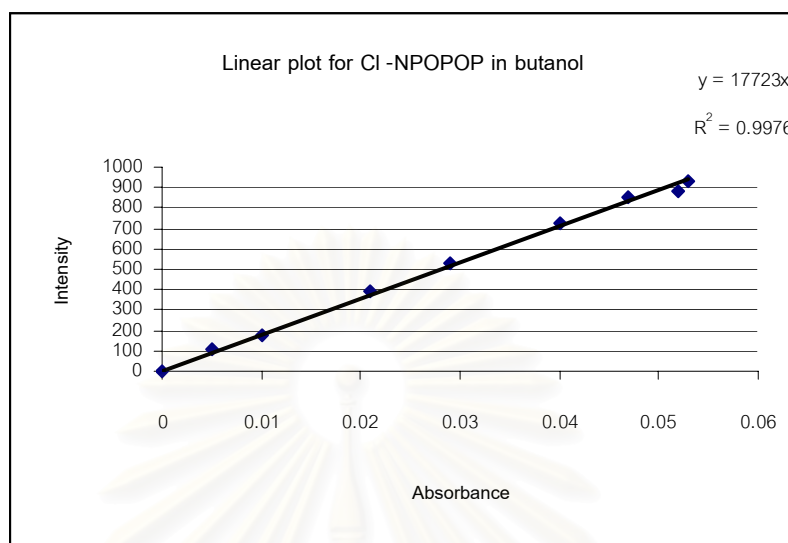
$$= 0.10$$

สถาบันวิทยบริการ  
จุฬาลงกรณ์มหาวิทยาลัย





1.3 Linear plot for 1,4-bis(4-chloro-2-phenyloxazol-5-yl)benzene between Intensity vs Absorbance



Slope = 17723

While;

$$\phi_x = \frac{\phi_{st} [\text{slope}_x] [\eta_x^2]}{[\text{slope}_{st}] [\eta_{st}^2]}$$

as x = n-butanol

st = ethanol

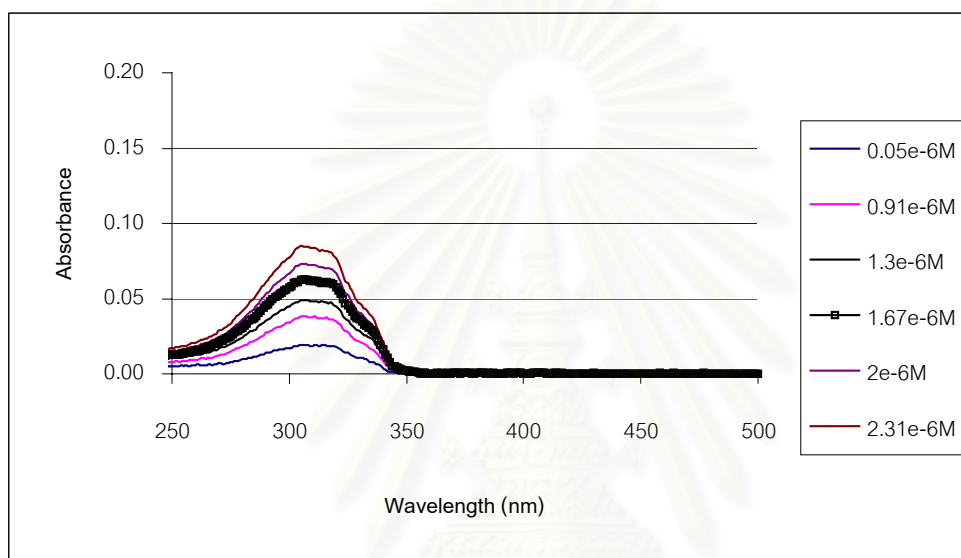
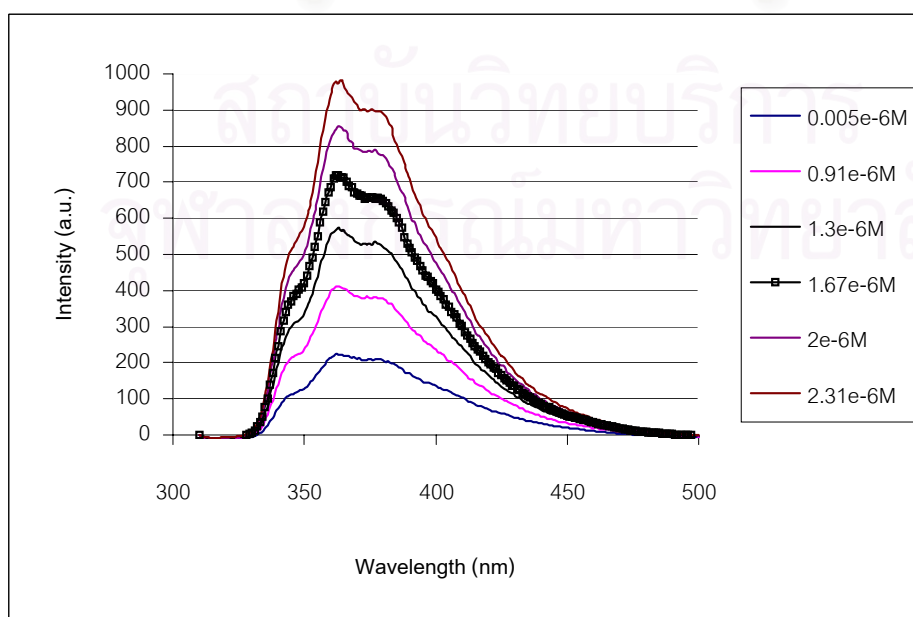
$$= \frac{0.27 [17723] [1.3992^2]}{[23085] [1.3594^2]}$$

$$= 0.22$$

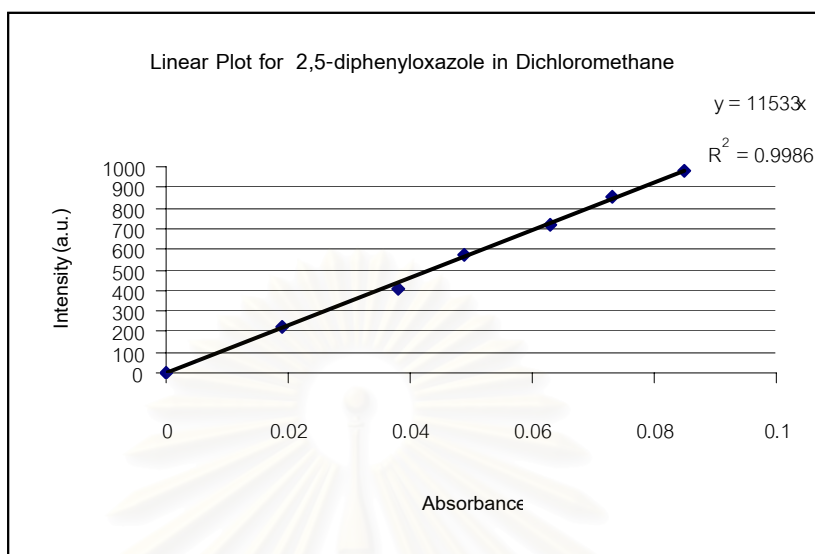
สถาบันวิทยบริการ  
จุฬาลงกรณ์มหาวิทยาลัย

Figure C8. Data Fluorescence Spectrum of 2,5-diphenyloxazole in dichloromethane

## 1. Fluorescence Spectrum

1.1 Excitation spectra,  $\lambda_{\text{ex}} = 306 \text{ nm}$ 1.2 Emission spectra,  $\lambda_{\text{em}} = 363.07 \text{ nm}$ 

## 1.3 Linear plot for 2,5-diphenyloxazole between Intensity vs Absorbance



Slope = 11533

While;

$$\phi_x = \frac{\phi_{st} [\text{slope}_x] [\eta_x^2]}{[\text{slope}_{st}] [\eta_{st}^2]}$$

as x = dichloromethane

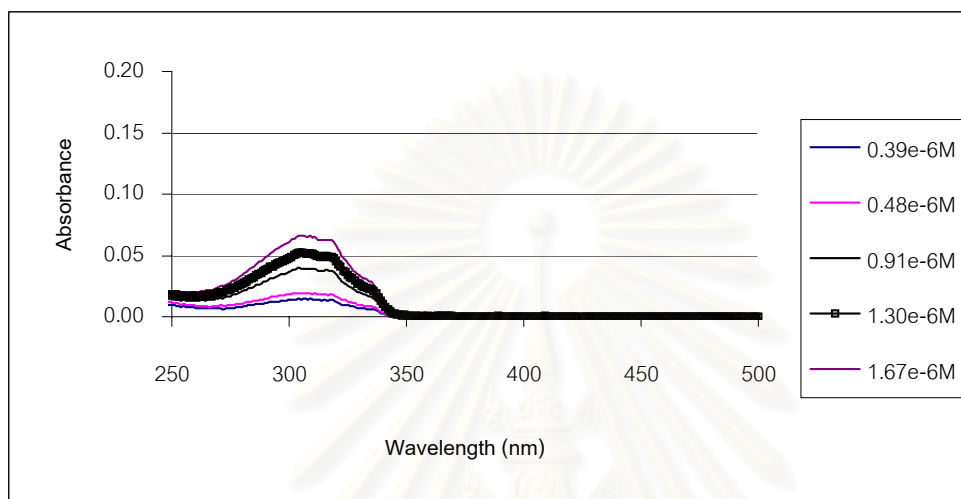
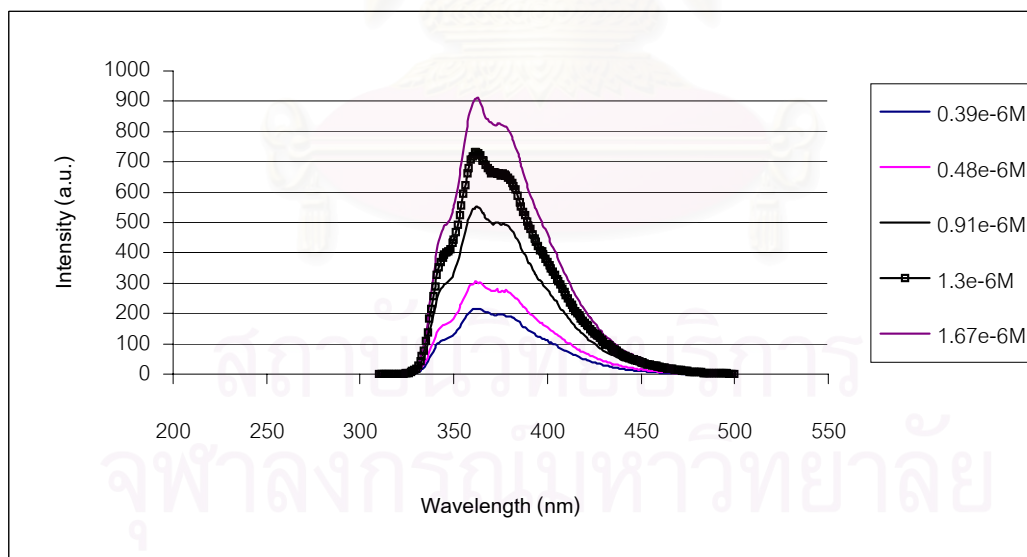
st = ethanol

$$= \frac{0.27 [11533] [1.4246^2]}{[23085] [1.3594^2]}$$

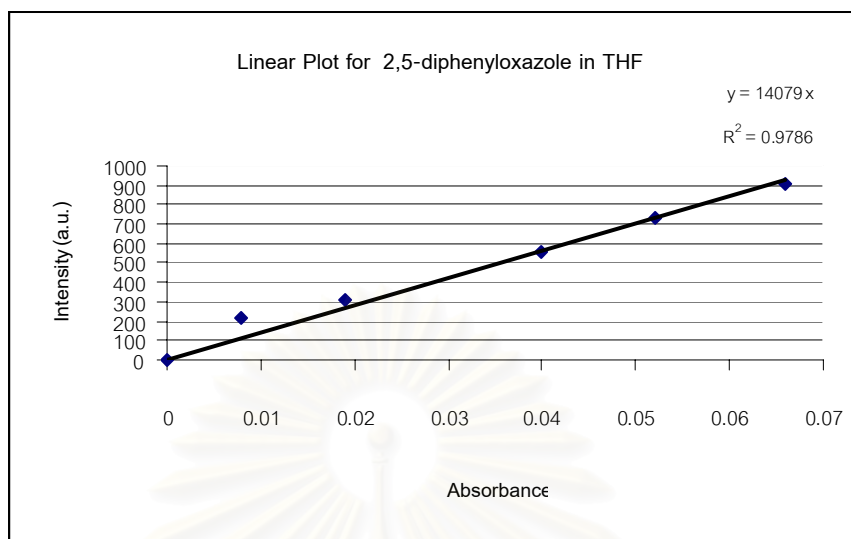
$$= 0.148 = 0.15$$

Figure C9. Data Fluorescence Spectrum of 2,5-diphenyloxazole in THF

## 1. Fluorescence Spectrum

1.1 Excitation spectra,  $\lambda_{\text{ex}} = 306 \text{ nm}$ 1.2 Emission spectra,  $\lambda_{\text{em}} = 362 \text{ nm}$ 

## 1.3 Linear plot for 2,5-diphenyloxazole between Intensity vs Absorbance



Slope = 14079

While;

$$\phi_x = \frac{\phi_{st} [\text{slope}_x] [\eta_x^2]}{[\text{slope}_{st}] [\eta_{st}^2]}$$

as x = THF

st = ethanol

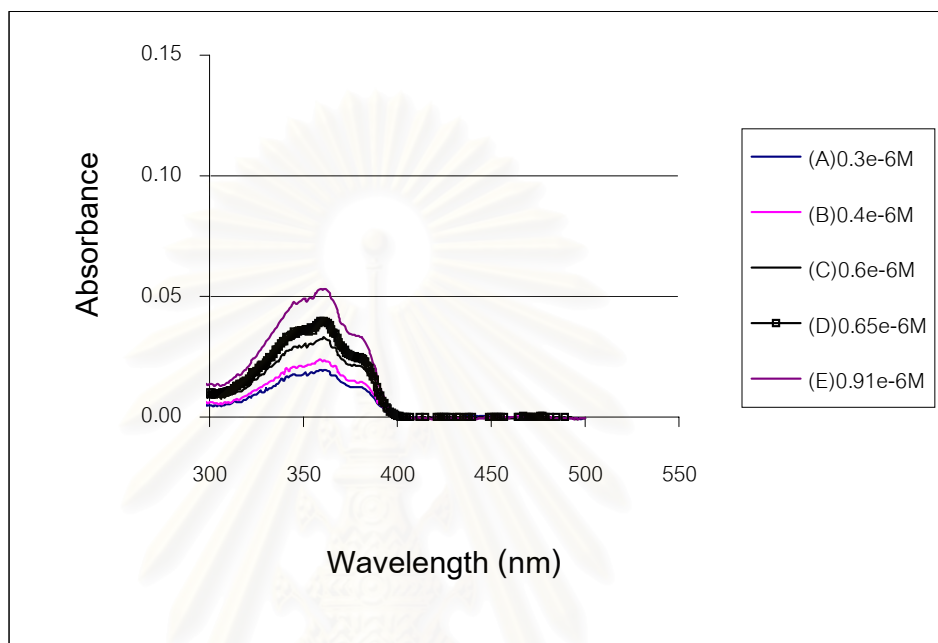
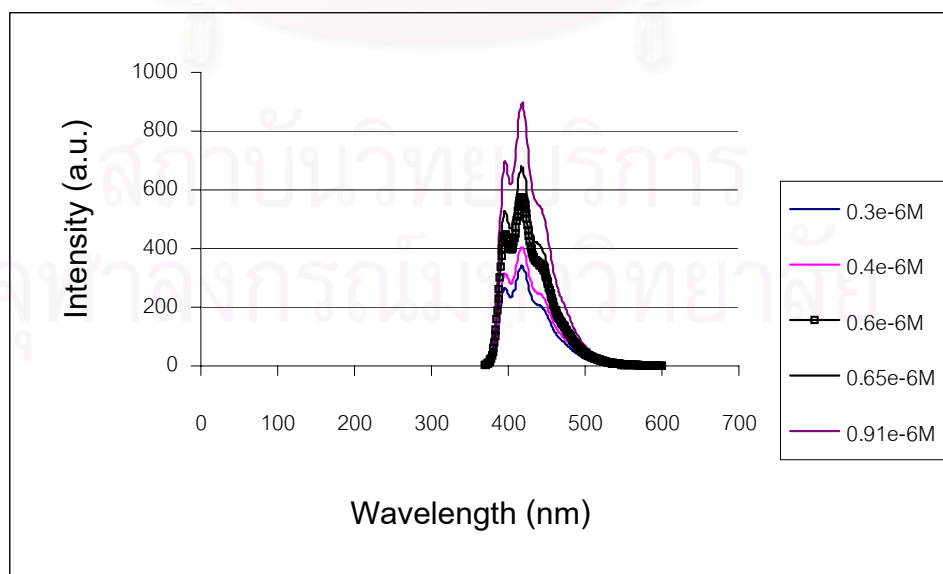
$$= \frac{0.27 [14079] [1.4072^2]}{[23085] [1.3594^2]}$$

$$= 0.176 = 0.18$$

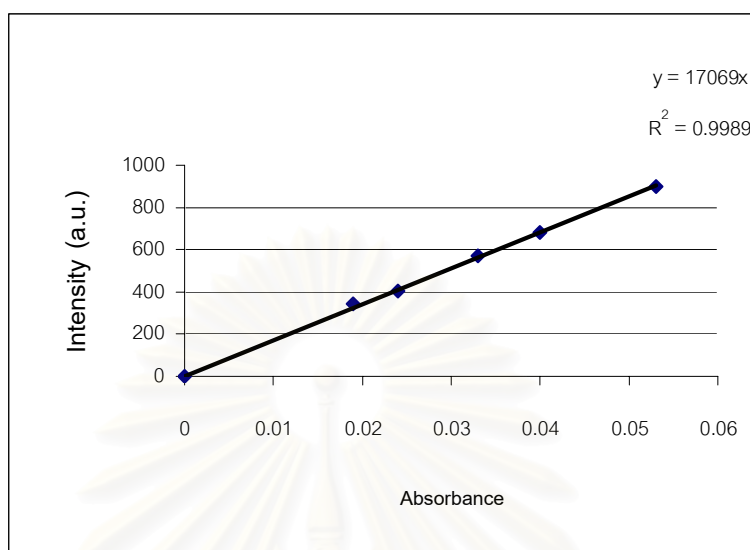
ศูนย์บริการ  
จุฬาลงกรณ์มหาวิทยาลัย

Figure C10. Data Fluorescence Spectrum of POPOP in dichloromethane

## 1. Fluorescence Spectrum

1.1 Excitation spectra,  $\lambda_{\text{ex}} = 361 \text{ nm}$ 1.2 Emission spectra,  $\lambda_{\text{em}} = 418 \text{ nm}$ 

## 1.3 Linear plot for POPOP between Intensity vs Absorbance



Slope = 17069

While;

$$\phi_x = \frac{\phi_{st} [\text{slope}_x] [\eta_x^2]}{[\text{slope}_{st}] [\eta_{st}^2]}$$

as x = dichloromethane

st = ethanol

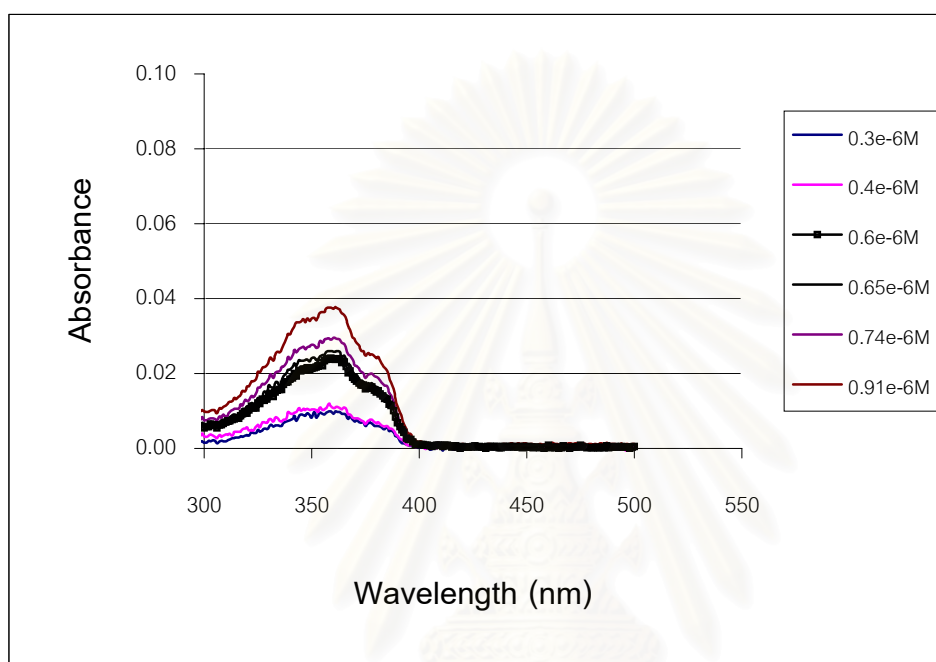
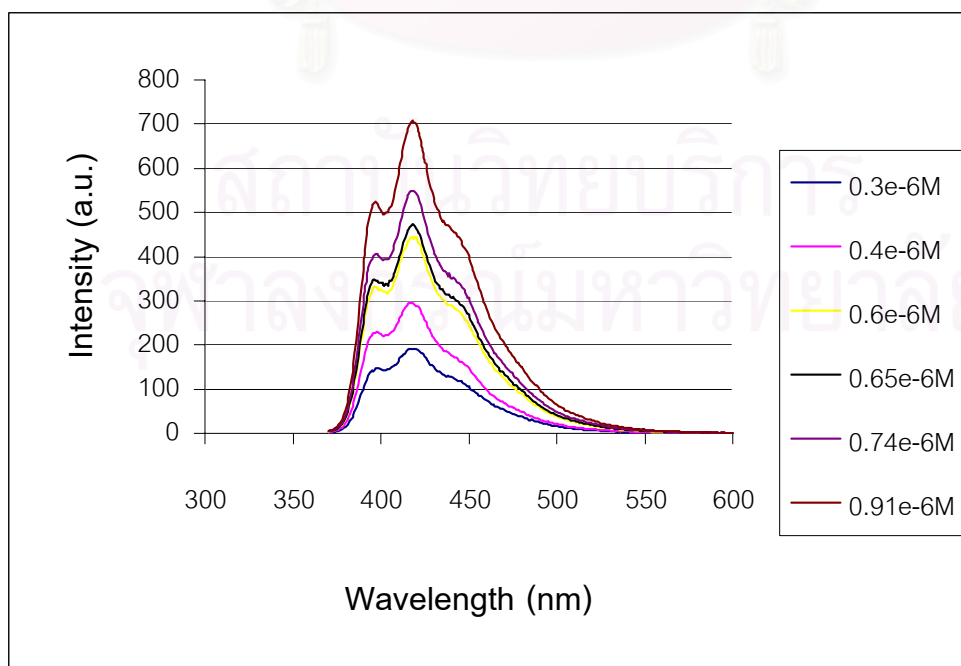
$$= \frac{0.27 [17069] [1.4246^2]}{[23085] [1.3594^2]}$$

$$= 0.22$$

สถาบันวิทยบริการ  
จุฬาลงกรณ์มหาวิทยาลัย

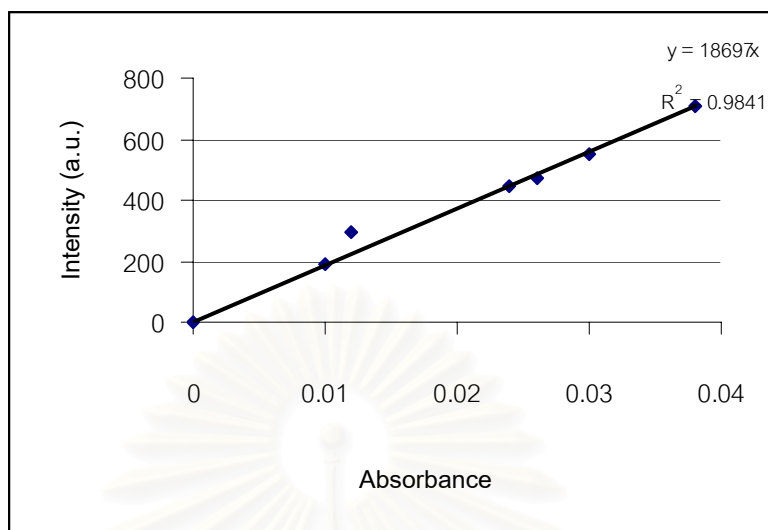
Figure C11. Data Fluorescence Spectrum of POPOP in *n*-butanol

## 1. Fluorescence Spectrum

1.1 Excitation spectra,  $\lambda_{\text{ex}} = 359 \text{ nm}$ 1.2 Emission spectra,  $\lambda_{\text{em}} = 418 \text{ nm}$ 



## 1.3 Linear plot for POPOP between Intensity vs Absorbance



Slope = 18697

While;

$$\phi_x = \frac{\phi_{st} [\text{slope}_x] [\eta_x^2]}{[\text{slope}_{st}] [\eta_{st}^2]}$$

as x = n-butanol

st = ethanol

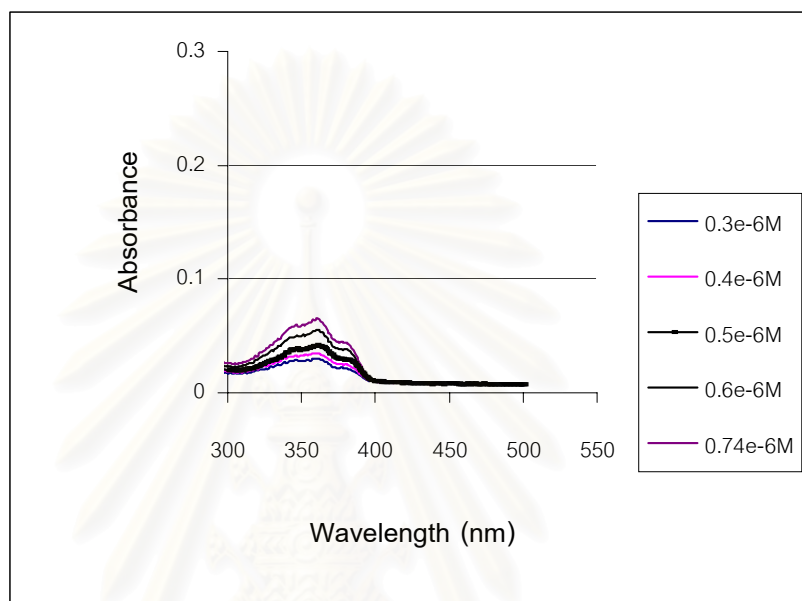
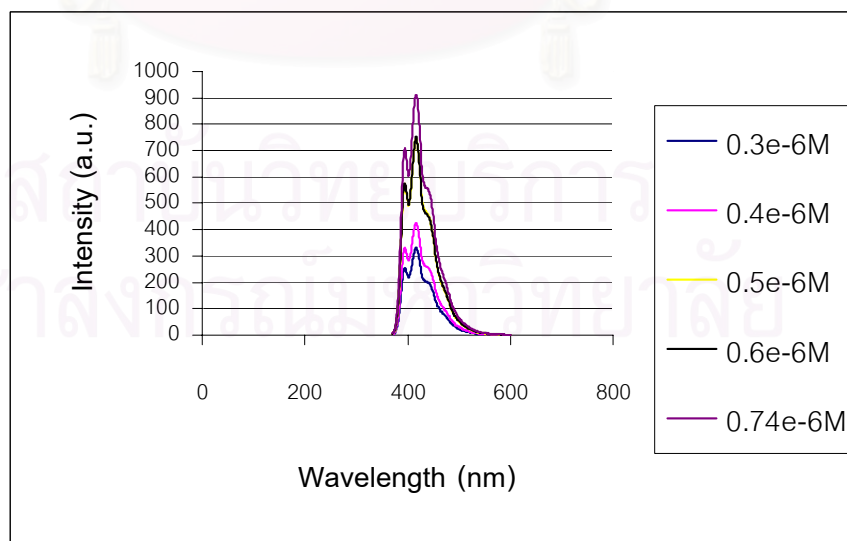
$$= \frac{0.27 [18697] [1.3992^2]}{[23085] [1.3594^2]}$$

$$= 0.23$$

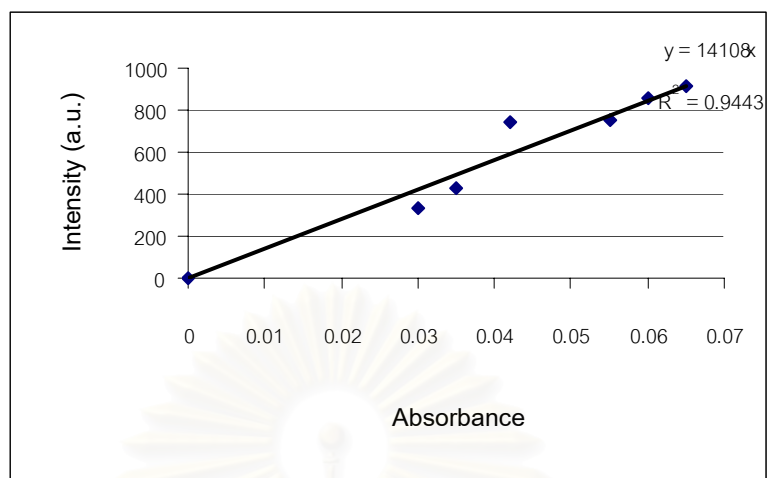
สถาบันวิทยบริการ  
จุฬาลงกรณ์มหาวิทยาลัย

Figure C12. Data Fluorescence Spectrum of POPOP in THF

## 1. Fluorescence Spectrum

1.1 Excitation spectra,  $\lambda_{\text{ex}} = 361 \text{ nm}$ 1.2 Emission spectra,  $\lambda_{\text{em}} = 416 \text{ nm}$ 

## 1.3 Linear plot for POPOP between Intensity vs Absorbance



Slope = 14108

While;

$$\phi_x = \frac{\phi_{st} [\text{slope}_x] [\eta_x^2]}{[\text{slope}_{st}] [\eta_{st}^2]}$$

as x = THF

st = ethanol

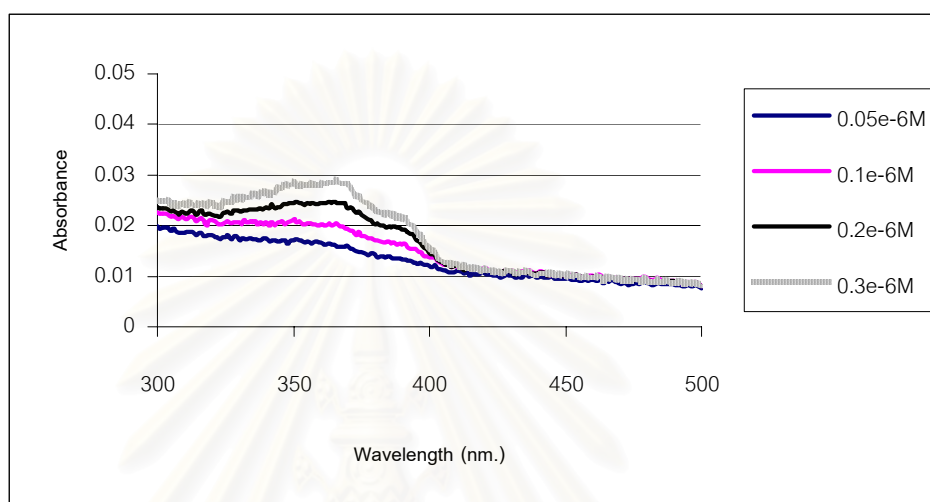
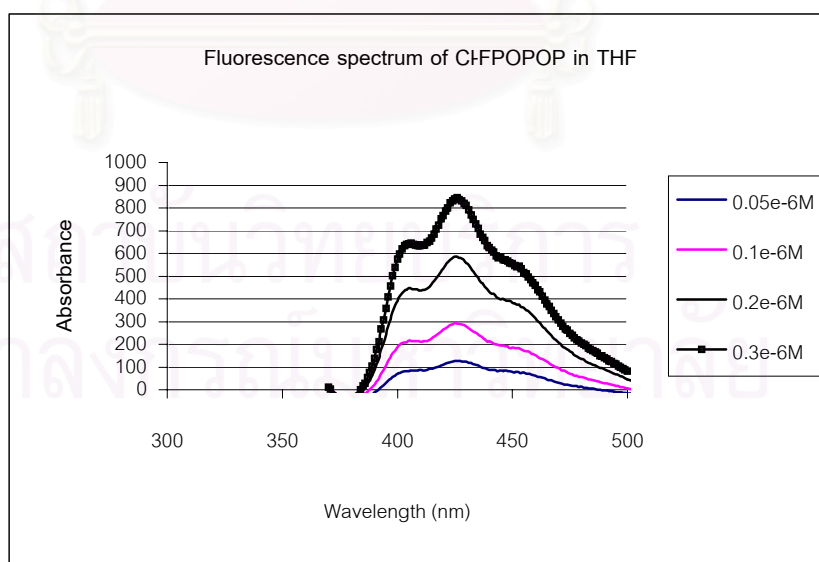
$$= \frac{0.27 [14108] [1.4072^2]}{[23085] [1.3594^2]}$$

$$= 0.18$$

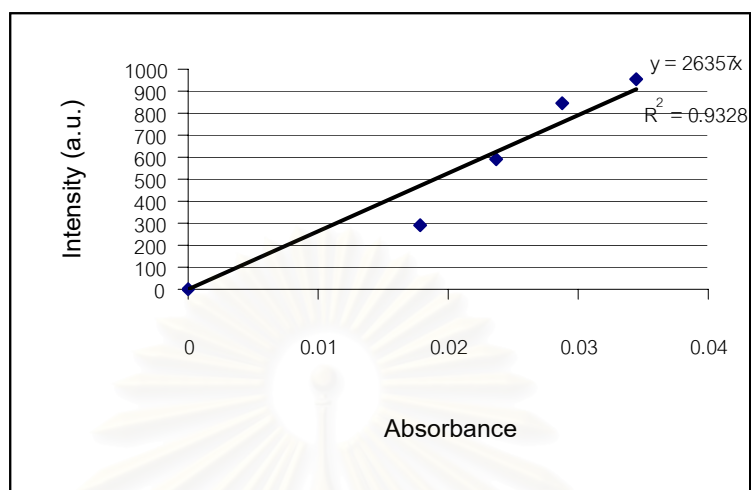
สถาบันวิทยบริการ  
จุฬาลงกรณ์มหาวิทยาลัย

Figure C13. Data Fluorescence Spectrum of 1,4-bis(4-chloro-5-phenyloxazol-2-yl)benzene in THF

## 1. Fluorescence Spectrum

1.1 Excitation spectra,  $\lambda_{\text{ex}} = 367 \text{ nm}$ 1.2 Emission spectra,  $\lambda_{\text{em}} = 425 \text{ nm}$ 

1.3 Linear plot for 1,4-bis(4-chloro-5-phenyloxazol-2-yl)benzene between Intensity vs Absorbance



Slope = 26357

While;

$$\phi_x = \frac{\phi_{st} [\text{slope}_x] [\eta_x^2]}{[\text{slope}_{st}] [\eta_{st}^2]}$$

as x = THF

st = ethanol

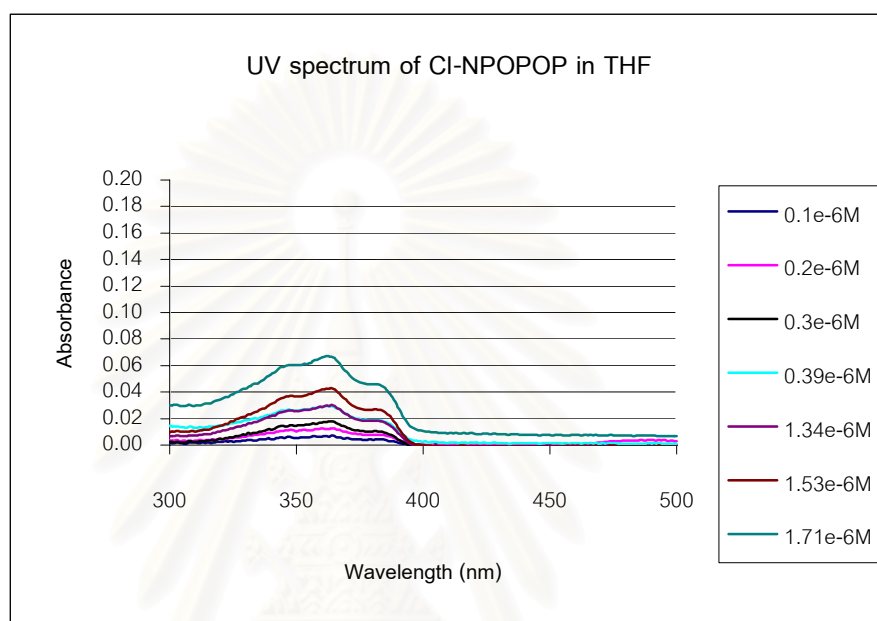
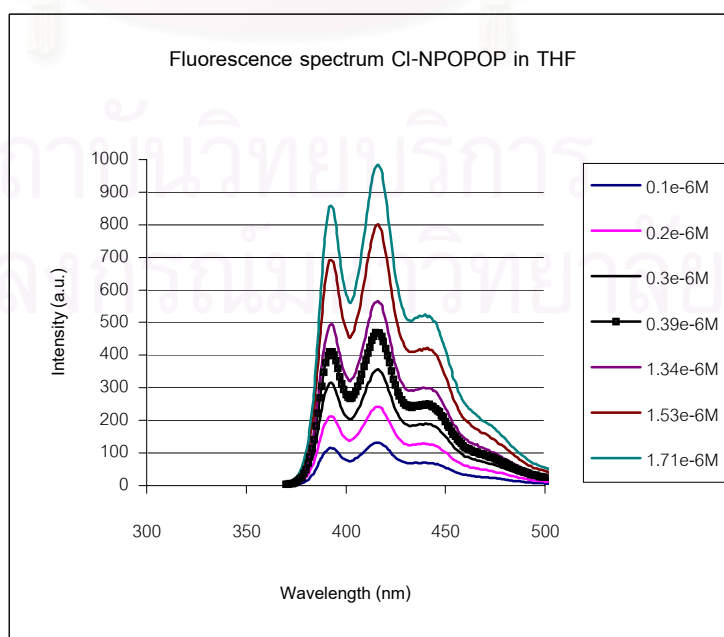
$$= \frac{0.27 [26357] [1.4072^2]}{[23085] [1.3594^2]}$$

$$= 0.33$$

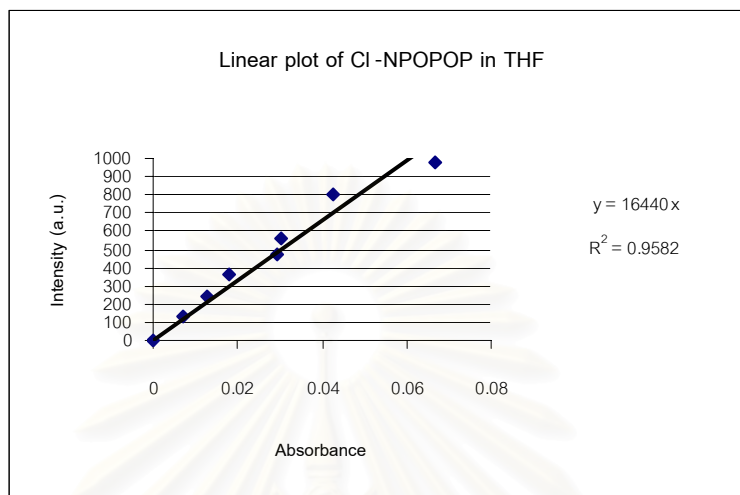
สถาบันวิทยบริการ  
จุฬาลงกรณ์มหาวิทยาลัย

Figure C14. Data Fluorescence Spectrum of 1,4-bis(4-chloro-2-phenyloxazol5-yl)benzene in THF

## 1. Fluorescence Spectrum

1.1 Excitation spectra,  $\lambda_{\text{ex}} = 363 \text{ nm}$ 1.2 Emission spectra,  $\lambda_{\text{em}} = 416 \text{ nm}$ 

1.3 Linear plot for 1,4-bis(4-chloro-2-phenyloxazol-5-yl)benzene between Intensity vs Absorbance



Slope = 16440

While;

$$\phi_x = \frac{\phi_{st} [\text{slope}_x] [\eta_x^2]}{[\text{slope}_{st}] [\eta_{st}^2]}$$

as x = THF

st = ethanol

$$= 0.27 [16440] [1.4072^2]$$

$$[23085] [1.3594^2]$$

$$= 0.21$$

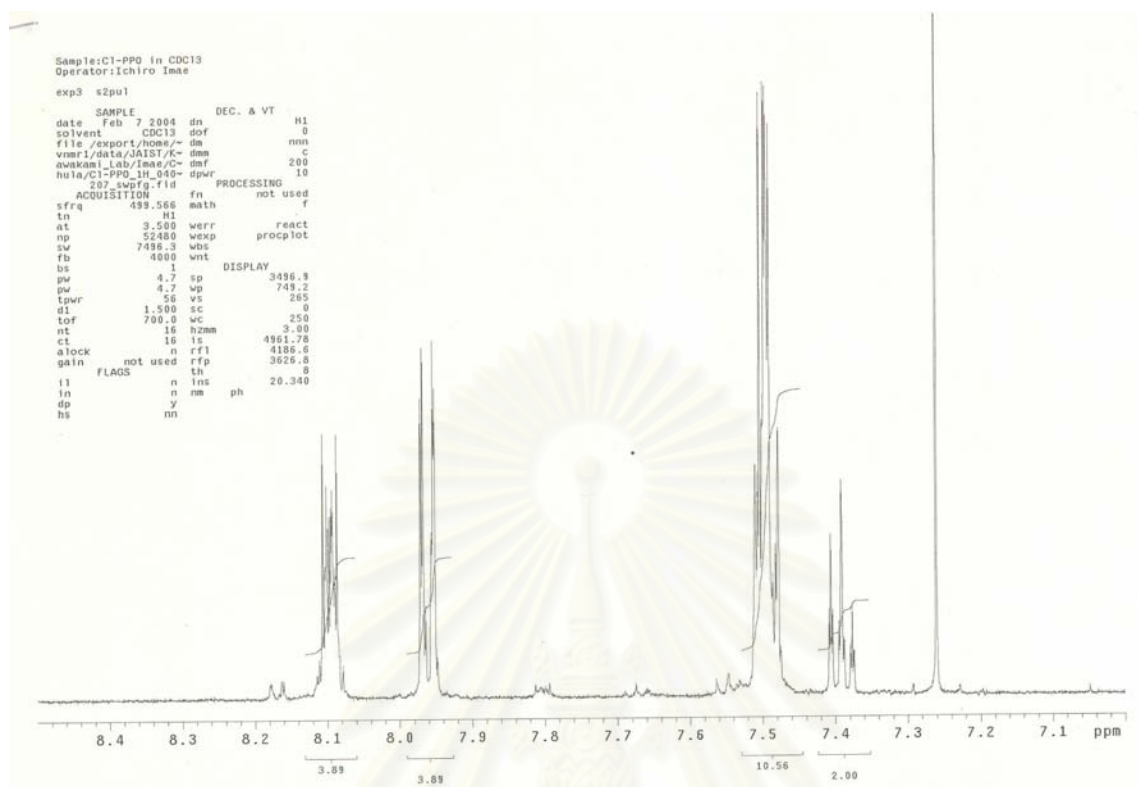
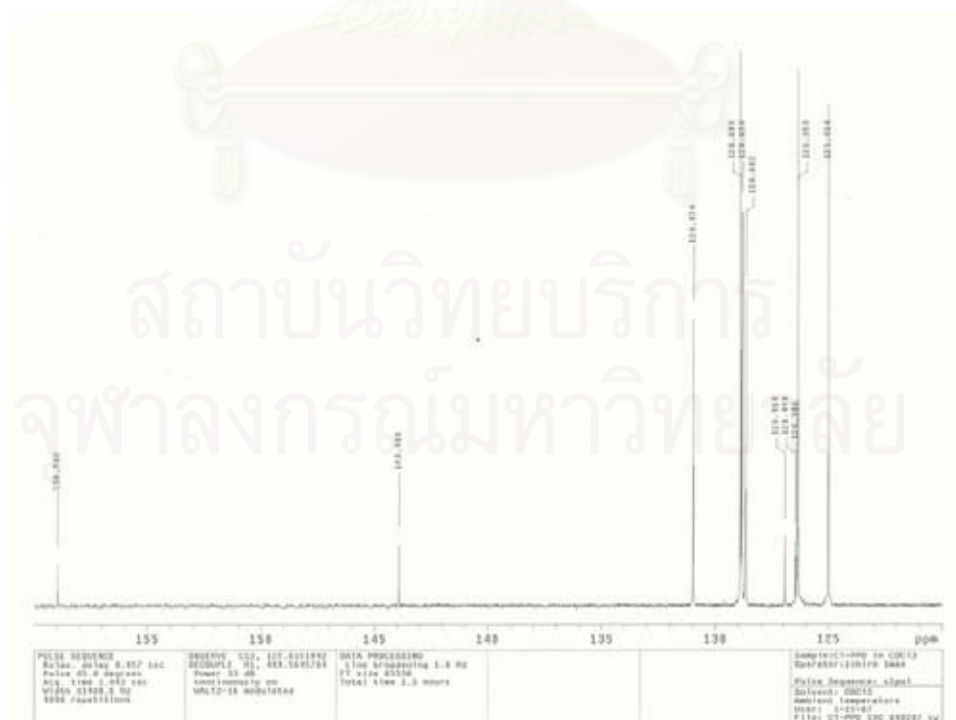


Appendix D

สถาบันวิทยบริการ  
จุฬาลงกรณ์มหาวิทยาลัย



## 4-Chloro-2,5-diphenyloxazole

Figure D1 500MHz  $^1\text{H}$  NMR spectrum of 4-chloro-2,5-diphenyloxazoleFigure D2 125 MHz  $^{13}\text{C}$  NMR spectrum of 4-chloro-2,5-diphenyloxazole

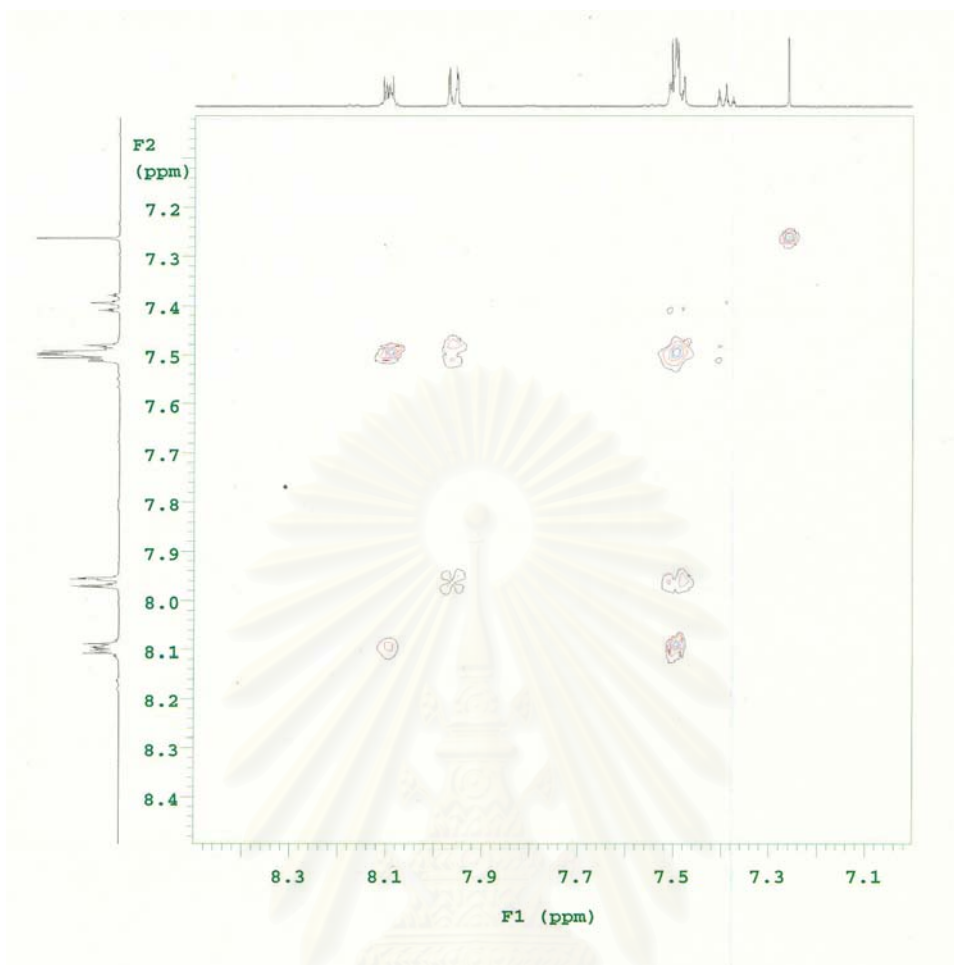


Figure D3 COSY spectrum of 4-chloro-2,5-diphenyloxazole

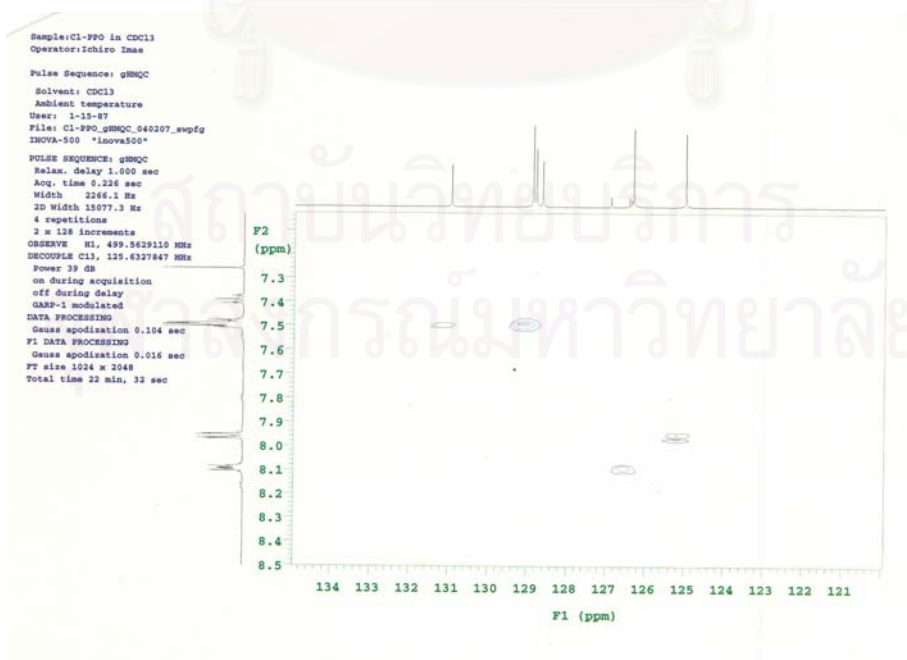


Figure D4 HMBC spectrum of 4-chloro-2,5-diphenyloxazole

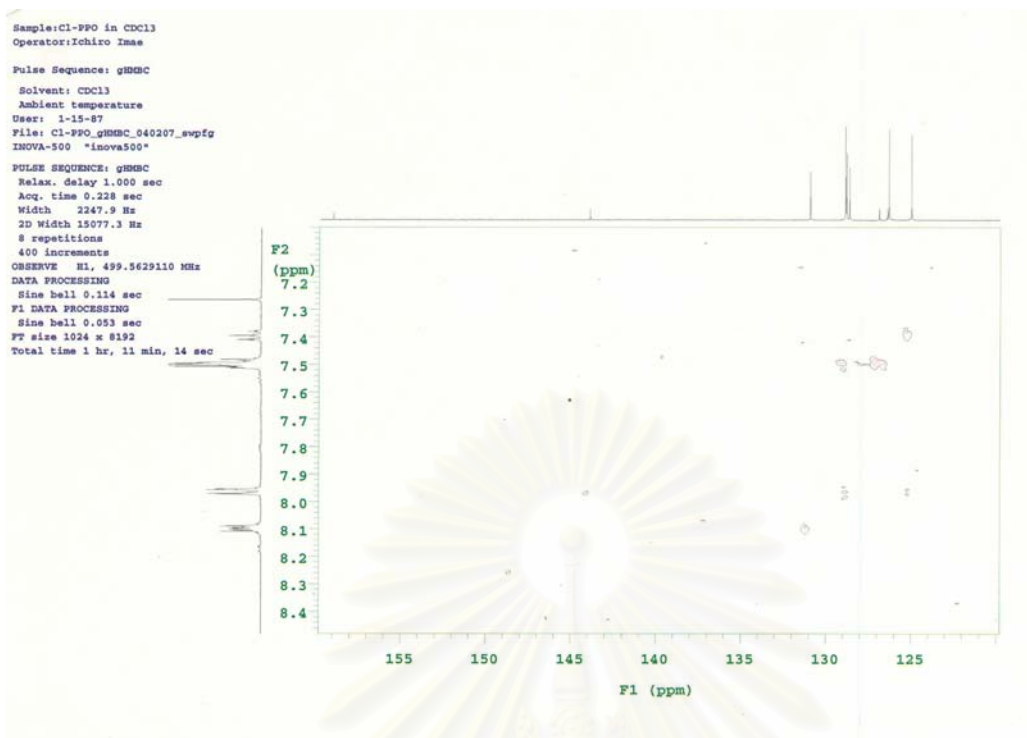


Figure D5 HMBC spectrum of 4-chloro-2,5-diphenyloxazole

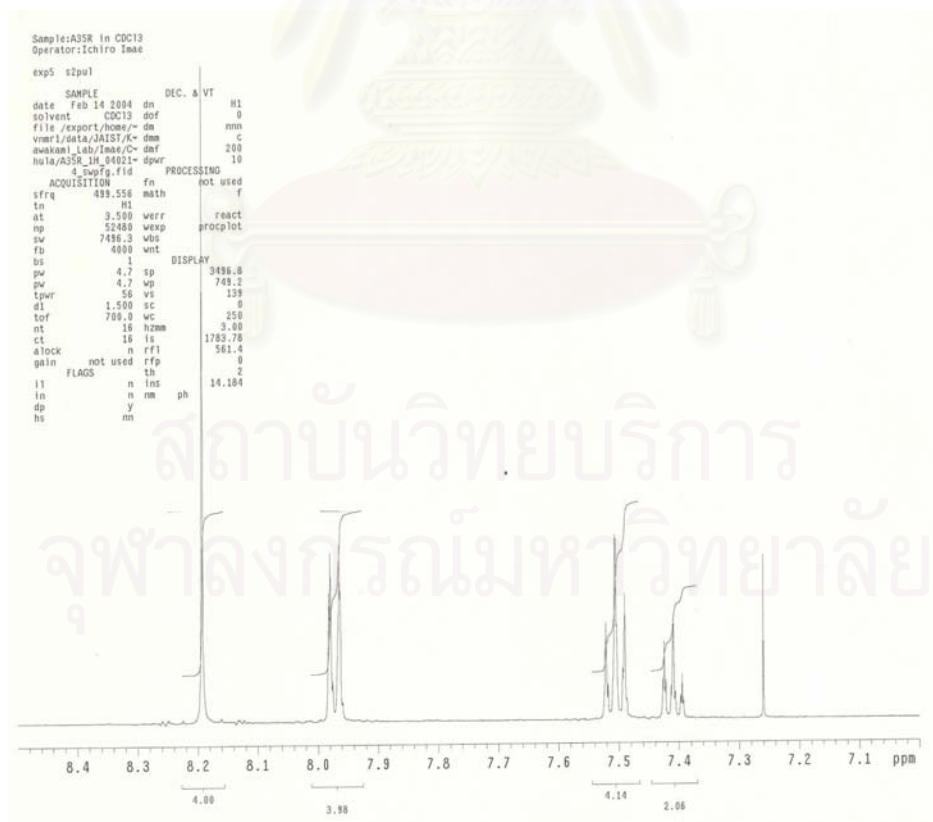
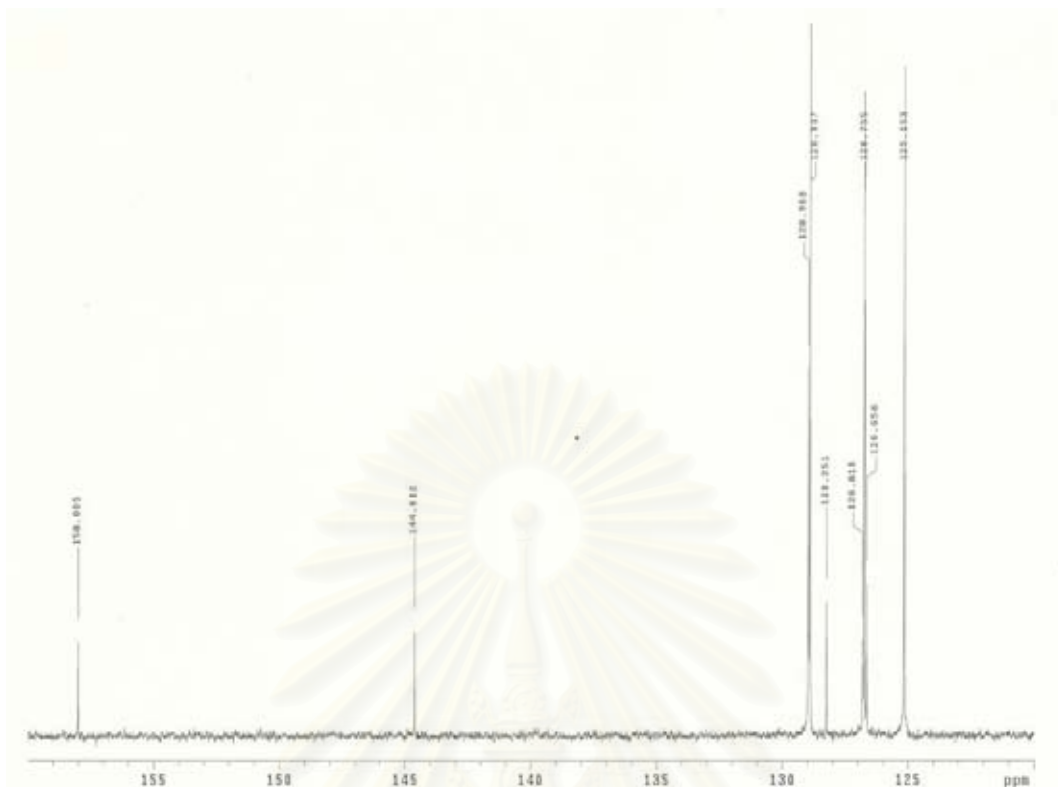
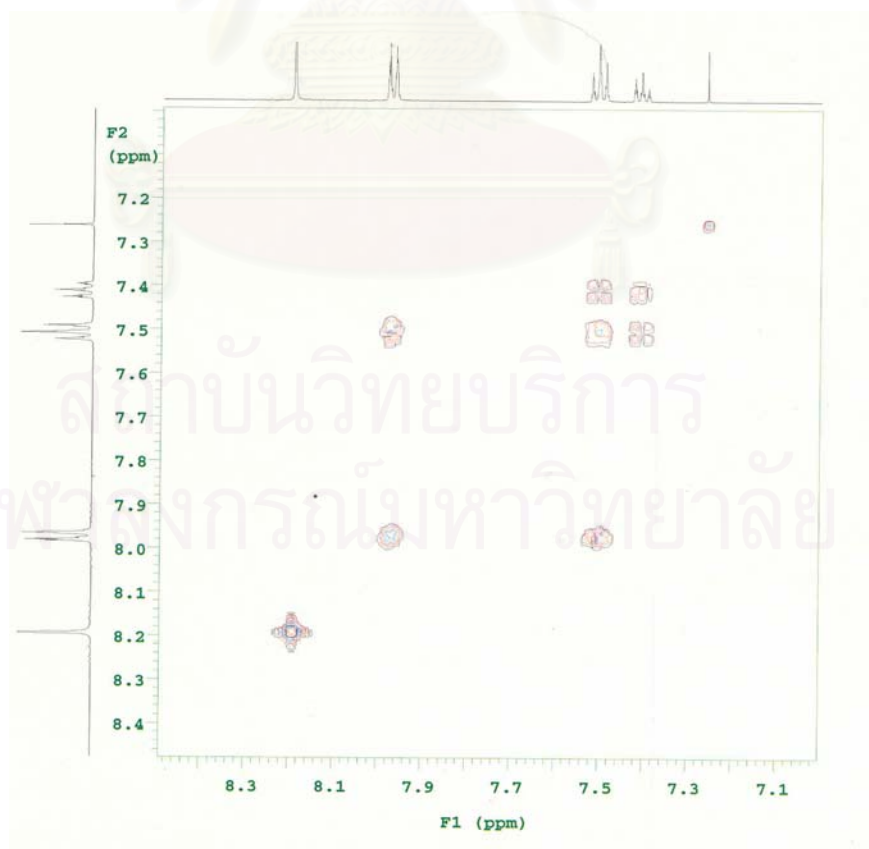


Figure D6 500 MHz  $^1\text{H}$  NMR spectrum of 1,4-bis(4-chloro-5-phenyloxazol-2-yl)benzene



**Figure D7** 125 MHz <sup>13</sup>C NMR spectrum of 1,4-bis(4-chloro-5-phenyloxazol-2-yl)benzene



**Figure D8** COSY spectrum of 1,4-bis(4-chloro-5-phenyloxazol-2-yl)benzene

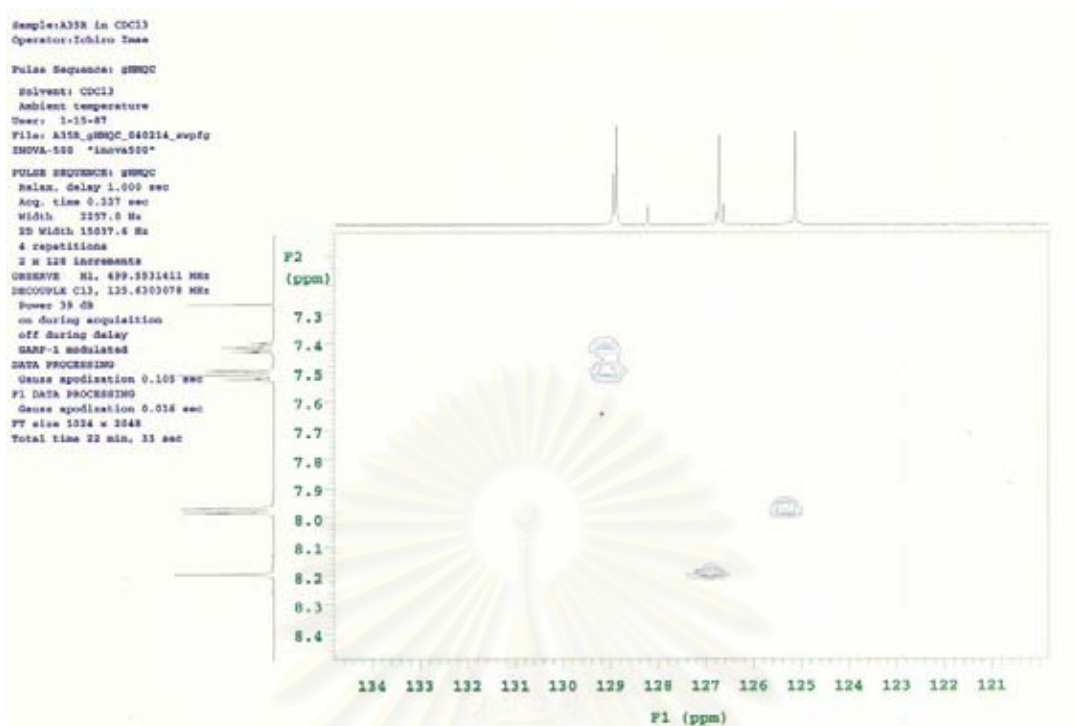


Figure D9 HMQC spectrum of 1,4-bis(4-chloro-5-phenyloxazol-2-yl)benzene

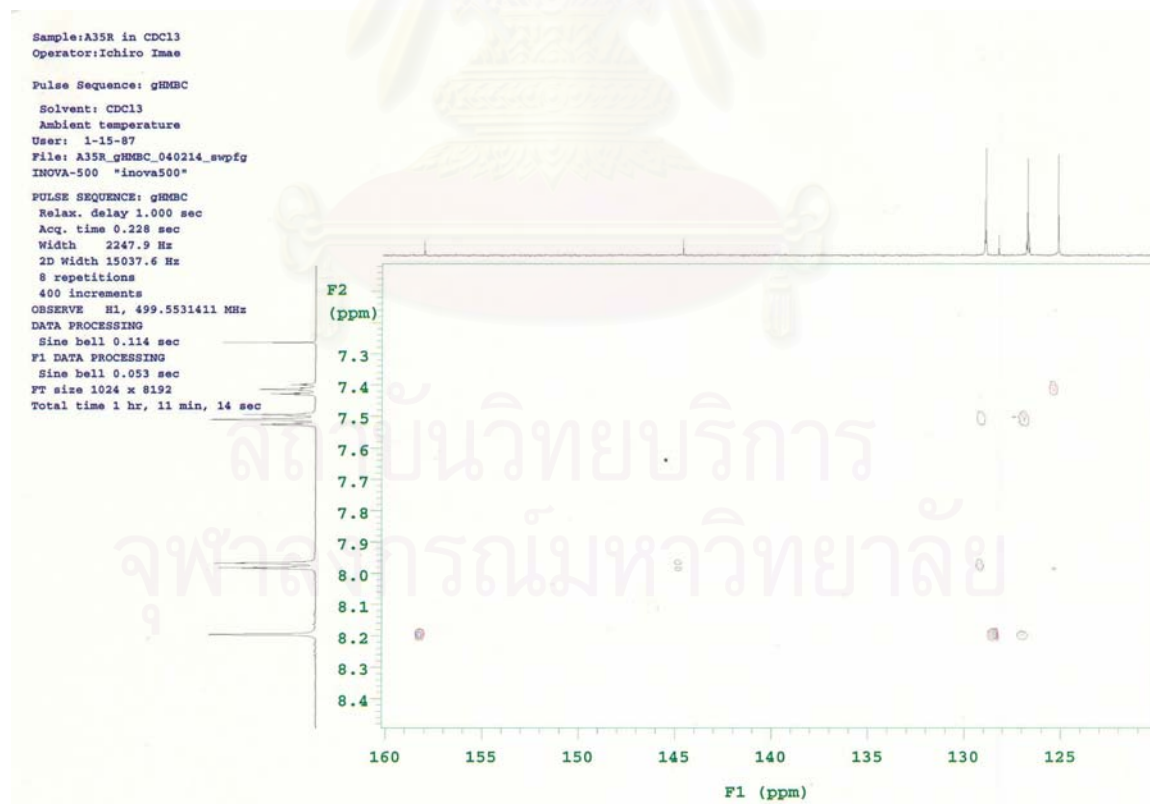
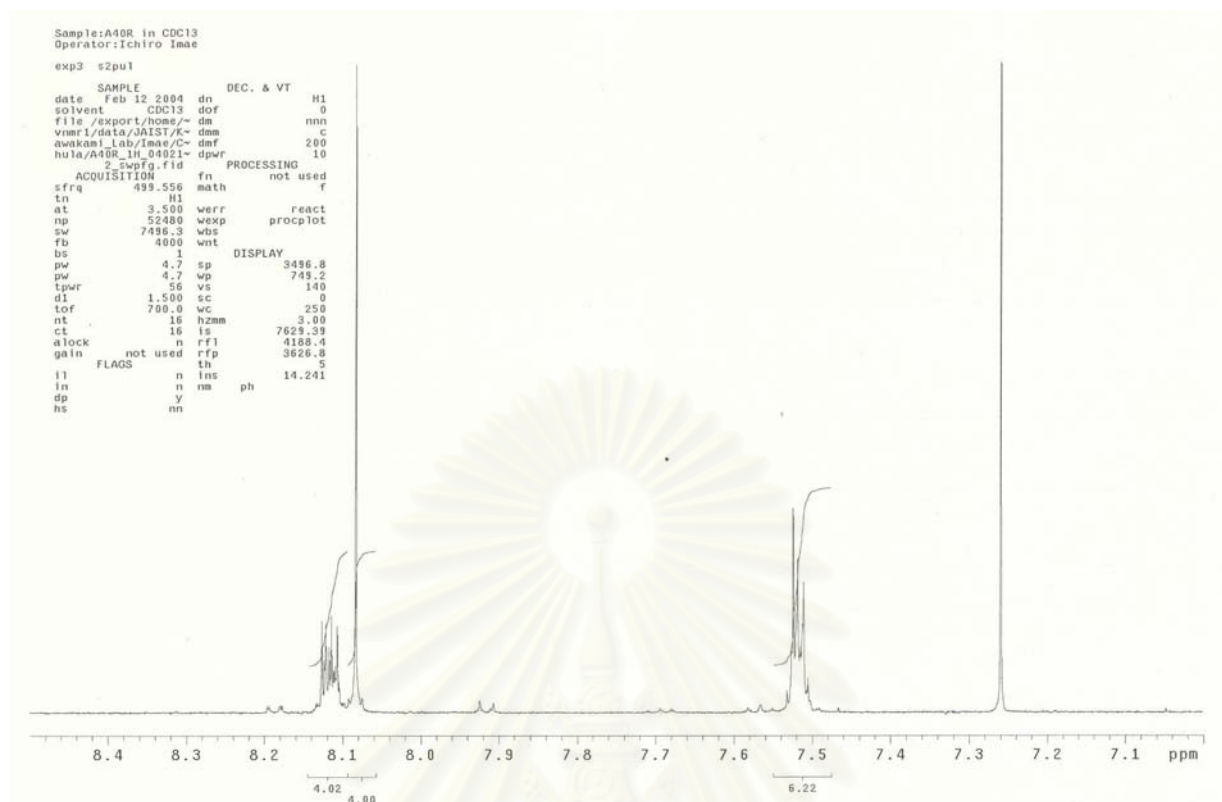
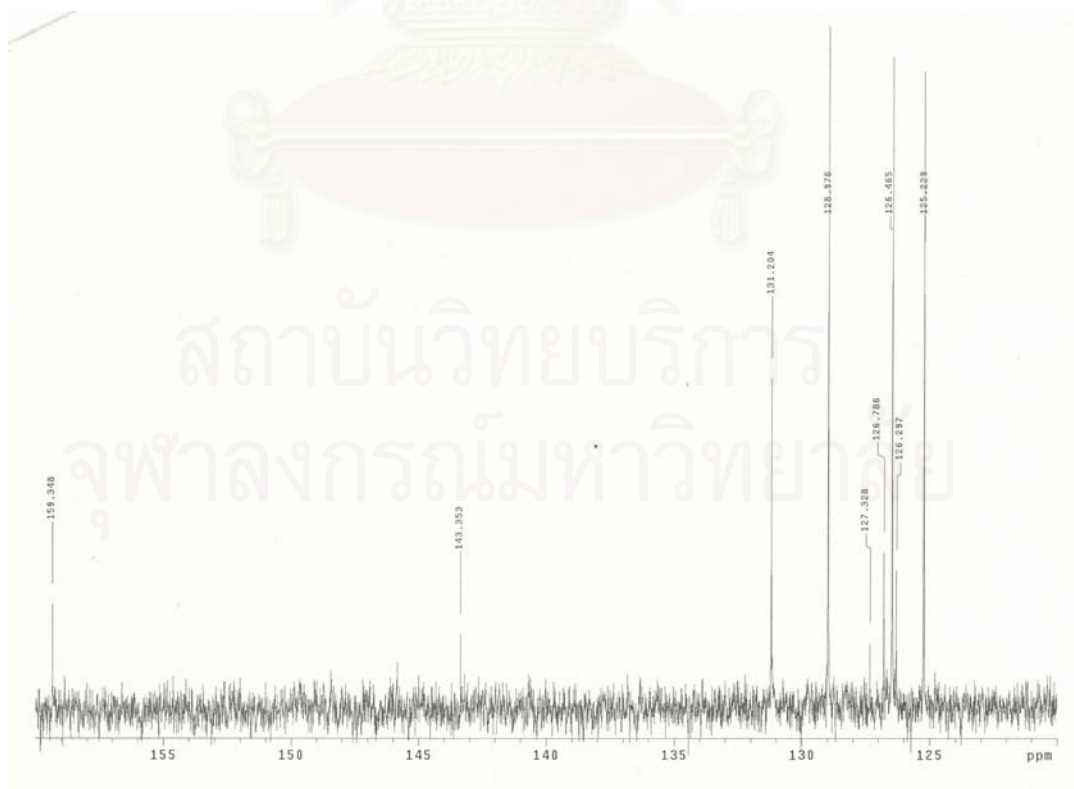


Figure D10 HMBC spectrum of 1,4-bis(4-chloro-5-phenyloxazol-2-yl)benzene



**Figure D11** 500 MHz  $^1\text{H}$  NMR spectrum of 1,4-bis(4-chloro-2-phenyloxazol-5-yl)benzene



**Figure D12** 125 MHz  $^{13}\text{C}$  NMR spectrum of 1,4-bis(4-chloro-2-phenyloxazol-5-yl)benzene



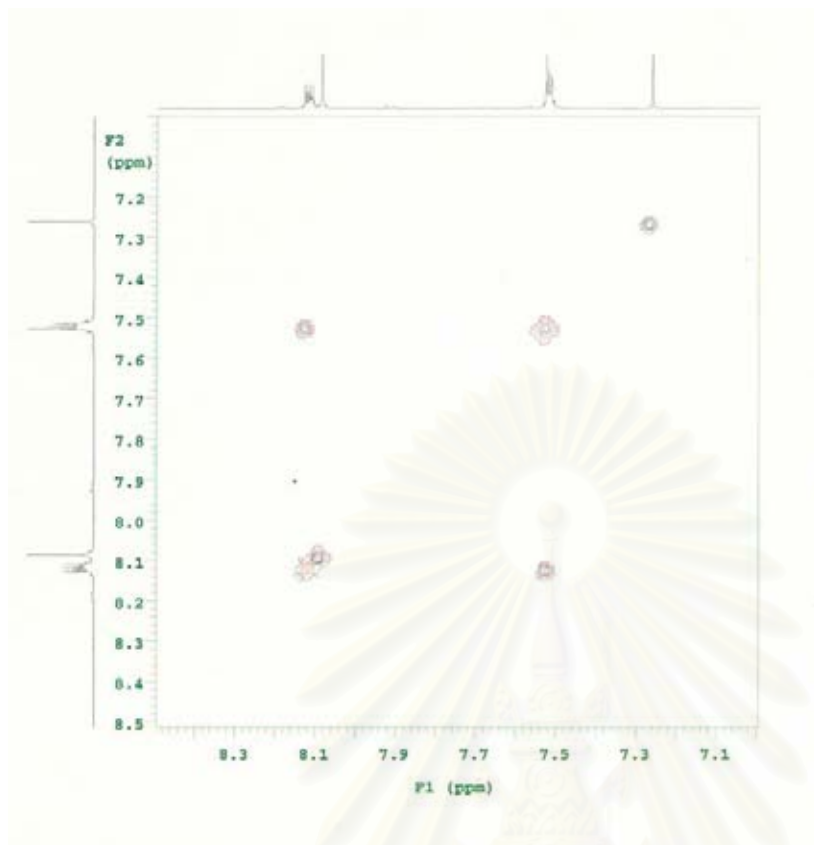


Figure D13 COSY spectrum of 1,4-bis(4-chloro-2-phenyloxazol-5-yl)benzene

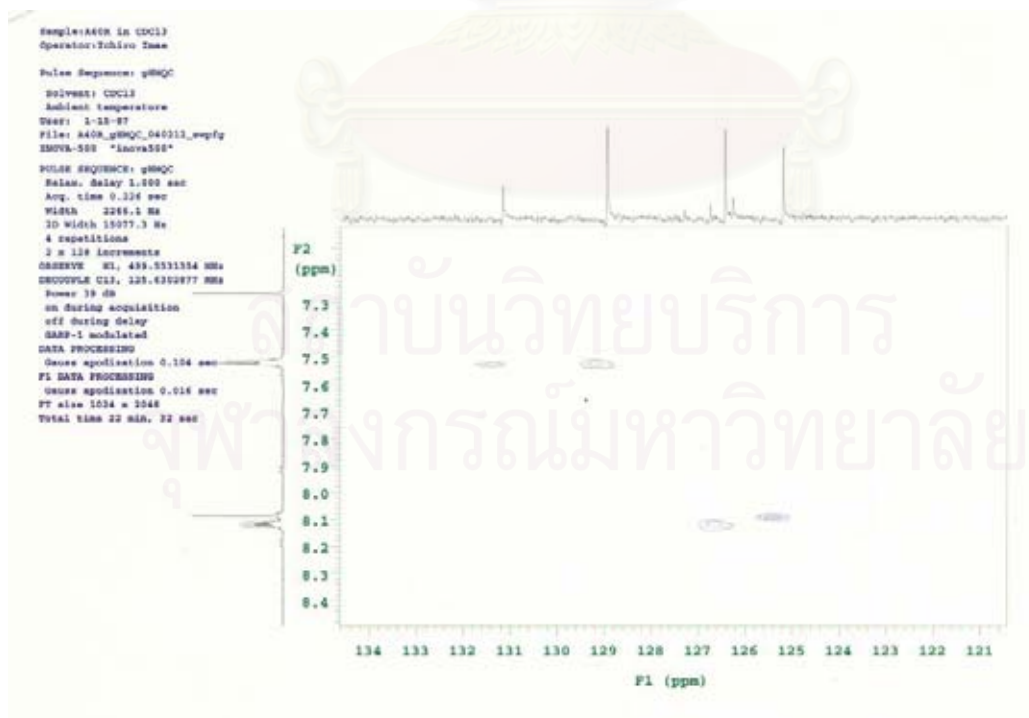
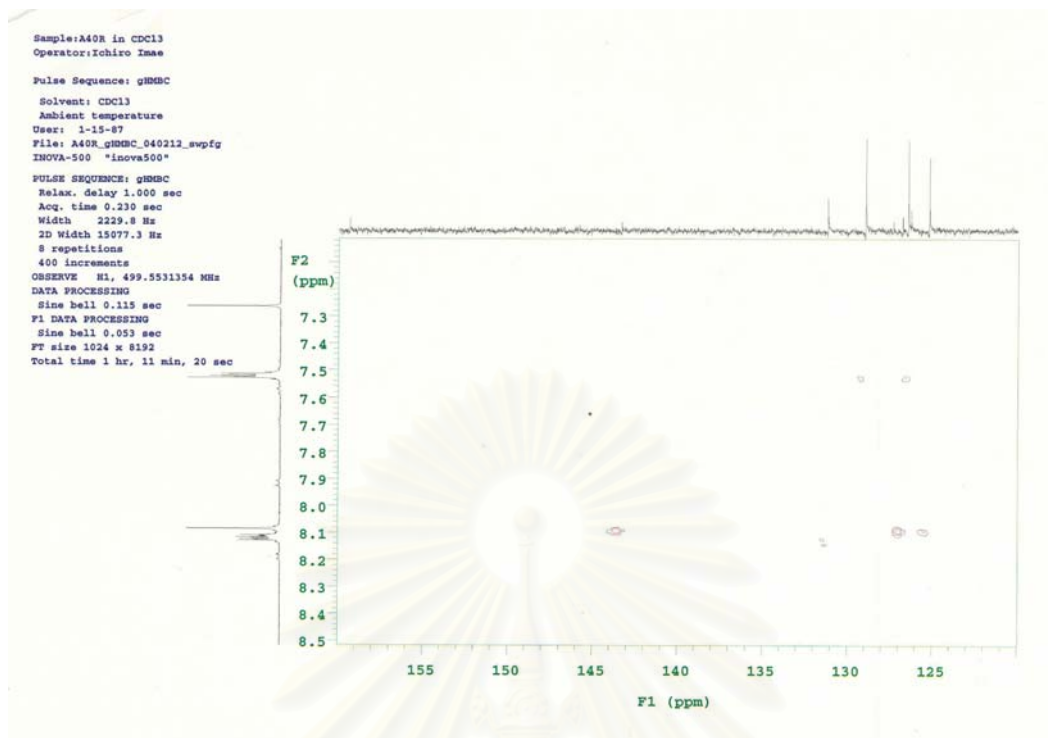


Figure D14 HMQC spectrum of 1,4-bis(4-chloro-2-phenyloxazol-5-yl)benzene



**Figure D15** HMBC spectrum of 1,4-bis(4-chloro-2-phenyloxazol-5-yl)benzene

สถาบันวิทยบริการ  
จุฬาลงกรณ์มหาวิทยาลัย



## VITA

Miss Vorapun Sivaleepunth was born on August 27, 1979 in Bangkok, Thailand. She finished high school at St. Joseph Convent School, Bangkok in 1998. In 2002, she received a Bachelor's Degree of Science in Chemistry at Chulalongkorn University. After graduated with the B.Sc. degree in 2002, she was accepted as a graduate student in Program of Petrochemistry and Polymer Science, Faculty of Science, Chulalongkorn University. She received a Master's Degree program of Science in Polymer Science, in 2004.



สถาบันวิทยบริการ  
จุฬาลงกรณ์มหาวิทยาลัย